

NRDL-12-68-86

7 May 1968

AD 676883

# TURBULENCE IN AN UNBOUNDED UNIFORM-SHEAR FLOW: A COMPUTER ANALYSIS

by

T. H. Gawn

J. W. Pritchett

DDC  
RECEIVED  
OCT 31 1968  
REGISTED  
B

This document has been approved  
for public release and sales its  
distribution is unlimited

U.S. NAVAL RADIOLOGICAL  
DEFENSE LABORATORY

SAN FRANCISCO • CALIFORNIA • 94135

Reproduced by the  
CLEARINGHOUSE  
for Federal Scientific & Technical  
Information Springfield Va. 22151

173

**BEST  
AVAILABLE COPY**

## ABSTRACT

Fluid turbulence is of crucial significance in many problems of scientific and technical importance. Current developments in computer technology offer the possibilities of solving the fundamental equations of turbulent flow in a way never before possible. In order to accomplish this aim, however, it is first necessary to formulate the essential theoretical concepts in a suitable manner. This report summarizes the progress achieved to date in this connection. Various essential basic equations are derived, but the emphasis is as much on fundamental concepts as on mathematical details. More specifically, a method is established for the computer simulation of the detailed stationary turbulence in a uniform shear flow. The results obtainable in this way are far more comprehensive than any which could reasonably be obtained by physical experiment. The data generated represents fundamental information which may be subsequently analyzed to establish overall phenomenological characteristics of the turbulence. The concepts in this report should provide a sound basis for a systematic, sustained and productive research plan. They have already been successfully applied to a computer program which is now going into operation. Results of a typical computer run are included and illustrate qualitative agreement with theoretical predictions; it is hoped to present far more comprehensive and definitive numerical results in future reports.

## SUMMARY

### The Problem

For solution of the flow in complex hydrodynamic systems at high Reynolds number (for example, upward flow following underwater nuclear explosions), a basic understanding of the mechanism of fluid turbulence is required. The Reynolds stresses applied to the mean flow, various "eddy diffusion coefficients," as well as the rate of energy dissipation from turbulence to heat, all depend on the state of the turbulence itself. Various experimental information is available concerning these phenomena for certain particular configurations of the mean flow, and various theories of turbulence exist which are applicable to a few special cases. The basic partial differential equations which govern all incompressible fluid flows (including turbulent ones) have been known for many years. To date, however, it has been impossible to derive from these equations the relevant overall statistical parameters describing turbulence which are required for technical applications.

### Findings

In the current investigation, the approach to the problem of obtaining this information is indirect rather than direct. That is, by the use of high-speed digital computers which have been available only recently, the exact, detailed nature of particular realizations of turbulence may be obtained numerically, by brute-force integration of the governing partial differential equations. This extremely large amount of detailed information concerning the flow may then be treated

statistically to extract the essential information required. This report describes techniques developed to obtain the desired detailed information, and presents a few results from a computer program which embodies these concepts. Methods are then discussed by which this data (which is analogous to a very large amount of physical experimental data) will be processed.

## CONTENTS

ABSTRACT. . . . .	1
SUMMARY . . . . .	11
1. INTRODUCTION. . . . .	1
2. THE BASIC FLOW FIELD. . . . .	7
3. DIMENSIONAL ANALYSIS OF THE BASIC FLOW. . . . .	13
4. BLOCK SIZE, CELL SIZE, AND MEMORY SIZE. . . . .	16
5. EQUIVALENT REFERENCE FRAMES. . . . .	23
6. BOUNDARY AND INITIAL CONDITIONS. . . . .	29
7. NUMERICAL REPRESENTATION OF AN ARBITRARY SCALAR FUNCTION OF POSITION. . . . .	36
8. DIFFERENCING AND INTERPOLATION: METHOD A . . . . .	38
9. DIFFERENCING AND INTERPOLATION: METHOD B . . . . .	43
10. DIFFERENCING AND INTERPOLATION: METHOD C. . . . .	48
11. COMPARISON OF DIFFERENCING METHODS. . . . .	51
12. INITIAL NUMBER OF DEGREES OF FREEDOM. . . . .	53
13. PARTIAL DERIVATIVES IN TERMS OF SURFACE INTEGRALS . . . . .	56
14. CONTINUITY EQUATION. . . . .	63
15. MOMENTUM EQUATION. . . . .	65
16. TURBULENT PRESSURE DISTRIBUTION . . . . .	70
17. BASIC SURFACE INTEGRALS FOR A FINITE ELEMENT: METHOD C. . . . .	74
18. SCALE OF TURBULENCE. . . . .	79
19. MEAN EFFECTIVE TURBULENCE STRESSES. . . . .	83
20. COMPUTATIONAL VERSUS HYDRODYNAMIC INSTABILITY . . . . .	95
21. GENERATION VERSUS ANALYSIS OF TURBULENCE DATA . . . . .	97
22. PARTIAL SUMMARY OF PRINCIPAL CONCEPTS. . . . .	99
23. TYPICAL COMPUTER RESULT. . . . .	104
24. POSTSCRIPT. . . . .	107
REFERENCES. . . . .	111
APPENDIX A DEVELOPMENT OF BASIC DIFFERENCE EQUATIONS (METHOD C). . . . .	112
A.1 LOCATION OF GRID POINTS . . . . .	112
A.2 SURFACE CONSTANTS. . . . .	115
A.3 DIVERGENCE. . . . .	118
A.4 MEAN STRESSES FROM IMPOSED SHEAR RATE . . . . .	119
A.5 MOMENTUM FLUX. . . . .	121
A.6 LOCAL VISCOUS STRESSES . . . . .	122
A.7 MEAN VISCOUS STRESSES . . . . .	123
A.8 RESULTANT PRIMARY STRESSES. . . . .	125
A.9 NET PRIMARY FORCES. . . . .	126

A.10	MEAN PRIMARY FORCES. . . . .	127
A.11	PRESSURE COMPATIBILITY EQUATION. . . . .	128
A.12	SOLUTION FOR PRESSURE BY ITERATION . . . . .	130
A.13	NET PRESSURE FORCES. . . . .	133
A.14	VELOCITY TIME DERIVATIVES. . . . .	134
A.15	NEW VELOCITIES. . . . .	135
APPENDIX B DIVERGENCE CORRECTION AT SLIDING BOUNDARIES . . . . .		136
B.1	SLIDING INTERPOLATION. . . . .	136
B.2	DIVERGENCE CORRECTIONS . . . . .	140
APPENDIX C EVALUATION OF KINETIC ENERGY, REYNOLDS STRESSES, VORTICITY AND SCALE OF TURBULENCE. . . . .		145
C.1	REYNOLDS STRESSES AND ENERGY. . . . .	145
C.2	VORTICITY. . . . .	148
C.3	SURFACE CONSTANTS. . . . .	150
C.4	SCALE OF TURBULENCE. . . . .	152
APPENDIX D FOURIER ANALYSIS OF TURBULENCE IN A UNIFORM SHEAR FLOW. . . . .		154
D.1	COORDINATE SYSTEMS. . . . .	154
D.2	FOURIER SERIES APPROXIMATION FOR VELOCITY PERTURBATIONS. . . . .	156
D.3	SOLUTION FOR THE FOURIER COEFFICIENTS. . . . .	160
TABLES		
3.1	Summary of Dimensionless Variables. . . . .	14
19.1	Types of Turbulent Flows. . . . .	85
23.1	Typical Computer Output. . . . .	105
FIGURES		
2.1	Laminar and Turbulent Flows Between Oppositely Moving Parallel Walls. . . . .	10
2.2	The Basic Mean Flow Field . . . . .	12
5.1	Relative Positions and Velocities of Equivalent Reference Blocks. . . . .	24
6.1	True and Spurious Correlations Resulting From Blockwise Periodicity. . . . .	35
8.1	Basic Grid for Differencing Method A . . . . .	39
9.1	Basic Grid for Differencing Method B . . . . .	44
9.2	Grid Point Relationships for Differencing Method B . . . . .	46
13.1	Volume Elements for Definition of Partial Derivatives. . . . .	57
17.1	Surface Element in Z Plane. . . . .	76
18.1	Velocity Component $v$ in Reference Wave. . . . .	81
19.1	Reference Axes and Mohr's Circles of Strain Rate and Stress. . . . .	90

FIGURES (Contd)

23.1	Dissipation of Turbulent Energy for Sub-Critical Block Size. . . . .	106
26.1	Differencing Method for Grid Points Which Move with Mean Flow. . . . .	109

## 1. INTRODUCTION

The present investigation of turbulence originated in connection with a project involving the numerical simulation of the mean flow in underwater nuclear explosions.\* It was realized quite early in the course of the explosion study that a significant fraction of the energy released in the explosion goes into the creation of intense turbulence, and that the turbulence and the mean flow have a profound mutual influence upon each other. Of course, it is possible to simulate the mean flow phenomena to a first order of approximation, which is sufficient for some engineering purposes, by ignoring the complexities of turbulence and simulating them rather crudely in the form of a fictitious increase in apparent viscosity. In fact, some such procedure is required in any case to ensure that the numerical calculation procedure shall itself be stable.

It is apparent, however, that further progress in the underwater explosion problem requires a deeper understanding of the associated turbulence. Furthermore, the phenomenon of turbulence has an enormous technical and scientific importance in its own right, quite apart from the specific application to underwater explosions. Most fluid flows of technical importance are turbulent, so that progress in understanding the fundamentals of turbulence has potentially an enormous range of application.

---

\*Pritchett, J. W., "MACYL - A Two Dimensional Cylindrical Coordinate Incompressible Code", U. S. Naval Radiological Defense Laboratory, USNRDL-LR-67-97, 20 Oct. 1967.

It is an interesting fact that the basic partial differential equations which govern the detailed motion involved in fluid turbulence have been known for a very long time. However, no one has yet succeeded in deriving from these detailed equations the resulting overall statistical and phenomenological characteristics of the turbulence which are important for technical applications. Typical statistical features of these kinds are mean kinetic energy, mean turbulent stresses, scale of turbulence, various correlation coefficients, etc. The ultimate mutual interrelationships among these statistical characteristics of the turbulence and the relevant features of the mean flow field remain shrouded in mystery.

One reason for the difficulty is that the detailed structure of the turbulence is extremely complex in relation to that of the mean flow and requires an enormously greater number of degrees of freedom for its full description. This fact is crucial for analysis by purely numerical methods. It should be borne in mind that in the underwater explosion problem, for example, the mean flow itself is quite complex and requires a very large number of degrees of freedom for its adequate numerical description. This is true even after advantage has been taken of the polar symmetry which reduces the mean-flow problem from three to two dimensions. The mean-flow requirements still tax the memory capacity of the best modern computers. If we now were to attempt to add turbulence effects by a direct numerical assault, this would require a much finer mesh and an extension from two to three dimensions. The demands on computer memory capacity and computing time would be increased by a fantastic amount! Clearly, such an attack by sheer force would be wholly impractical.

In view of the foregoing difficulties with a direct numerical attack, and in the absence of any demonstrably valid analytical solutions, most attempts to incorporate the effects of turbulence into various problems of fluid mechanics have been based on a more or less empirical approach. Thus the unknown relation between the mean effective turbulence stresses

and the mean flow may be assumed to follow some more or less plausible mathematical form, perhaps one derived by a rough analogy with the known mechanism which governs the viscous stresses. Various assumptions of this kind can and have been postulated, but none so far suggested have been convincingly demonstrated to follow from the fundamental equations of continuity and motion. Consequently, heuristic models of this type generally contain one or more empirical coefficients whose values can be determined only by physical experiment. Nevertheless, results can be obtained in this way which do have a certain usefulness for particular purposes. However, such results tend to be rather limited in scope, are subject to occasionally serious inconsistencies and errors, and do not provide sufficient insight into the real underlying mechanism involved.

There is, however, another possible alternative. We may subdivide the overall problem into several successive phases, each one of which does lie within the capabilities of modern computers. In the first place, we can turn attention to the study of situations in which the character of the mean flow has been substantially simplified. All nonessential complications of the mean flow are at first eliminated. In this way the inherent and essential mechanism of turbulence is all the better isolated and displayed for detailed study and analysis. Secondly, we can subdivide the turbulence itself into two parts, namely, small-scale and large-scale turbulence. The small-scale turbulence can be studied first, utilizing the full capabilities of the computer to this end. While the numerical data obtained in this way is enormously detailed and complex, the significant overall statistical and phenomenological features of this data presumably lend themselves to summary and generalization in some much simpler way. Thus the mean effective turbulence stresses associated with the small-scale turbulence can be consolidated into an appropriate formula. In fact the analysis given in a later section of this report sheds some light on the essential nature of such a relation. The resulting formula can then be treated as part of the known input in the treatment of the large-scale turbulence. Again the full power of

the computer is utilized in dealing with the large-scale turbulence. The detailed numerical data obtained in this second stage can again be generalized so as to summarize the mean effective turbulence stresses and other phenomenological characteristics of the overall turbulence. These results, in turn, can be treated as known inputs in the treatment of the mean flow field, and can be applied to progressively more complex mean flows.

Of course, the relationships obtained for a simplified mean flow do not necessarily apply to mean flows of more general types. Nevertheless, if fundamental insight is our goal, the natural progression of study must be from the simpler to the more complex cases. Eventually, it should be possible to re-introduce some of the complicating factors which are excluded from the initial studies. The resulting mathematical models should gradually become more pertinent and general. Meanwhile, however, even the earlier models can be used to advantage as first-order approximations and introduced provisionally into rather general types of flow fields, such as the unsteady mean flows involved in underwater explosions, for example. This, at least, is the philosophy upon which the present line of investigation is based.

A more detailed discussion of the problem of modelling the mean effective turbulence stresses is presented in a later section of this report.

The principal purpose of the present investigation is, therefore, to begin a fundamental study of the basic mechanism of turbulence by means of a numerical solution of the equations of continuity and motion on a modern high-speed digital computer.

So far as the present report itself is concerned, its main objective is to document the progress that has thus far been achieved, and to summarize the key concepts that have evolved. A certain amount of exploratory theoretical work and preliminary computer calculations were carried out in the early stages before the essential ideas were adequately

developed. It is not the purpose of this report to dwell on these early attempts which have played a useful role but which are now largely superseded.

It is perhaps appropriate to mention in passing, however, that some efforts were made to formulate the problem in wave space, using concepts of spectral and Fourier analysis. While these methods have certain attractive theoretical features, it was finally concluded, nevertheless, that numerical analysis can be carried out more efficiently by a more straightforward approach expressed in terms of ordinary physical space. However, the results computed in this more direct way can subsequently be re-analyzed from the spectral point of view. In fact, it is expected that such supplementary calculations of the spectral type will definitely be made and will prove useful. (See Appendix D.)

While several preliminary computer programs have so far been produced, the first program which embodies present guiding concepts to a sufficient degree is that one designated as "TURBOCODE, MARK V." As of the date of this writing (January 1968), this program has just been developed to the point where serious calculations can now begin on a moderate scale. Results of a typical computer run are given later in this report. However, extended discussion of actual numerical results must await a future report. The present report is aimed primarily at documenting the theoretical concepts which are largely embodied in TURBOCODE, MARK V. In fact, the present theory goes somewhat beyond that on which the above code is based. It is anticipated that a more up to date version will ultimately replace MARK V. At this time, however, it is considered advisable to obtain a certain amount of numerical data from MARK V before proceeding with any major program revision.

The anticipated progress of the present research program can be classified into several successive, but somewhat overlapping stages, as follows:

- (1) Development of basic concepts, equations and computer program for simulation of turbulence.

- (2) Generation and analysis of turbulence data, and development of phenomenological models.
- (3) Application and extension of results to various mean flow fields of technical importance.

The present report, however, is largely limited to the first item in this list. The second stage will also require a strong analytical effort. Only then can the technological pay-off represented by the third stage be fully achieved.

## 2. THE BASIC FLOW FIELD

The simplest possible mean flow field relating to the problem at hand is one which is both steady and incompressible.

The simplest possible state of turbulence is one which is both stationary and homogeneous. Stationary turbulence is characterized by time invariance of all statistical properties at all points. Homogeneous turbulence is characterized by spatial invariance of all statistical properties at all times. These statements also imply constant viscosity over space and time.

The turbulence can be stationary and homogeneous only if the mean flow itself is steady and homogeneous. For homogeneity, the mean flow must have a uniform and constant vorticity vector, and a uniform and constant strain rate tensor. If, in addition, we require that the streamlines of the mean flow field be straight and parallel, say parallel to the x axis, the mean flow reduces to the definite and unique case of a simple uniform shear flow. We can, without loss of generality, orient the y axis in the direction of the shearing gradient. Therefore the mean velocity becomes simply

$$\hat{U} = \hat{i} [U_0 + \Omega y] \quad (2-1)$$

where  $\hat{i}$  is a unit vector in the positive x direction, and  $\Omega$  is the constant shear rate.  $U_0$  is a constant which depends only on the arbitrary location of coordinates.

A further simplification of Eq. (2-1) would be to impose the restriction of zero shear rate, that is

$$\frac{\partial \hat{U}}{\partial y} = \hat{i} \Omega = 0 \quad (2-2)$$

whereupon

$$\hat{U} = \hat{i} U_0 = \text{constant} \quad (2-3)$$

This represents a uniform mean flow. It is in fact equivalent to no flow at all, since a set of axes can now be defined which move along with the mean flow, with respect to which axes the mean velocity is everywhere zero.

The case of uniform mean flow has attracted much attention because it is isotropic. Naturally, the condition of isotropy represents a very considerable simplification of the turbulence problem, and has been extensively studied.

Unfortunately, however, this degree of simplification is excessive in the present context, for with isotropic turbulence and zero shear rate of the mean flow the average turbulent shear stresses are zero, and there can be no transfer of energy from the mean flow to the turbulence. Hence the turbulent energy dissipated into heat by viscous action is not replenished, and the turbulent energy decays with time. The turbulence therefore is not stationary with respect to time, as originally required. (It becomes steady only in the limit as zero amplitude is approached.

But this limit is trivial, in that it really amounts to the absence of turbulence.)

For non-zero shear rate, however, the mean turbulent shear stress is also non-zero, and the sense is such that net energy is transferred from the mean flow into the turbulence. Hence an equilibrium is eventually reached between the mean rate of energy input and the mean rate of viscous dissipation. Consequently, a stationary non-zero amplitude of turbulent energy is ultimately established, as required.

In short, the required flow field involves

(a) A steady, incompressible, parallel mean shear flow with constant non-zero shear rate, and constant viscosity.

(b) Stationary and homogeneous turbulence which is, however, anisotropic.

Now consider the flow between two parallel walls of infinite extent, as shown in Fig. 2.1. The walls move in opposite directions with constant velocities  $\pm U_w$  as indicated. Spacing between the walls is  $2h$ . The fluid has constant density  $\rho$  and constant kinematic viscosity  $\nu$ .

A Reynolds number may be defined for this flow in the form

$$R_e = \left( \frac{U_w h}{\nu} \right) \quad (2-4)$$

It is a well known principle of fluid mechanics that for any given geometrical configuration, there exists a corresponding critical Reynolds number which marks the boundary between laminar and turbulent flow. For the present case, the critical Reynolds number is about 750 (Ref. 1). Below this critical value the above flow is laminar and the velocity varies according to the simple linear law.

$$U = \Omega y \quad (2-5)$$

where

$$\Omega = \frac{\partial U}{\partial y} = \text{constant shear rate} \quad (2-6)$$

At Reynolds numbers above the critical, however, the flow becomes unstable with respect to small velocity perturbations, and a stationary turbulent condition is soon established. In this case the velocity distribution becomes strongly non-linear, somewhat as shown in the diagram.

Next, consider a sequence of turbulent flows of the above type at successively higher Reynolds numbers. Suppose this sequence is generated by increasing both  $U_w$  and  $h$  in such a way that the slope  $\frac{\partial U}{\partial y}$  remains finite in the mid-region near  $y = 0$ , far from both walls. In the limit as  $R_e \rightarrow \infty$ , we once again recover a linear distribution of the mean velocity far from the walls, but now the flow is turbulent. This is the

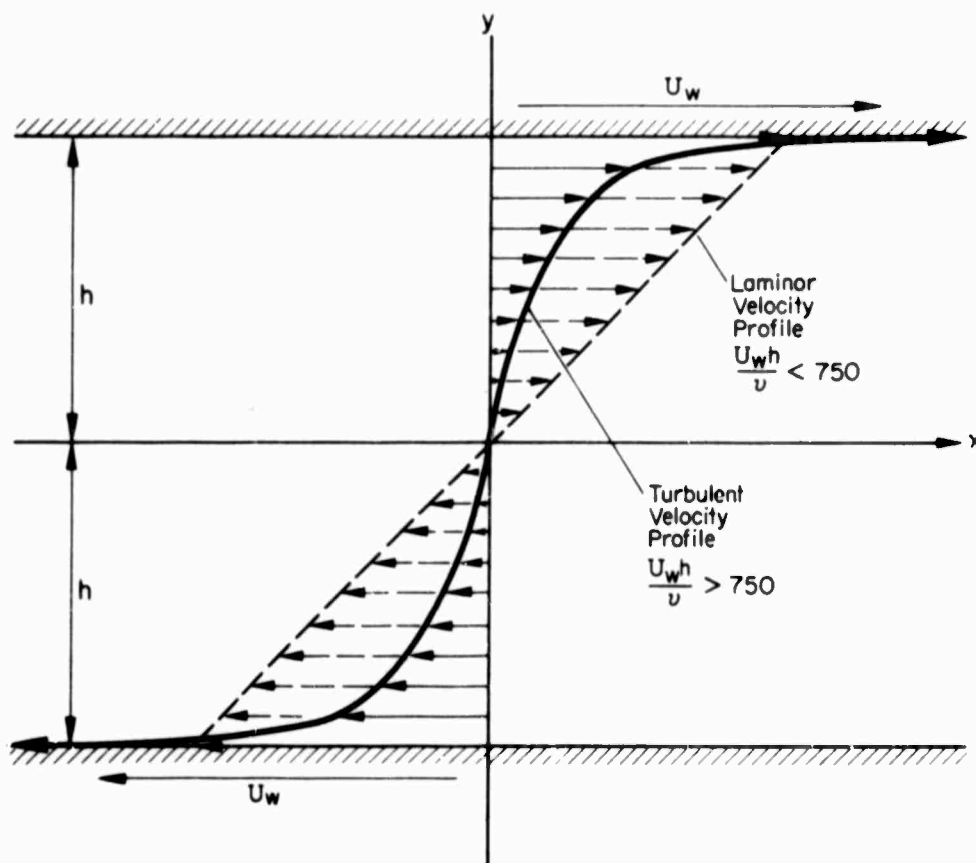


Fig. 2.1 Laminar and Turbulent Flows Between Oppositely Moving Parallel Walls.

situation we wish to analyze (see Fig. 2.2). It represents perhaps the simplest conceptual example of stationary, homogeneous non-isotropic turbulence. Analysis of this flow should reveal important basic information concerning the irreducible essence of stationary turbulence.

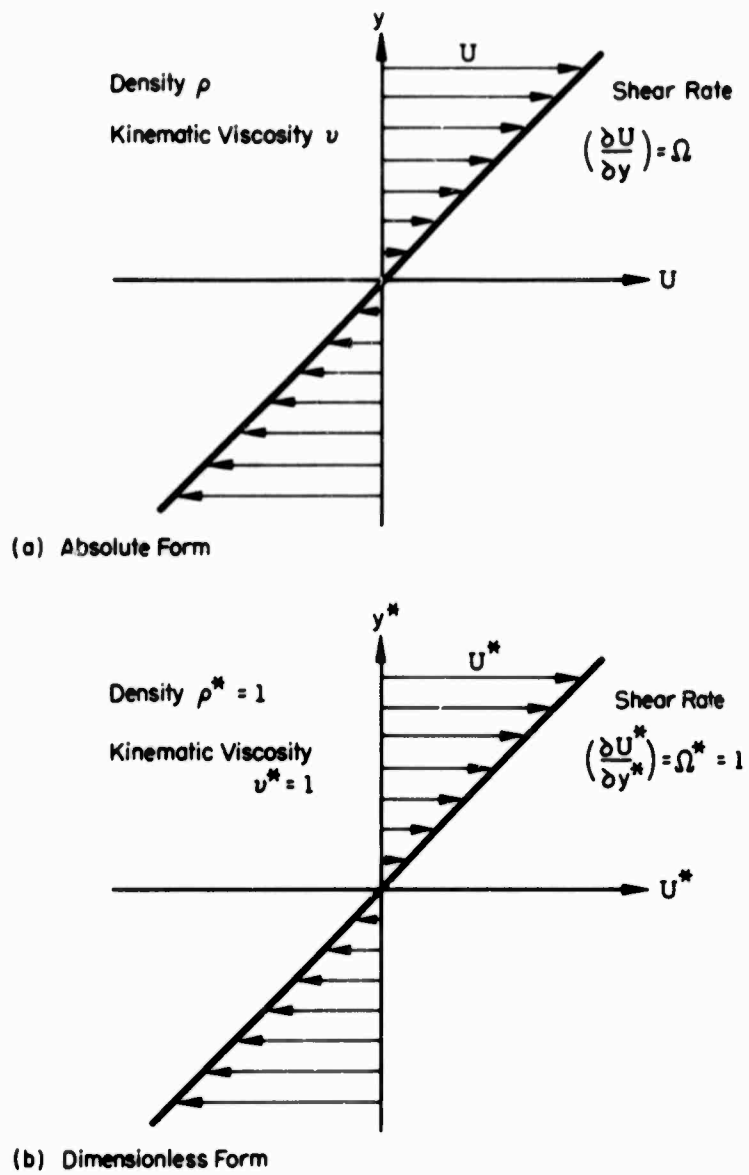


Fig. 2.2 The Basic Mean Flow Field.

### 3. DIMENSIONAL ANALYSIS OF THE BASIC FLOW

The basic flow field described in the previous section, and illustrated in Fig. 2.2, is fully defined by three characteristic parameters, namely,

$\Omega = \frac{\partial u}{\partial y}$  = the constant shear rate, 1/sec

$\rho$  = the constant fluid density, slugs/ft<sup>3</sup>

$\nu$  = the constant kinematic viscosity, ft<sup>2</sup>/sec

The present problem lies in the realm of dynamics. This amounts to saying that all significant quantities which occur in it are reducible dimensionally to certain combinations of not more than three fundamental dimensions. These can be force  $F$ , length  $L$  and time  $T$ . However, the requisite reference force, length and time can be expressed, in turn, by combinations of three parameters appropriate to the specific problem under study. For the present problem, the necessary and sufficient parameters are clearly  $\Omega$ ,  $\rho$  and  $\nu$ . These three quantities suffice to establish a system of natural reference units in terms of which all other physical quantities can be expressed in an appropriate dimensionless form. Thus, for example, if  $X$  is any relevant quantity having arbitrary physical dimensions, a dimensionless form  $X^*$  may always be defined such that

$$X^* = \frac{X}{\rho^a \Omega^b \nu^c}$$

The appropriate exponents  $a$ ,  $b$ ,  $c$  can always be found so as to render  $X^*$  dimensionless.

This principle is illustrated by the examples listed in Table 3.1.

The last three entries in the table show that the basic dimensional reference quantities, namely  $\rho$ ,  $\nu$  and  $\Omega$ , when themselves expressed in dimensionless terms, turn out, of course, to have unit amplitude.

TABLE 3.1  
Summary of Dimensionless Variables

Quantity	Symbol	Dimensions	Dimensionless Form
<u>Principal Variables:</u>			
Length	x	L	$x^* = x \sqrt{\frac{\Omega}{\nu}}$
Time	t	T	$t^* = \Omega t$
Velocity	u	L/T	$u^* = \frac{u}{\sqrt{\nu \Omega}}$
Velocity Time Derivative	$\frac{\partial u}{\partial t}$	L/T <sup>2</sup>	$\frac{\partial u^*}{\partial t^*} = \frac{1}{\sqrt{\Omega^3 \nu}} \frac{\partial u}{\partial t}$
Force per Unit Mass	f	$\frac{F}{M} = \frac{L}{T^2}$	$f^* = \frac{f}{\sqrt{\Omega^3 \nu}}$
Pressure per Unit Density	$\phi = \frac{p}{\rho}$	$\frac{FL}{M} = \frac{L^2}{T^2}$	$\phi^* = \frac{p}{\rho \nu \Omega}$
Kinetic Energy per Unit Mass	E	$\frac{FL}{M} = \frac{L^2}{T^2}$	$E^* = \frac{E}{\nu \Omega}$
<u>Reference Parameters:</u>			
Density	$\rho$	$\frac{M}{L^3} = \frac{FT^2}{L^4}$	$\rho^* = \frac{\rho}{\rho} = 1$
Kinematic Viscosity	$\nu$	$\frac{L^2}{T}$	$\nu^* = \frac{\nu}{\nu} = 1$
Mean Shear Rate	$\Omega$	$\frac{1}{T}$	$\Omega^* = \frac{\Omega}{\Omega} = 1$

This fact is important. It shows that all cases of unbounded parallel flow with constant shear rate are reducible, when expressed dimensionlessly, to a single case! This represents a substantial simplification and generalization of the problem. Using dimensionless nomenclature, we may say that all cases are equivalent in a certain sense to the case of a fluid of unit mass and unit viscosity undergoing unit shear rate.

It can be shown rigorously that any equation that is valid when expressed in absolute dimensional form is also valid when expressed in corresponding dimensionless form. Hence we may replace absolute quantities  $x$ ,  $t$ ,  $u$ , ..... etc. by the equivalent dimensionless forms denoted by  $x^*$ ,  $t^*$ ,  $u^*$  .....etc. In this process the quantities  $\rho$ ,  $\nu$ ,  $\Omega$  are replaced by  $\rho^* = 1$ ,  $\nu^* = 1$ ,  $\Omega^* = 1$  and hence cease to appear explicitly in the equations.

The above non-dimensionalizing procedure is followed in some of the mathematical developments of this report. Whenever the context is such that there is no ambiguity involved, it becomes permissible to drop the symbol\* which was introduced above to distinguish dimensionless forms from their dimensional counterparts. On the other hand, in some discussions it is clearer to retain the fully dimensional form. This variation of usage should cause no difficulty, as the context makes the intended meaning clear.

#### 4. BLOCK SIZE, CELL SIZE, AND MEMORY SIZE

In analysis of the flow by finite difference methods, it is obviously necessary to confine the numerical operations to a finite region. Extension of the boundaries to infinity, such as is frequently convenient when one is using analytical techniques, is not feasible when numerical methods are employed.

Fortunately, an adequate approximation can be made on the basis of a finite region, provided that the chosen region is sufficiently large to constitute a representative sample of the field. The term "large" is, of course, relative. We must ask, "Large relative to what?"

The answer is that the region should be large relative to the "scale of turbulence." There are various possible definitions of scale of turbulence. Perhaps the most useful definition in the present context is based on the concept of statistical correlation. Let us therefore summarize the essential features of this concept.

For this purpose, let  $\hat{x}_P$  and  $\hat{x}_Q$  denote the position vectors of two arbitrary but known fixed points in the flow field. The relative displacement vector between the two points is then

$$\hat{r}_{PQ} = \hat{x}_Q - \hat{x}_P \quad (4-1)$$

Let  $\hat{u}_P(t)$  and  $\hat{u}_Q(t)$  be the respective turbulent velocity vectors at the two points as functions of time. Assuming that the turbulence is stationary, we may define the following three time-average scalar products, namely,

$$\overline{\hat{u}_P \cdot \hat{u}_Q} = \frac{1}{T} \int_0^T \hat{u}_P(t) \cdot \hat{u}_Q(t) dt \quad (4-2)$$

$$\overline{\hat{u}_P \cdot \hat{u}_P} = \overline{u_P^2} = \frac{1}{T} \int_0^T \hat{u}_P(t) \cdot \hat{u}_P(t) dt \quad (4-3)$$

$$\overline{\hat{u}_Q \cdot \hat{u}_Q} = \overline{u_Q^2} = \frac{1}{T} \int_0^T \hat{u}_Q(t) \cdot \hat{u}_Q(t) dt \quad (4-4)$$

where the total time  $T$  is large.

Now the correlation coefficient  $R$  is defined as

$$R(\hat{r}_{PQ}) = \frac{\overline{\hat{u}_P \cdot \hat{u}_Q}}{\sqrt{\overline{u_P^2}} \sqrt{\overline{u_Q^2}}} \quad (4-5)$$

Since the field is also homogeneous, this expression simplifies further because in this case

$$\overline{u_P^2} = \overline{u_Q^2} = \overline{u^2} \quad (4-6)$$

Therefore

$$R(\hat{r}_{PQ}) = \frac{\overline{\hat{u}_P \cdot \hat{u}_Q}}{\overline{u^2}} \quad (4-7)$$

Furthermore, in a homogeneous field  $R$  has the same value for every possible choice of the point  $\hat{x}_P$ , provided  $\hat{r}$  is held fixed.

Now it is easy to show that if point  $Q$  is chosen to coincide with point  $P$ , we obtain perfect correlation, that is,

$$R(0) = 1 \quad (4-8)$$

On the other hand, we know from experiment that if point  $Q$  is remote from  $P$ , the velocities are completely uncorrelated. Hence

$$R(\infty) = 0 \quad (4-9)$$

There is much experimental information available which shows that the correlation coefficient  $R$  diminishes rapidly with increasing magnitude of the relative displacement vector,  $r = |\hat{r}_{PQ}|$ . In principle,

therefore, there exists some finite value  $r_{MAX}$  beyond which the magnitude of the correlation coefficient  $|R|$  is everywhere less than some very small preassigned quantity  $\epsilon$ . Thus

$$|R(r_{MAX})| \leq \epsilon \lll 1 \quad (4-10)$$

The actual value of  $r_{MAX}$  depends on the permissible error  $\epsilon$ . Of course, in any practical case there is always some limitation in the accuracy with which  $R$  itself can be measured or computed. If we choose  $\epsilon$  equal to the uncertainty in  $R$  itself, then there exists some corresponding finite  $r_{MAX}$ . We can say that beyond this distance the correlation  $R$  is truly negligible. Hence the smallest region which is sufficiently large with respect to the scale of turbulence to be acceptable as a representative sample of the field may be conceived, for example, as a sphere of radius  $r_{MAX}$ .

Another way to judge the size of the region is in relation to the wavelengths of the turbulent velocity spectral components. It is known that the wavelengths which play a significant role in entraining energy from the mean flow, in sustaining the kinetic energy of the turbulence, and in dissipating turbulent energy into heat, are largely confined within a certain limited range. The flow region selected for study must be large enough to include this range, of course, but any further increase in size can be expected to have negligible effects on the results.

Provided the region selected is sufficiently large along its smallest dimension, its exact shape should make no noticeable difference in the final results. Hence shape may be chosen on the basis of convenience. Now the shape which is by far most convenient for numerical analysis is a simple cubical block, say of length  $L$  along each edge.

The cubical control block must in turn be subdivided into small volume elements for purposes of numerical analysis by differencing techniques. Once again, the shape of the volume elements is relatively unimportant, provided they are reasonably compact and sufficiently small.

Clearly, it is by far most convenient to choose these as cubical cells of length  $(L/N)$  along each edge. It is essential, however, that the length  $(L/N)$  be sufficiently small relative to the scale of turbulence. In particular, it must be smaller than the shortest wavelength in the significant wavelength range as described above.

It follows that, ideally, we should like to use a block length  $L$  which lies above some upper critical limit, say  $L_{\max}$ , and simultaneously to use a cell length  $(L/N)$  which lies below some lower critical limit,  $L_{\min}$ . In principal, this can be achieved by choice of a sufficiently large value of  $N$ , that is,  $N \geq L_{\max}/L_{\min}$ .

The difficulty to be faced is that computer memory limitations will make it impossible to use a value of  $N$  large enough to satisfy the foregoing requirement. This is because computer storage requirements increase roughly in proportion to  $N^3$ . Moreover, computing times increase even more sharply, perhaps in proportion to  $N^4$ . Consequently, some type of partial simplification of the problem becomes mandatory.

One answer to this difficulty is to split the overall turbulence into several ranges of wavelength, and solve them in succession. The general idea has already been explained briefly. It is believed that existing third-generation computers have now reached a state of development such that the problem can probably be solved in just two stages, namely, by division of the turbulence into small-scale and large-scale effects. We can do this by choosing a length  $L_s$  which represents the block size for the small-scale turbulence, and which is at the same time equal to the cell size of the large-scale turbulence.

Thus we may write -

For the small-scale turbulence:

$$\begin{array}{ll} \text{Cell Size} & L_{\min} \\ \text{Block Size} & L_s \end{array} \left. \vphantom{\begin{array}{l} L_{\min} \\ L_s \end{array}} \right\} \frac{L_s}{L_{\min}} \leq N \quad (4-11)$$

For the large-scale turbulence:

$$\left. \begin{array}{l} \text{Cell Size } L_s \\ \text{Block Size } L_{\max} \end{array} \right\} \frac{L_{\max}}{L_s} \leq N \quad (4-12)$$

It follows that for a two-stage analysis of this kind, the required value of  $N$  is reduced to

$$N \geq \sqrt{\frac{L_{\max}}{L_{\min}}}.$$

Another problem is that the appropriate spectral wavelengths  $L_{\max}$  and  $L_{\min}$  are initially unknown, although existing experimental data might possibly provide this information. However, we now consider a method of numerical experimentation on the computer itself which can serve to establish a reasonable estimate for the lower limit  $L_{\min}$ .

Recall that energy input to the turbulence is mostly concentrated at the longer wavelengths while energy dissipation is mainly in the shorter wavelength range. Hence a reduction of the small-scale block size  $L_s$  amounts to cutting down energy input in relation to dissipation. It should result in a reduction in the mean steady kinetic energy of the turbulence. In fact, it should presumably be possible to find a critical limit  $L_{cr}$  below which the initially imposed turbulence cannot sustain itself and eventually dies out. This condition can be associated with a critical Reynolds number marking the border between laminar and turbulent flow. Thus

$$Re_{cr} = \frac{L_{cr}^2 \Omega}{\nu} = L_{cr}^{*2} \quad (4-13)$$

It may be argued that over distances smaller than  $L_{cr}$ , significant turbulence effects cannot be sustained. This therefore provides a reasonable measure for the minimum necessary cell size. That is, for the small-scale turbulence we may place

$$\frac{L_s}{N} = L_{cr} \quad (4-14)$$

Presumably it is possible to find  $L_{cr}$  by successive trials, using only the basic turbulence computer program itself. Let a series of runs be made varying only the block size  $L$ . For trial values of  $L$  smaller than  $L_{cr}$ , the initial turbulence may be expected always to die out. For values greater than  $L_{cr}$ , the turbulence kinetic energy may be expected eventually to reach a non-zero mean stationary state. Hence a systematic series of trials should theoretically suffice to establish  $L_{cr}$  to within any prescribed margin of uncertainty. When  $L_{cr}$  has been found in this way, we may then fix the required block size for the small-scale turbulence as equal to

$$L_s = N L_{cr} \quad (4-15)$$

Then the required block size for the large-scale turbulence becomes

$$L_L = N L_s = N^2 L_{cr} \quad (4-16)$$

If the large-scale block size  $L_L$  obtained in this way satisfies the condition

$$L_L \geq L_{max} \quad (4-17)$$

then all requirements relating to block and cell size will have been met.

Naturally, the higher the available value of  $N$ , the more accurate are the results obtained in this way. Theoretically, the exact result corresponds to the unattainable hypothetical limit of infinite  $N$ . It is believed, however, that by use of the two-stage approach outlined above, reasonably accurate results can be obtained with modest values of  $N$ , well within the memory capacity of modern computers. With computer technology itself still advancing at a brisk rate, there is every reason

to suppose that the accuracy and adequacy of the results attainable will improve steadily.

Of course, the use of two (or more) successive ranges of wavelengths, although it should enable us to compensate in part for limitations of computer capacity, is not without its drawbacks. For one thing, the basic equations become more complex as the quadratic terms in the momentum equation introduce interaction effects among the several wavelength regimes. A detailed treatment of the interaction problem lies outside the scope of the present report. It is believed, however, that this aspect can be successfully treated.

## 5. EQUIVALENT REFERENCE FRAMES

The present analysis is concerned with homogeneous turbulence. This means that all statistical features of the turbulence, such as the mean kinetic energy, for example, are uniform over the entire flow field. Consequently, it is immaterial just where the control block is located in the flow field. In fact, we may subdivide the entire unbounded flow region into a cubical array of blocks, somewhat as shown in Fig. 5.1, and select one of these at random as the system to be analyzed.

However, if the various blocks are to be considered equivalent to one another, they must all be related to the mean flow in a corresponding manner. Consider, for example, the array of blocks in Fig. 5.1. Block outlines are indicated by heavy lines, cell outlines within each block by lighter lines. Three rows of blocks are shown in the figure. Each of these rows has a mid-plane, which is the horizontal plane midway between the top and bottom boundaries of that row. The vertical spacing between the successive mid-planes is equal to the block size  $L$ . Let the middle row of blocks be regarded as fixed in the diagram. Suppose the mean velocity of the fluid is

$$\hat{U} = \hat{i} \Omega y \quad (5-1)$$

where  $y$  is measured vertically from the mid-plane of the middle row.

Suppose that the upper row of blocks is moving to the right with a speed  $\Omega L$ , and the lower row is moving to the left with speed  $\Omega L$ . Clearly there is now zero relative velocity between fluid and block at the mid-planes of all three rows. An observer in any one row of blocks, moving with that row, sees within his own row a distribution of the relative mean velocity which is identical with that seen by any other observer in the latter's own row. The velocity diagrams illustrate this fact. This is what is meant by the statement that all blocks must be related to the mean flow in a corresponding way.

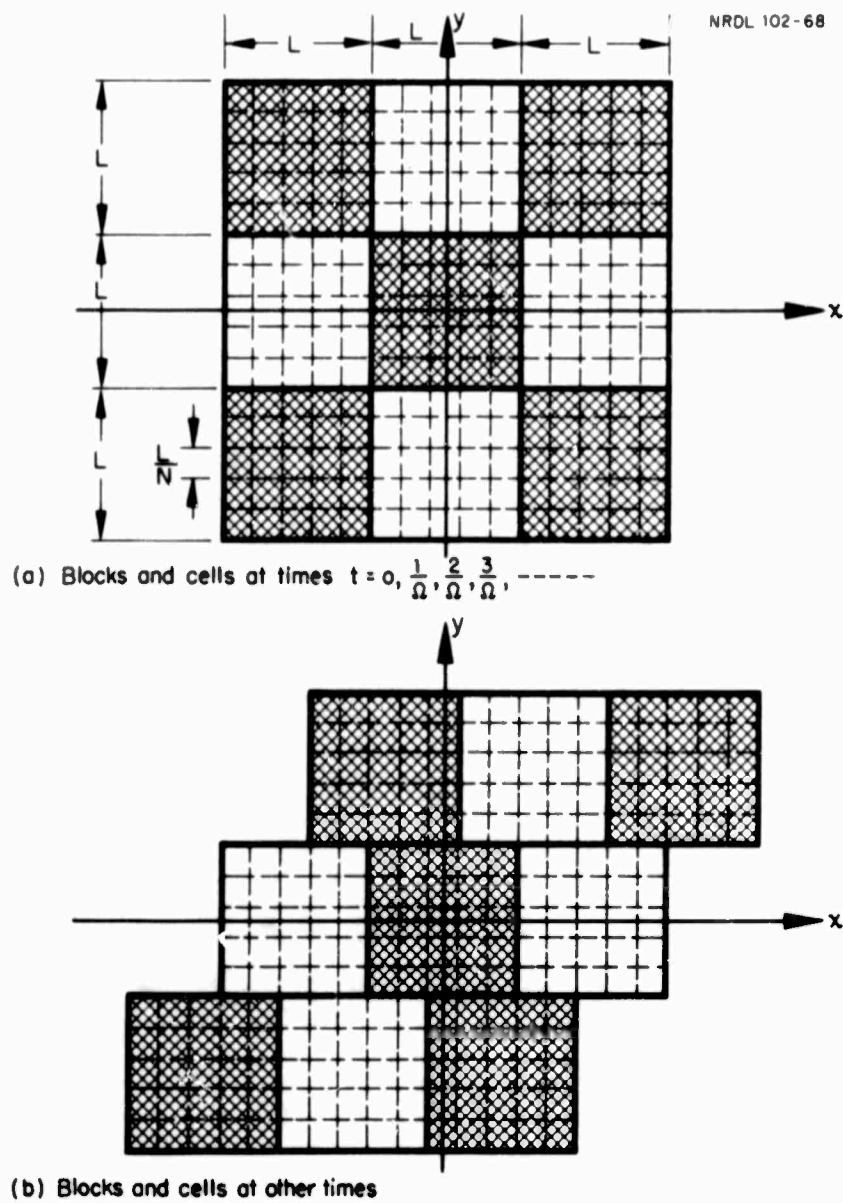
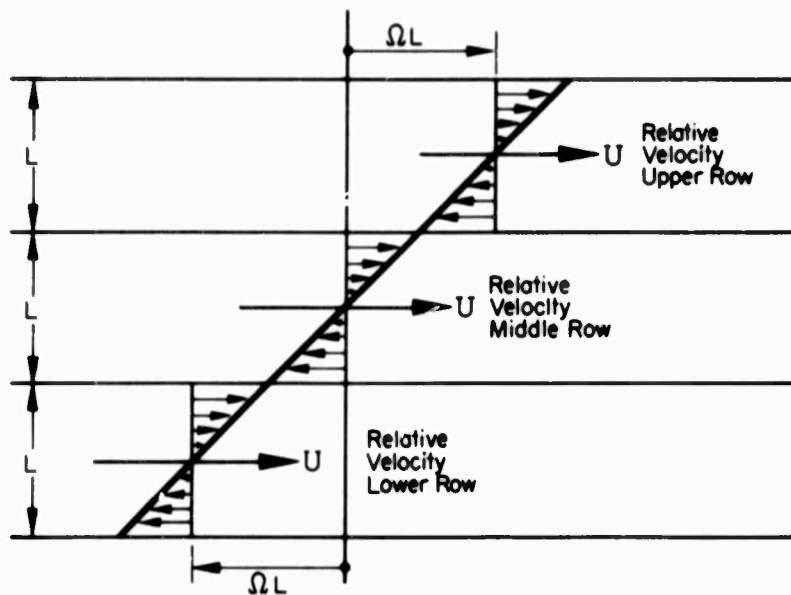


**Fig. 5.1** Relative Positions and Velocities of Equivalent Reference Blocks.

- (a) Blocks and cells at times  $t = 0, \frac{1}{\Omega}, \frac{2}{\Omega}, \frac{3}{\Omega}, \dots$
- (b) Blocks and cells at other times.



(c) Mean flow velocities relative to successive rows of blocks.

Fig. 5.1 (cont'd) (c) Mean Flow Velocities Relative to Successive Rows of Blocks.

Now any one of these blocks may be chosen at random as the system to be analyzed. From the point of view of a hypothetical observer within that block and moving along with it, the block and its associated grid of cells constitutes a stationary or Eulerian frame of reference. All the subsequent analytical equations are to be understood as being expressed with respect to such an Eulerian reference frame. It is an important point, however, that the different rows of blocks are to be considered as lying in different, though equivalent, reference frames. Since all of these reference frames are moving in straight lines parallel to one another and at constant relative velocities, they are all inertial systems.

It is convenient to assume that at some initial time  $t = 0$ , all of the blocks in the field are arranged in a simple cubical array, with their front and rear surfaces lying in common vertical planes through all rows, in the manner shown in Fig. 5.1(a). As time passes, the separate rows become gradually more staggered relative to one another, owing to their relative motion, as shown in Fig. 5.1(b). However, after each time interval of length  $(1/\Omega)$ , the relative movement between any two successive rows equals exactly one additional block length, so that a simple cubical alignment is once again established. It is seen, therefore, that the steady and progressive relative sliding of the various blocks gives to the structure of the reference framework a periodically recurring character, with period  $T = 1/\Omega$ . Expressed in appropriate dimensionless time units, the period becomes simply  $T^* = 1/\Omega^* = 1$ .

There is, however, a time span which is a true characteristic of the turbulence, and which should be mentioned at this point. It is associated with the concept of correlation over time, and is entirely analogous to the previously discussed concept of correlation over distance.

Let  $\hat{u}_p(t)$  and  $\hat{u}_p(t+T)$  be the velocity vectors at a fixed point  $\hat{X}_p$  at times  $t$  and  $(t+T)$  respectively. If the turbulence is stationary we can define the time averages

$$\overline{\hat{u}_P(t) \cdot \hat{u}_P(t+T)} = \frac{1}{T} \int_0^T \hat{u}_P(t) \cdot \hat{u}_P(t+T) dt \quad (5-2)$$

$$\begin{aligned} \overline{u^2} &= \overline{\hat{u}_P(t) \cdot \hat{u}_P(t)} = \overline{\hat{u}_P(t+T) \cdot \hat{u}_P(t+T)} \\ &= \frac{1}{T} \int_0^T \hat{u}_P(t) \cdot \hat{u}_P(t) dt = \frac{1}{T} \int_0^T \hat{u}_P(t+T) \cdot \hat{u}_P(t+T) dt \end{aligned} \quad (5-3)$$

Now the correlation coefficient  $R$  is defined as

$$R(T) = \frac{\overline{\hat{u}_P(t) \cdot \hat{u}_P(t+T)}}{\overline{u^2}} \quad (5-5)$$

If the turbulence is homogeneous, then for a fixed  $T$ , the value of  $R$  is the same for every possible choice of the point  $\hat{x}_P$ .

It is seen that if we place  $t = 0$ , we obtain perfect correlation, that is,

$$R(0) = 1 \quad (5-6)$$

On the other hand, we know from experiment that at times sufficiently far apart, the velocities are completely uncorrelated, that is

$$R(\infty) = 0 \quad (5-7)$$

Now it follows that there exists some time span  $t=T$  beyond which the value of  $R$  differs from zero by an amount less than the small inherent uncertainty in  $R$  itself.

It follows that if we wish to calculate any time-average property of the turbulence, an integration over a time interval of say  $2T$  will be ample to provide a just average. Also, if we wish to approximate the turbulence by Fourier methods, it is permissible, for example, to treat

the phenomenon as periodic in time, provided that we choose the basic reference period as at least equal to  $2T$ . Actually, our present method of solution does not assume this kind of periodicity in time; it will be seen, however, that the assumption of periodicity in space proves to be most useful.

## 6. BOUNDARY AND INITIAL CONDITIONS

Solution of the fluid turbulence problem involves the application of the principles of mass and momentum conservation to all the individual small cubical cells which comprise the large fluid block under study. The resulting difference equations which embody these physical principles may be termed field equations because they apply to all the small volume elements throughout the field. They play a role in the numerical difference method analogous to that of partial differential equations.

However, such a set of field equations is capable of establishing an indefinitely large number of distinct solutions, depending on the boundary and initial conditions which are involved. For the present case, the boundary conditions are simply the velocity and pressure distributions occurring as functions of time over the six square bounding surfaces of the block. The initial conditions are the distributions existing over the entire control volume at the initial time  $t = 0$ .

From a purely mathematical point of view, the boundary and initial conditions may be arbitrarily prescribed; the field equations then establish the corresponding complete time-dependent distributions over the volume of the block. Thus the field equations do not in themselves fully determine the phenomena, but merely propagate the effects of the boundary and initial conditions in the proper manner.

But for the purpose of simulating turbulence, what are the appropriate boundary and initial conditions to apply? The field equations themselves do not enlighten us directly on this crucial point. Nevertheless, there are other considerations which do lead to fairly satisfactory answers. In this connection, it is convenient to consider the initial conditions and the boundary conditions separately.

In regard to the initial conditions, it is shown elsewhere in this report that for a simple cubical grid of  $N^3$  points, there are  $2N^3$  initial

degrees of freedom. This means that  $2N^3$  initial velocity components may be prescribed arbitrarily. Hence the number and variety of conceivable initial combinations is extremely large. So how shall a specific suitable initial combination be selected or prescribed?

The key to the answer lies in the fact that fluid turbulence is an instability phenomenon. It is characteristic of instability processes that initial perturbations serve mainly as a triggering mechanism; the state ultimately attained is essentially independent of the exact nature of the triggering disturbance. The reason is that certain components of the turbulence tend to grow and others to decay until an inner dynamic equilibrium is attained. This ultimate equilibrium depends on the intrinsic mechanism of turbulence rather than upon the exact form of the triggering perturbation.

It is known, however, that the initial response of a particular flow field to an imposed disturbance may be relatively sensitive to certain ranges of frequencies or wavelength and comparatively immune to others, although the ultimate state is independent of these details. Hence it is probably advantageous, though not essential, to assume an initial velocity perturbation which contains a wide range of wavelengths and frequencies. Apart from this rather mild requirement, however, the exact form of the initial perturbation should be immaterial in the long run.

From this it appears that any random set of initial velocity perturbations is adequate for starting the calculation procedure. In any case, the precise influence traceable to the specific initial input used may be expected to fade out with time in a roughly exponential manner, quickly leading to a state of the system which may for all practical purposes be regarded as stationary and representative. At least, this is the assumption made in the present analysis.

Turning now to the conditions along the bounding surfaces, we find a more difficult problem. The reason is that the influence of the boundaries, unlike that of the initial state, does not diminish with

time. Hence there is no possibility of obtaining a valid solution unless the boundary conditions are defined in an appropriate way.

In this connection, one important clue is that the flow field is homogeneous. Therefore, the exact placement of the reference grid is arbitrary and immaterial. Thus the overall statistical results obtained from a certain system of blocks should be the same as those from another system of blocks displaced with respect to the first by arbitrary amounts along all three axes. Of course, if there is a vertical displacement between these two reference systems, there must also be a corresponding horizontal relative velocity between them. As has already been shown, this is necessary in order that both systems of reference blocks shall have corresponding velocity relationships with respect to the mean flow passing through them.

Another way to view the matter is that the translation of any plane by any amount in any direction should not change any overall statistical characteristics pertaining to that plane, provided only that it remains parallel to its original orientation and that it retains a corresponding velocity relative to the mean flow.

Another clue concerning the character of the boundary conditions is that each bounding surface is the common interface between two adjacent blocks. It serves as a medium of transmission of the influence of each of the blocks upon the other. Furthermore, there is a kind of symmetry in this two-way transmission. The reason is that both blocks are sufficiently large that all statistical characteristics of the turbulence are sensibly equal in the two volumes. It is seen therefore that each bounding surface is the common interface between two large volumes whose fluid contents exhibit statistically equivalent behavior.

Another significant attribute of turbulence that should be borne in mind in formulation of appropriate boundary conditions is the element of randomness in the phenomena. The statistical concept of correlation, as explained in an earlier section, is helpful in this connection. In particular, we require that the velocity correlation coefficient  $R(\hat{f}_{PQ})$

shall be negligible if the distance  $\hat{r}_{PQ}$  between the two points involved is sufficiently large, say equal to block size  $L$ .

Consider specifically two points  $P$  and  $Q$ , point  $P$  being somewhere on the left bounding surface and point  $Q$  being somewhere on the right bounding surface of the block. The distance between  $P$  and  $Q$  is never less than the block size  $L$  regardless of the precise locations of  $P$  and  $Q$  on the respective faces. Hence the velocity correlation between  $P$  and  $Q$  must be negligible for all possible pairs of locations. Similar conclusions can be drawn for another pair of points  $P'$  and  $Q'$  on the front and rear bounding faces of the block, respectively. Similarly for points  $P''$  and  $Q''$  on the upper and lower faces.

At first glance, the above restriction seems to rule out the idea of treating the spacewise velocity components as periodic functions of wavelength  $L$ , equal to block size. For if such periodicity were assumed, then pairs of points could always be found on opposite faces for which the correlation coefficient, instead of vanishing, would equal unity!

What seems to be demanded, instead, is a certain statistical randomness in the boundary conditions. It is well understood, of course, that turbulence is a partly stochastic process. Since the field equations themselves are strictly deterministic, the stochastic aspects can only enter via the initial and boundary conditions.

It is undoubtedly possible to devise some calculation procedure of the Monte Carlo type to simulate the stochastic element in the boundary conditions, while still preserving the various types of statistical equivalence previously discussed. The advantage of such a procedure would be that all the foregoing requirements could be met, including the requirement for high correlation at small distances and zero correlation at large distances. Hence this possibility is worth more detailed study.

It has been concluded, however, that a very slight relaxation of the above requirements leads to a great simplification of the problem, without any serious disadvantages. Also, it effectively minimizes the

stochastic aspects, and puts the calculations on an essentially deterministic basis.

The simplification consists of selecting for the initial perturbation a pattern which, although it may be somewhat random in other respects, is "blockwise periodic." By this term we mean that at the initial instant of time, the distributions of the turbulent velocity and pressure perturbations are identical in all blocks.

Now it follows rigorously from the equations of motion that if the turbulence is blockwise periodic at the initial instant, it remains blockwise periodic thereafter.

To define this concept mathematically, let us take the typical scalar velocity component  $u(x,y,z,t)$ , for example. The function  $u$  will be said to be blockwise periodic if, and only if, for all values of  $x,y,z$  and  $t$  we have

$$u(x', y', z', t) = u(x,y,z,t) \quad (6-1)$$

$$\begin{aligned} \text{where } x' &= x + pL + qL\Omega t & ) \\ y' &= y + qL & ) \\ z' &= z + rL & ) \end{aligned} \quad (6-2)$$

$$\begin{aligned} \text{and where } p & ) \\ q & ) = 0, \pm 1, \pm 2, \pm 3, \dots, \pm \infty \\ r & ) \end{aligned} \quad (6-3)$$

The term of  $qL\Omega t$  in the above expression accounts for the difference in mean flow velocity in two horizontal planes separated by the vertical distance  $qL$ .

This assumption of periodicity among the blocks, is, of course, stronger than the requirement for merely statistical equivalence. The distributions in the various blocks could be statistically equivalent without necessarily being identical at every corresponding point of space and time. On the other hand, if they are treated as strictly periodic in this special way, then they satisfy statistical equivalence

identically. That is to say all volumetric integrals, averages, variances etc. will be exactly equal for all blocks.

It turns out that this assumption of blockwise periodicity supplies exactly the information needed to establish the unknown boundary conditions in a completely determinate manner, without recourse to auxiliary statistical hypotheses or ad hoc arguments. In other words, the hypothesis is very attractive because it succeeds so well!

The method is also efficient numerically in the sense that the stored numerical information now is representative not just of one block but of all blocks, and hence of the entire infinite field.

One requirement that the assumption of blockwise periodicity does not fully meet is that velocity correlations should vanish at large distances. Instead, it is found that the correlation coefficient itself becomes periodic in character. However, there is no great harm in this, provided that the basic **wavelength** is sufficiently large that the recurring correlation peaks are well separated. In fact if the correlation is negligible at the midpoints between successive peaks, each peak may be regarded as essentially isolated, and the spurious correlation at the full **wavelength** may be safely disregarded. Figure 6.1 may help to clarify these ideas.

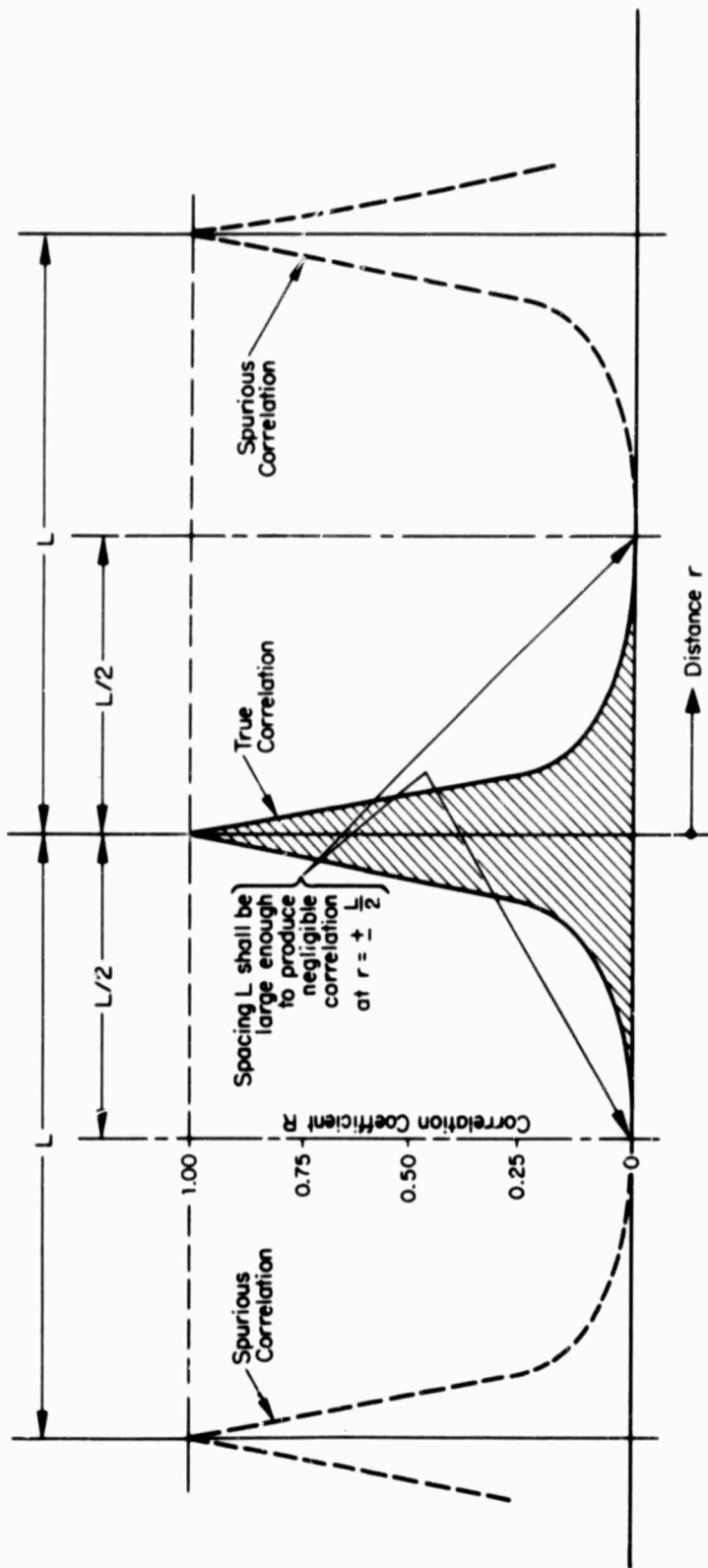


Fig. 6.1 True and Spurious Correlations Resulting From Blockwise Periodicity.

## 7. NUMERICAL REPRESENTATION OF AN ARBITRARY SCALAR FUNCTION OF POSITION

In this analysis we deal with scalar functions such as the velocity components  $u$ ,  $v$ ,  $w$ , and the pressure function  $\phi$ . Typically these quantities are continuous functions of the spatial coordinates  $x$ ,  $y$ ,  $z$  and of time  $t$ . Symbolically we may write, for example,

$$u = u(x,y,z,t) \quad (7-1)$$

Furthermore, the various partial derivatives of all orders exist and are continuous functions of space and time.

At any specified instant of time, however, the quantities of interest are functions of the space coordinates only. Thus

$$u = u(x,y,z) \quad (7-2)$$

Unfortunately, the functions of interest possess very intricate spatial distributions which fluctuate erratically with the passage of time. In principle, these functions may theoretically be approximated by Fourier series (or Fourier integrals). In practice, however, the number of terms required in the series is of the same order as the number of grid points in the block. It is easy to see that round-off errors, even if negligible on individual terms of the series, will accumulate when summed over the very large number of terms required in the whole series. This leads to excessive errors which vitiate the calculation. The plain fact is, therefore, that we do not have available any suitable analytical expressions for describing such intricate distributions in a way that is adequate for purposes of numerical analysis.

The problem, therefore, is to devise a numerical scheme for approximating the required functions to the requisite degree of accuracy. The scheme must also be flexible and efficient.

For this purpose we define a suitable gridwork of reference points uniformly distributed throughout the space in question. The values of the function are then specified for all points of the grid. In addition, a suitable three-dimensional interpolation rule is needed for estimating the value of the function at an arbitrary point lying anywhere in the space between the specified grid points. Since the function being approximated is single-valued everywhere, it is desirable that the interpolation rule adopted be definite and unambiguous. In other words, once the values of the function are specified at the reference grid points, the function should be uniquely determined over the entire space.

In the course of this research, several different schemes of differencing and interpolation have been conceived. Three of these methods are described in the succeeding sections of this report. They are discussed in order of increasing complication. However, the third (Method C) was actually developed first and used in the work to be discussed. It was only later that it was realized that the simple Method A could be made to yield precise results.

## 8. DIFFERENCING AND INTERPOLATION: METHOD A

Consider a cubical region of length  $L$  on a side. Let each side be subdivided into  $N$  equal intervals, thus defining a set of  $N^3$  cubical cells, each cell of length  $(L/N)$ , as illustrated in Fig. 8.1. Let these cells represent the control volumes for the finite-element analysis.

Each of the above control volumes has a definite centroidal point. The centroids of the control volumes constitute a cubical array of grid points. There are, of course,  $N^3$  grid points in all.

For purposes of the present discussion, let us choose an origin of coordinates as shown in Fig. 8.1. Then the coordinates of the centroidal points may be expressed in the form

$$x_i = (i - \frac{1}{2}) \frac{L}{N} \quad i = 1, 2, 3, \dots, N \quad (8-1)$$

$$y_j = (j - \frac{1}{2}) \frac{L}{N} - \frac{L}{2} \quad j = 1, 2, 3, \dots, N \quad (8-2)$$

$$z_k = (k - \frac{1}{2}) \frac{L}{N} \quad k = 1, 2, 3, \dots, N \quad (8-3)$$

We wish to describe, to within a suitable degree of approximation, the distribution, over the volume of the block, of an arbitrary scalar function of position, say  $u(x, y, z)$ .

The first part of the description consists of specifying the values of  $u = u(i, j, k)$  at each of the foregoing  $N^3$  grid points. So far as the immediate discussion is concerned, these  $N^3$  values may be regarded as arbitrary.

The second part of the description consists of a suitable interpolation rule for determining the value of the function at any point other than a centroidal grid point. For this purpose we define a second set of cubical cells which we may designate as interpolation spaces or cells.

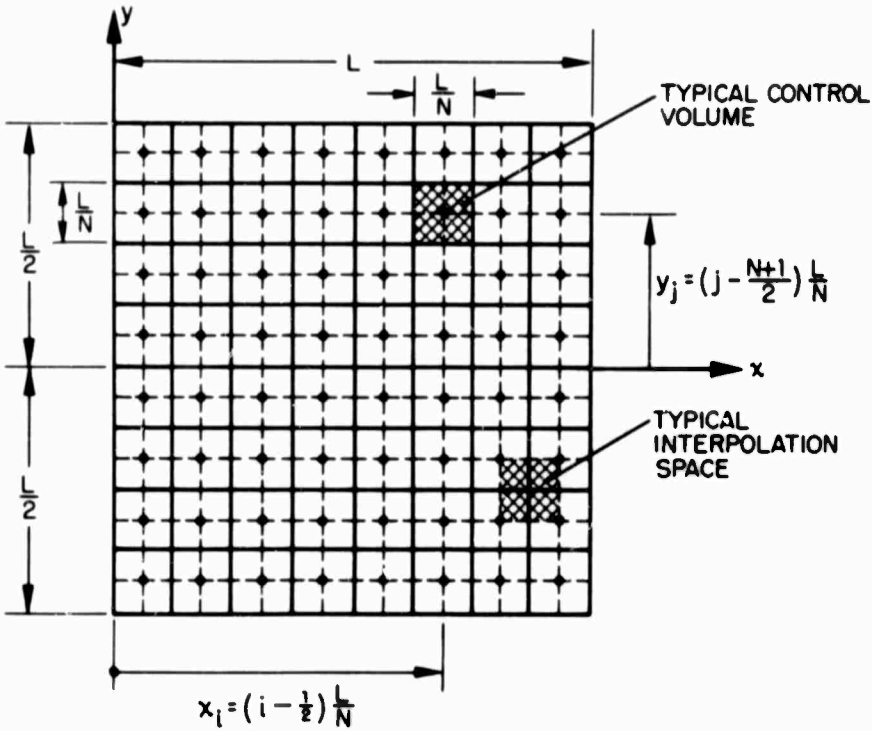


Fig. 8.1 Basic Grid for Differencing Method A.

An interpolation space is also a small cubical cell of length  $L/N$  on a side. However, it is displaced with respect to the control volumes. The previously defined grid points which are at the centroids of the control volumes lie at the corners of the interpolation spaces. It follows that the control volumes and the interpolation cells are mutually staggered relative to one another. Thus each octant of a control volume is in a different interpolation space. Conversely, each octant of an interpolation space lies in a different control volume.

Next, we adopt the rule that within each interpolation space, the variation of the function  $u$  shall be linear along every line parallel to one of the coordinate axes. This rule can be expressed in algebraic form.

For this purpose, it is convenient to introduce the following auxiliary notation. Let

$$\xi = \frac{N}{L} (x - x_1) \quad 0 \leq \xi \leq 1 \quad (8-4)$$

$$\eta = \frac{N}{L} (y - y_j) \quad 0 \leq \eta \leq 1 \quad (8-5)$$

$$\zeta = \frac{N}{L} (z - z_k) \quad 0 \leq \zeta \leq 1 \quad (8-6)$$

Thus the dimensionless coordinates  $\xi$ ,  $\eta$ ,  $\zeta$  may each vary over the range from zero to unity within any interpolation space.

Now the variation of  $u$  within any particular interpolation space may be expressed by the polynomial

$$u = A_0 + A_1 \xi + A_2 \eta + A_3 \zeta + A_4 \eta \zeta + A_5 \xi \zeta + A_6 \xi \eta + A_7 \xi \eta \zeta \quad (8-7)$$

The  $A$ 's are initially unknown constants whose values must be determined from the known values of  $u$  at the eight corners of the particular interpolation space in question. At these eight corners, each of the coordinates,  $\xi$ ,  $\eta$ ,  $\zeta$ , is either zero or unity. Hence the foregoing equation

can be written eight times, with the appropriate values of  $\xi$ ,  $\eta$ ,  $\zeta$ , and  $u$  substituted each time. The resulting set of eight simultaneous equations just suffices to determine the eight initially unknown constants. Because of the symmetry and the many zeros, the solution turns out to be quite simple.

Note that Eq. (8-7) does, in fact, satisfy the requirement that  $u$  shall vary linearly along any line parallel to any one of the coordinate axes. This is because the coordinates  $\xi$ ,  $\eta$ ,  $\zeta$  occur individually only to the zeroth or first powers. Furthermore, this equation contains all eight of the possible combinations of these factors, and is therefore the most general possible expression capable of satisfying this three-dimensional linearity rule.

Note that the interpolation spaces along the six surfaces of the block extend into the adjacent blocks. However, the variation within these spaces can be handled in much the same way as for the interior spaces. In this connection, it is convenient to take advantage of the assumed spacewise periodicity of the function  $u$  in the  $x$  and  $z$  directions. Thus

$$u(1 + N, j, k) = u(1, j, k) \quad (8-8)$$

$$u(1, j, k + N) = u(1, j, k) \quad (8-9)$$

There is also a periodicity in the  $y$  direction, but it is of a slightly more complicated kind. This matter is discussed elsewhere in this report. It suffices here to say that an appropriate periodicity rule is available for the  $y$  direction which makes the variation of  $u$  perfectly determinate also for the interpolation spaces along the top and bottom surfaces of the block.

The foregoing discussion shows that once the values of  $u(i,j,k)$  are arbitrarily specified at the  $N^3$  grid points, the above interpolation rule defines the function  $u(x,y,z)$  uniquely over the entire volume of the block.

This means, of course, that the distribution of  $v(x,y,z)$  is also uniquely determined over each of the six square surfaces which enclose each control volume. This fact is important, because the application of the fundamental mass and momentum conservation laws involves the evaluation of certain integrals over these bounding surfaces.

In addition, the determination of certain overall flow characteristics, such as the mean kinetic energy of turbulence, for example, involves the evaluation of corresponding volume integrals. Consequently, a unique rule for the variation of any function over the entire volume is necessary.

The six quadratic velocity products  $u^2$ ,  $v^2$ ,  $w^2$ ,  $vw$ ,  $wu$ ,  $uv$  play an important role in the analysis. In dealings with these products, the usual quasi-linear interpolation rule is taken to apply to the individual factors, rather than simply to the product itself. Hence the variation of the product between grid points is quadratic along lines parallel to the coordinate axes, rather than linear. While this complicates the calculations somewhat, it yields a higher level of consistency and accuracy than could otherwise be attained. In view of the basic importance of these products, which are associated with the Reynolds stresses, the added accuracy appears to be well worth the extra complications.

Since the entire spacewise distribution of any function is determined when the values are known at the  $N^3$  grid points, it follows that all pertinent surface and volume integrals must be ultimately expressible directly in terms of these grid values. When these relationships are expressed in explicit form, they constitute the "differencing formulas" appropriate to the task at hand.

## 9. DIFFERENCING AND INTERPOLATION: METHOD B

In this scheme, two distinct families of grid points are used, as shown in Fig. 9.1. It is convenient to designate these families by means of superscripts <sup>I</sup> and <sup>II</sup>, respectively.

Points of family I are defined by the coordinates

$$x_1^I = (1 - \frac{1}{2}) \frac{L}{N} \quad i = 1, 2, 3, \dots, N \quad (9-1)$$

$$y_j^I = (j - \frac{1}{2}) \frac{L}{N} - \frac{L}{2} \quad j = 1, 2, 3, \dots, N \quad (9-2)$$

$$z_k^I = (k - \frac{1}{2}) \frac{L}{N} \quad k = 1, 2, 3, \dots, N \quad (9-3)$$

Points of family II are defined by the coordinates

$$x_1^{II} = 1 \left( \frac{L}{N} \right) \quad i = 0, 1, 2, \dots, N \quad (9-4)$$

$$y_j^{II} = j \left( \frac{L}{N} \right) - \frac{L}{2} \quad j = 0, 1, 2, \dots, N \quad (9-5)$$

$$z_k^{II} = k \left( \frac{L}{N} \right) \quad k = 0, 1, 2, \dots, N \quad (9-6)$$

Note that the two grids are mutually staggered relative to each other by the distance of half a cell width,  $L/2N$ , with respect to each of the coordinate planes.

Corresponding to the two families of interlaced grid points, there are two families of interlaced control volumes. All control volumes are cubical cells of length  $(L/N)$  on a side. The grid points of family I are the centroids of the control volumes of the first family. Likewise, the grid points of family II are the centroids of the control volumes of the second family. Furthermore, the grid points of family II lie at the corners of the control volumes of family I. Similarly, the grid points of family I lie at the corners of the control volumes of family II.

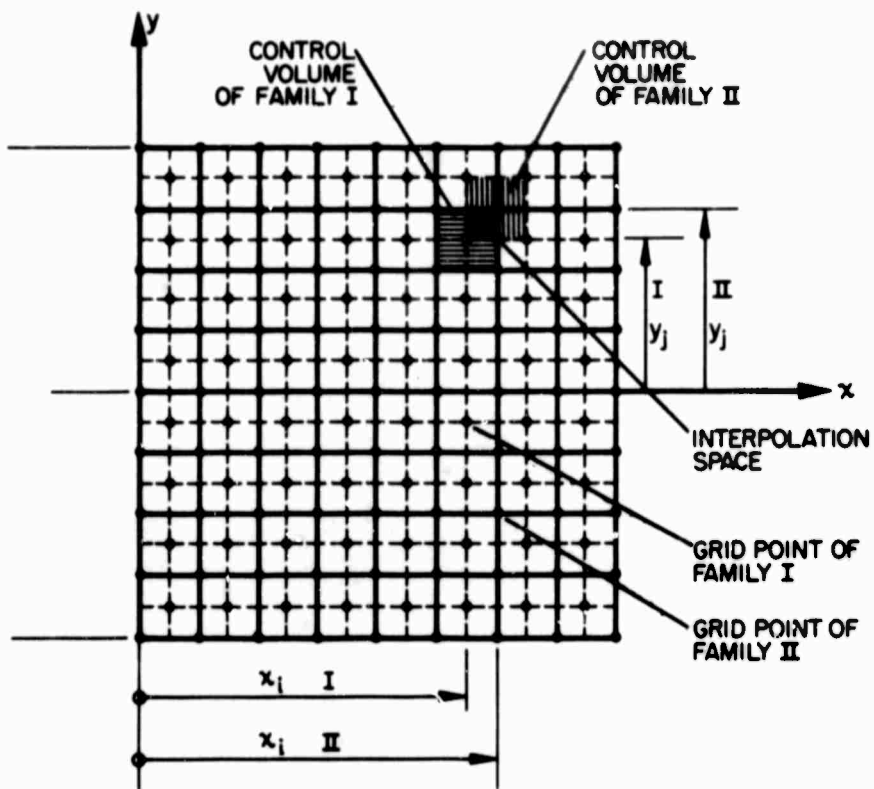


Fig. 9.1 Basic Grid for Differencing Method B.

These various relations are inherently three-dimensional and are not easy to portray adequately in two-dimensional diagrams. Nevertheless, Figs. 9.1 and 9.2 may be of some help in visualizing the essential facts.

Note that the overall volume of the cubical block under study is represented twice in this scheme: once by the control volumes of family I, and once by the control volumes of family II. There is a mutual overlapping of the individual control volumes. Thus the individual octants of a single cell of family I lie within eight separate cells of family II. Conversely, the individual octants of a cell of family II lie within eight separate cells of family I.

Consider any one such octant as shown, for example, in Fig. 9.2. It is itself a cube of length  $(L/2N)$  on a side. One corner of this cube is always a grid point of family I. The diagonally opposite corner is always a grid point of family II. We define each distinct octant as a distinct interpolation space. There are therefore  $8N^3$  distinct interpolation spaces within the block.

We note for comparison that Method A involves only  $N^3$  distinct interpolation spaces. This does not imply, however, that Method B involves an eightfold improvement in resolution. The reason is that the interpolation spaces of Method A are "complete" in the sense that all eight of their corners are principal grid points. The interpolation spaces of Method B are initially "incomplete" in the sense that only two of the eight corners are principal grid points. To "complete" these spaces, we must define the values of the unknown function at the other six corners of each space.

Fortunately, each of these six corners is itself a midpoint between two principal grid points. Hence using linear interpolation consistently throughout, we may assign a value at each of these six points. The assigned value is always the simple arithmetic mean of the known values at the two corresponding principal grid points involved. Thus, for example, in Fig. 9.2 the value at point QII is the mean of the values at

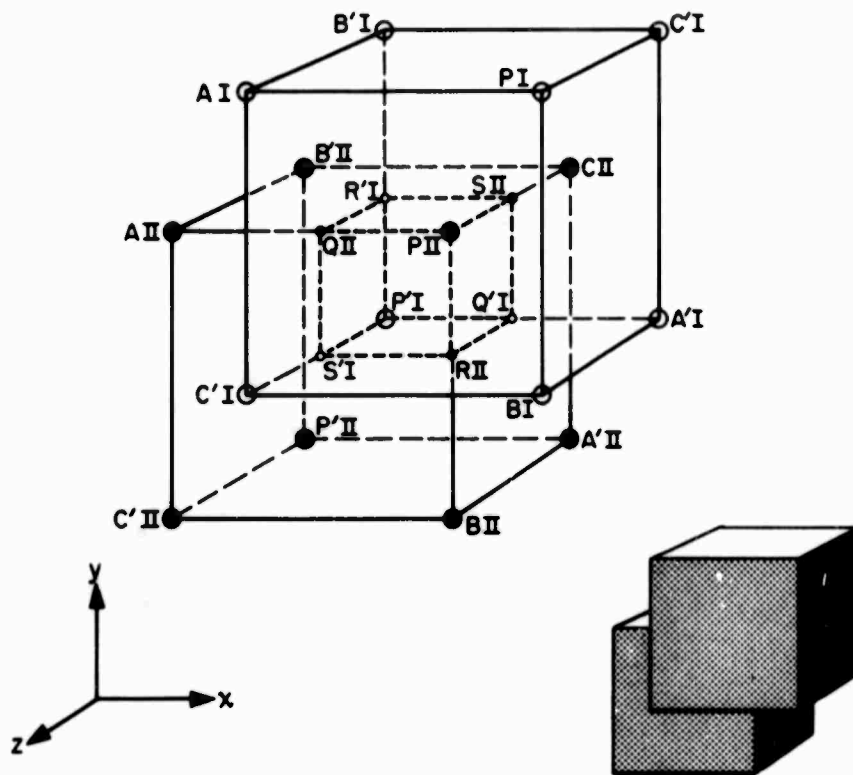


Fig. 9.2 Grid Point Relationships for Differencing Method B.

points PII and AII. Similarly, the value at point Q'I is the mean of the values at points P'I and A'I. Note that three of the interpolated values are derived from values at grid points of family I, the other three from grid points of family II. Thus both families are represented exactly equally and symmetrically within each interpolation space.

With the eight corner values defined, we can once more write the variation over the volume and/or surfaces of the interpolation space in the form

$$u = A_0 + A_1\xi + A_2\eta + A_3\zeta + A_4\eta\xi + A_5\zeta\xi + A_6\xi\eta + A_7\xi\zeta \quad (9-7)$$

where, for example,

$$\xi = (x - x_1) \frac{2N}{L} \quad 0 \leq \xi \leq 1 \quad (9-8)$$

$$\eta = (y - y_j) \frac{2N}{L} \quad 0 \leq \eta \leq 1 \quad (9-9)$$

$$\zeta = (z - z_k) \frac{2N}{L} \quad 0 \leq \zeta \leq 1 \quad (9-10)$$

and where the point at the "inner" corner  $x_1, y_j, z_k$  may be of either family, depending on the particular interpolation space being considered.

It is apparent that the foregoing definitions suffice to determine uniquely the complete spacewise distribution of any scalar function  $u(x, y, z)$  in terms of the assigned values at the  $2N^3$  principal grid points. Consequently all surface and volume integrals over the control cells can be uniquely expressed in terms of the appropriate grid point values. Hence the method leads to specific "differencing formulas" for such quantities as partial derivatives, gradients, divergences, etc.

## 10. DIFFERENCING AND INTERPOLATION: METHOD C

The differencing scheme described under this heading is merely an earlier and somewhat less fully developed version of the staggered scheme described as Method B. It is important however, because the currently available computer program, TURBOCODE MARK V, is based on this system.

Method C uses the two families of grid points and control volumes described previously. The interpolation spaces and interpolation rules are defined differently, however. In fact the interpolation spaces in this scheme are taken as identical with the respective control volumes themselves; there are therefore two distinct and overlapping sets of interpolation spaces.

Thus within the volume and along the surfaces of any cell of family I, the variation of any scalar function  $u(x,y,z)$  is assumed to follow the rule

$$u^I = A_0^I + A_1^I \xi + A_2^I \eta + A_3^I \zeta + A_4^I \eta \zeta + A_5^I \zeta \xi + A_6^I \xi \eta + A_7^I \xi \eta \zeta + A_8^I (1-\xi^2)(1-\eta^2)(1-\zeta^2) \quad (10-1)$$

where

$$\xi = (x-x_1^I) \frac{2N}{L} \quad -1 \leq \xi \leq +1 \quad (10-2)$$

$$\eta = (y-y_j^I) \frac{2N}{L} \quad -1 \leq \eta \leq +1 \quad (10-3)$$

$$\zeta = (z-z_k^I) \frac{2N}{L} \quad -1 \leq \zeta \leq +1 \quad (10-4)$$

Similarly for any cell of family II, the corresponding rule is

$$\begin{aligned}
U^{II} = & A_0^{II} + A_1^{II}\xi + A_2^{II}\eta + A_3^{II}\zeta + A_4^{II}\eta\zeta + A_5^{II}\xi\zeta + A_6^{II}\xi\eta \\
& + A_7^{II}\xi\eta\zeta + A_8^{II}(1-\xi^2)(1-\eta^2)(1-\zeta^2)
\end{aligned} \tag{10-5}$$

where

$$\xi = (x - x_1^{II}) \frac{2N}{L} \quad -1 \leq \xi \leq +1 \tag{10-6}$$

$$\eta = (y - y_j^{II}) \frac{2N}{L} \quad -1 \leq \eta \leq +1 \tag{10-7}$$

$$\zeta = (z - z_k^{II}) \frac{2N}{L} \quad -1 \leq \zeta \leq +1 \tag{10-8}$$

There are a number of critical observations to be made about this scheme.

Note first that any given arbitrary point in the field is simultaneously in two different interpolation spaces. Two distinct interpolation formulas apply which do not, in general, agree exactly. Such an ambiguity is not desirable, although it may be argued that the discrepancies involved are small quantities of higher order, and hence relatively unimportant. However, the existence of two distinct rules makes it necessary to compute certain volume integrals twice, thus increasing the corresponding computation times in an undesirable way.

Note secondly that the interpolation polynomial contains not eight but nine constants. These are determined by matching the known values at the eight corners of the cell and the ninth known value at the centroid.

It may be seen that the last term of the interpolation expression, unlike the others, is quadratic rather than linear in the coordinates. The presence of this term markedly complicates the computation of volume integrals for the cell. This is especially true in connection with the volume integration of quadratic terms like  $u^2$ ,  $uv$ , etc. The linear terms among themselves have certain properties of symmetry and orthogonality which tend to simplify the resulting expressions. The

characteristics of the quadratic term are more complex, and introduce various additional terms into the final results.

Fortunately, the quadratic term has been so devised that it vanishes at all six of the bounding surfaces of the cells. Consequently it does not enter into the evaluation of any of the surface integrals.

As compared with Method B, it would seem that Method C does not intermesh the data of the two families as closely and completely as might be desirable. Thus in Method B, four of the data points in each interpolation space are of one family and four are of the other family. In Method C, on the other hand, eight of the data points are always of one family, and only one is of the opposite family; furthermore, the influence of even this one point of the opposite family vanishes along the bounding surfaces of the cell.

Fortunately, Method C does possess some compensating computational advantages. For one thing, the distribution of any function  $u(x,y,z)$  over any bounding surface is expressed solely in terms of the grid values at the four corners of that surface. While this assumption does not fully utilize all of the information actually available, it does, of course, shorten and simplify the evaluation of all surface integrals.

## 11. COMPARISON OF DIFFERENCING METHODS

In the course of the present research there has been a steady improvement in the conceptual basis for the numerical differencing techniques employed. At first the equations to be solved were regarded simply as partial differential equations. The numerical techniques at this stage consisted mainly of replacement of infinitesimals by small but finite differences, with a largely intuitive approach.

It was soon realized, however, that much better accuracy and computational stability could be achieved for a given mesh size by adoption of a finite-element approach. An essential point is that the small but finite control volumes are not treated as mere infinitesimals. Accuracy is greatly improved by estimation of mass and momentum fluxes not merely from approximate local point values but as true surface integrals, in accordance with the previous carefully established interpolation rules.

It was at about this stage that the interpolation method C was formulated and successfully applied in the program TURBOCODE MARK V. When first formulated, it represented a considerable advance in numerical technique.

Further theoretical progress since that time makes it clear that certain revisions of that scheme are desirable. These are described under Method B.

However, the same concepts that lead to the above revision, when followed to their logical conclusions, lead even further and so to Method A.

The main advantage of Method A lies in its relative simplicity. It avoids the complexities of dealing with two distinct families of points. It avoids the duplication of covering the same overall volume with two distinct families of control cells. The application of the proper boundary conditions should be correspondingly simplified. It

seems that the programming can be simplified and computation times reduced by adoption of this scheme.

It is intended that Method A will ultimately be programmed for the computer. Meanwhile, however, the present program based on Method C represents investment of a considerable research effort. It is believed that this program, which has only recently been developed into a practicable form, is capable of generating much useful basic information. Hence the immediate effort will be to obtain this information with the existing program, and to study and evaluate it, before proceeding with any major revision of the computer program.

## 12. INITIAL NUMBER OF DEGREES OF FREEDOM

In this discussion, let  $G$  represent the number of grid points in one block. For differencing method A,  $G$  equals  $N^3$ ; for differencing methods B and C,  $G$  equals  $2N^3$ .

At the initial instant of time, the velocity vector distribution over the cubical block is fixed when the distributions of the three individual scalar components,  $u$ ,  $v$ ,  $w$ , are fixed. But if we are to establish the initial distribution of  $u$ , values must be specified at all  $G$  grid points. Similarly for  $v$  and  $w$ . Hence  $3G$  values are required to describe the initial velocity field.

However, if the fluid is incompressible, not all of these  $3G$  values may be specified independently. In fact, we must satisfy a mass conservation condition or continuity law for each one of the  $G$  control volumes centered at each grid point. Hence there are  $G$  constraint conditions to be satisfied among the  $3G$  velocity components. Consequently, only  $2G$  of these quantities may be independently prescribed. We say that there are  $2G$  initial degrees of freedom.

For example, if the  $u$  and  $v$  components are arbitrarily specified at all grid points, the  $w$  components are then fixed by the foregoing continuity conditions. If the distributions were not blockwise periodic, continuity constraints would determine  $w$  only to within an arbitrary additive function of  $x$  and  $y$  alone. However, the assumption of periodicity eliminates this arbitrary element and renders the solution for  $w$  unique.

The initial values of the pressures do not count as initial degrees of freedom. The reason is that once the velocities are specified, the pressures are also determined thereby. The pressures cannot be assigned independently.

It follows that for differencing method A, there are  $2N^3$  initial degrees of freedom; for differencing methods B and C, there are  $4N^3$  initial degrees of freedom.

However, the apparent arbitrariness of the 2G initial degrees of freedom requires qualification, as it can be somewhat misleading. This enormous degree of latitude is permissible only because, at the initial instant, the turbulence has not yet attained its ultimate stationary and homogeneous statistical structure. Once this state is reached, it will impose certain corresponding relations of statistical correlation, and thereby reduce the number of arbitrary or random degrees of freedom remaining. Nevertheless, turbulence necessarily involves some irreducible core of randomness, and hence there will always be some large residual number of arbitrary or random degrees of freedom. If we knew what the essential constraints were, it might be useful to impose them at the outset, much as we have done with regard to the continuity condition. But we do not know them, at least not initially, so the matter is academic. It is rather lucky that the calculation can proceed from such arbitrary initial conditions. The reason this is allowable is that the turbulent structure has an inherent self-correcting character which drives it asymptotically toward a limit which is essentially independent of the initial conditions.

The persistence through space and time of the net overall influence of the deterministic equations of motion, in addition to that of the continuity equation, is what imparts to the turbulent field its underlying orderly structure, upon which are superimposed phenomena of a more random character. One method of expressing the orderly structure is in terms of the correlation coefficient  $R$  defined in an earlier section. Let us here apply this concept to a simple grid of type A, with  $N^3$  grid points. In the present context, the appropriate definition of correlation coefficient is in the form of the matrix:

$$R(p,q,r,\tau) = \frac{1}{N^3} \sum_{i=1}^N \sum_{j=1}^N \sum_{k=1}^N \frac{1}{T} \int_0^T u(i,j,k,t) \cdot u(i+p,j+q,k+r,t+\tau) dt \quad (12-1)$$

where  $\begin{matrix} p) \\ q) \\ r) \end{matrix} = 0, 1, 2, 3, \dots, (N-1)$  (12-2)

Since each of the indices  $p, q, r$  varies over  $N$  distinct values, the expression (12-1) defines  $N^3$  separate equations. These equations fix the values of the  $N^3$  elements of the correlation matrix  $R(p, q, r, \tau)$ . Each element is a function of the time parameter  $\tau$ . This matrix of functions provides a reasonably adequate description of the orderly structure of the turbulent field. Ultimately, the matrix functions can be calculated from the computer simulation results.

Now consider the special case  $\tau = 0$  which establishes all spacewise correlations at any fixed time. The  $N^3$  elements of the matrix  $R$  are now fixed constants. Suppose these  $N^3$  values are known or assumed, and are imposed as essential initial conditions. This additional constraint reduces the initial number of degrees of freedom from  $2N^3$  to  $N^3$ . Presumably, the remaining  $N^3$  degrees of freedom may now be selected at random from some suitable probability distribution without appreciably affecting the structure of the turbulence.

### 13. PARTIAL DERIVATIVES IN TERMS OF SURFACE INTEGRALS

In dealing with functions of position, we usually need to estimate not only the values of the function itself, but also values of its various partial derivatives. Now a direct analytical differentiation of the approximate quasi-linear distribution as defined by any of the foregoing methods, A, B or C, is not adequate for this purpose. The reason is that such an approximate distribution is only piecewise continuous. Estimates of first-order derivatives obtained by direct differentiation of this approximation would be discontinuous; estimates of higher order derivatives would be indeterminate. This accords with the well known fact that the derivatives of an approximating function tend to be less accurate and well behaved than the approximating function itself. On the other hand, integrals of an approximating function tend to be more accurate and well behaved than the approximating function itself. Fortunately, it turns out to be possible to express the derivatives of a function in terms of certain surface integrals, as explained below. Estimation of derivatives by this method of integration avoids the rapid deterioration of accuracy associated with direct analytical differentiation; consequently, the integration method is always used in our work.

With the integral method explained below, derivatives are calculated at all principal grid points; derivative values between grid points are then estimated, as usual, by quasi-linear interpolation. This process may be repeated as often as necessary to obtain estimates of the higher order derivatives.

In the calculus of vectors, the gradient of a scalar function at a point is defined as the resultant of a certain limiting process. First, a small volume element  $\delta v$  is defined whose surface  $\delta S$  encloses a point in question. See Fig. 13.1. Secondly, an average value of the gradient within the small enclosed volume is defined. This definition involves

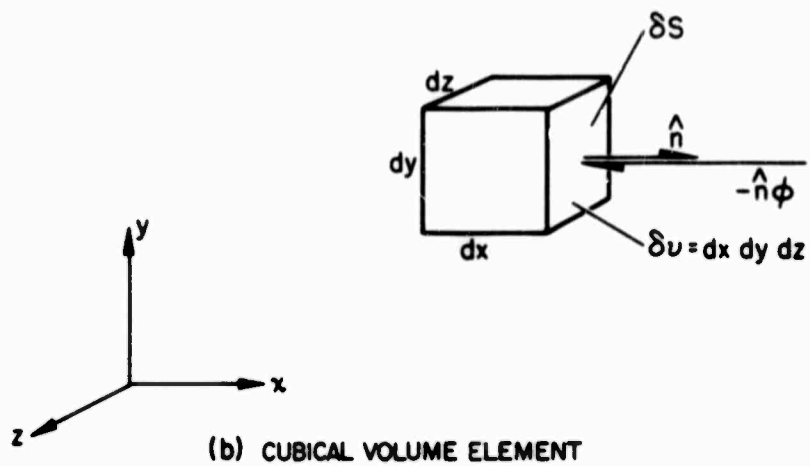
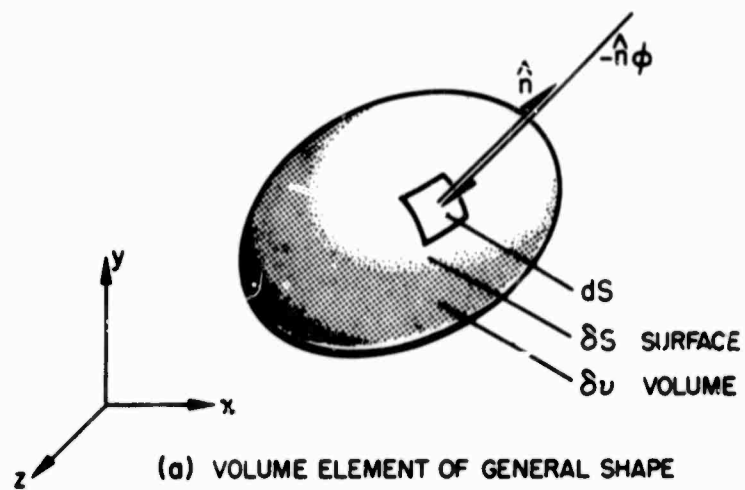


Fig. 13.1 Volume Elements for Definition of Partial Derivatives.

the evaluation of a certain integral over the bounding surface of the element. Finally, the volume of the element is allowed to shrink to zero. The resulting limit of the average gradient is defined as the local gradient at the point.

This rather complicated definition may be written symbolically in the form

$$\nabla\varphi = \lim_{\delta V \rightarrow 0} \frac{1}{\delta V} \int_{\delta S} \hat{n} dS \quad (13-1)$$

where  $dS$  is an infinitesimal surface element on the bounding surface  $\delta S$ , while  $\hat{n}$  is an outward unit vector normal to area  $dS$ .

Inasmuch as the gradient is expressible in terms of partial derivatives in the form

$$\nabla\varphi = \hat{i} \left( \frac{\partial\varphi}{\partial x} \right) + \hat{j} \left( \frac{\partial\varphi}{\partial y} \right) + \hat{k} \left( \frac{\partial\varphi}{\partial z} \right) \quad (13-2)$$

it follows that the partial derivatives of  $\varphi$  are also definable in terms of surface integrals, that is,

$$\left( \frac{\partial\varphi}{\partial x} \right) = \hat{i} \cdot \nabla\varphi = \lim_{\delta V \rightarrow 0} \left\{ \frac{1}{\delta V} \int_{\delta S} \hat{i} \cdot \hat{n} dS \right\} \quad (13-3)$$

$$\left( \frac{\partial\varphi}{\partial y} \right) = \hat{j} \cdot \nabla\varphi = \lim_{\delta V \rightarrow 0} \left\{ \frac{1}{\delta V} \int_{\delta S} \hat{j} \cdot \hat{n} dS \right\} \quad (13-4)$$

$$\left( \frac{\partial\varphi}{\partial z} \right) = \hat{k} \cdot \nabla\varphi = \lim_{\delta V \rightarrow 0} \left\{ \frac{1}{\delta V} \int_{\delta S} \hat{k} \cdot \hat{n} dS \right\} \quad (13-5)$$

Likewise, the divergence of a vector function  $u$  may be written

$$\nabla \cdot u = \lim_{\delta V \rightarrow 0} \left\{ \frac{1}{\delta V} \int_{\delta S} \hat{n} \cdot \hat{u} dS \right\} \quad (13-6)$$

However, in work with numerical approximations of the present type in which the functions involved are specified only at discrete grid points, and the variation between these points is merely estimated by a kind of three-dimensional quasi-linear interpolation, the above process of going to the limit of zero volume cannot be accomplished with sufficient accuracy. As mentioned above, the previously described interpolation schemes do not in themselves provide sufficient continuity in the representation of the function to define accurate local values of derivatives at a specified point by direct differentiation.

Suppose, however, that we omit the above limiting process. Instead we choose small but finite cubical elements as established by the finite spacing of the basic grid points. Now the quasi-linear interpolation scheme permits us to evaluate the various surface integrals required in the above definitions with excellent precision. Hence we may calculate very accurate average values of gradient, partial derivative, velocity divergence, etc., over the volume element as a whole.

In some instances, average values over the element are all that we require. Thus in dealings with incompressible flows, an exact solution would theoretically require that the velocity divergence vanish at all points of the field, not just at the basic grid points. This ideal is, of course, neither attainable nor really necessary. For a practical numerical solution it is quite sufficient to require that the average divergence vanish for each of the small cubical cells into which the field is divided. Thus in Method A, for example, for an overall cubical region or block of length  $L$  along each edge, with a basic grid spacing of dimension  $(L/N)$ , there are  $N^3$  individual volume elements involved, each a cube of length  $(L/N)$  on a side. Hence the non-divergence requirement for the field boils down to requiring that the average divergence vanish for each of these  $N^3$  distinct volume elements.

In some cases, however, the concept of an average value over the volume does not suffice. What is required is a method of establishing local point values at the basic grid points, so that a complete spatial

distribution of the quantity may be estimated by means of the quasi-linear interpolation method previously mentioned. For example, in applying the momentum integral equations to volume elements, we establish accurate average time rates of change of the velocities over these volumes. This is not really sufficient. What is needed, of course, are local values at the basic grid points themselves.

To meet this requirement, we introduce one additional postulate, namely, that the average value of a quantity over a given volume element constitutes the best available estimate of its local value at the centroid of that element. Because of this postulate, it is of course necessary to establish the pattern of control volumes and grid points in such a way that the grid points are in fact located at the centroids of the control volumes. When this is done, the formulas of this section may readily be applied to calculate the values of divergence, gradient and partial derivatives at all the grid points.

The results obtained in this way will depend on the particular differencing and interpolation scheme adopted, such as the methods A, B or C described elsewhere in this report. Detailed results for differencing method C are presented in Appendix A.

The following results are presented as typical examples of specific differencing formulas which are obtainable by use of the foregoing methods. We show the typical partial derivative  $(\frac{\partial \phi}{\partial x})$  as defined by each of the differencing techniques A, B and C explained earlier. Other partial derivatives can also be found merely by systematic permutation of indices in the following formulas.

Method A

$$\begin{aligned}
 \frac{\partial}{\partial x} [\varphi(i, j, k)] &= \left(\frac{N}{L}\right) \left\{ \frac{2}{32} [\varphi(i+1, j, k) - \varphi(i-1, j, k)] \right. \\
 &+ \frac{3}{64} [\varphi(i+1, j, k-1) + \varphi(i+1, j-1, k) + \varphi(i+1, j+1, k) + \varphi(i+1, j, k+1) \\
 &\quad - \varphi(i-1, j, k-1) - \varphi(i-1, j-1, k) - \varphi(i-1, j+1, k) - \varphi(i-1, j, k+1)] \\
 &+ \frac{1}{128} [\varphi(i+1, j-1, k-1) + \varphi(i+1, j+1, k-1) + \varphi(i+1, j-1, k+1) + \varphi(i+1, j+1, k+1) \\
 &\quad \left. - \varphi(i-1, j-1, k-1) - \varphi(i-1, j+1, k-1) - \varphi(i-1, j-1, k+1) - \varphi(i-1, j+1, k+1)] \right\}
 \end{aligned} \tag{13-7}$$

Method B

$$\begin{aligned}
 \frac{\partial}{\partial x} [\varphi^I(i, j, k)] &= \left(\frac{N}{L}\right) \left\{ \frac{1}{8} [\varphi^I(i+1, j, k) - \varphi^I(i-1, j, k)] \right. \\
 &+ \frac{3}{16} [\varphi^{II}(i, j, k) + \varphi^{II}(i, j-1, k) + \varphi^{II}(i, j, k-1) + \varphi^{II}(i, j-1, k-1) \\
 &\quad \left. - \varphi^{II}(i-1, j, k) - \varphi^{II}(i-1, j-1, k) - \varphi^{II}(i-1, j, k-1) - \varphi^{II}(i-1, j-1, k-1)] \right\}
 \end{aligned} \tag{13-8}$$

$$\begin{aligned}
 \frac{\partial}{\partial x} [\varphi^{II}(i, j, k)] &= \left(\frac{N}{L}\right) \left\{ \frac{1}{8} [\varphi^{II}(i+1, j, k) - \varphi^{II}(i-1, j, k)] \right. \\
 &+ \frac{3}{16} [\varphi^I(i+1, j+1, k+1) + \varphi^I(i+1, j, k+1) + \varphi^I(i+1, j+1, k) + \varphi^I(i+1, j, k) \\
 &\quad \left. - \varphi^I(i, j+1, k+1) - \varphi^I(i, j, k+1) - \varphi^I(i, j+1, k) - \varphi^I(i, j, k)] \right\}
 \end{aligned} \tag{13-9}$$

Method C

$$\begin{aligned} \frac{\partial}{\partial x} [\varphi^I(i, j, k)] = \\ \left(\frac{N}{4L}\right) \{ \varphi^{II}(i, j, k) + \varphi^{II}(i, j-1, k) + \varphi^{II}(i, j, k-1) + \varphi^{II}(i, j-1, k-1) \\ - \varphi^{II}(i-1, j, k) - \varphi^{II}(i-1, j-1, k) - \varphi^{II}(i-1, j, k-1) - \varphi^{II}(i-1, j-1, k-1) \} \end{aligned} \quad (13-10)$$

$$\begin{aligned} \frac{\partial}{\partial x} [\varphi^{II}(i, j, k)] = \\ \left(\frac{N}{4L}\right) \{ \varphi^I(i+1, j+1, k+1) + \varphi^I(i+1, j, k+1) + \varphi^I(i+1, j+1, k) + \varphi^I(i+1, j, k) \\ - \varphi^I(i, j+1, k+1) - \varphi^I(i, j, k+1) - \varphi^I(i, j+1, k) - \varphi^I(i, j, k) \} \end{aligned} \quad (13-11)$$

It is also of interest to consider a simple differencing formula such as might have been used in the absence of the finite-element principles expounded in this report. Thus, for a simple grid of the same type as used in Method A, we might have simply written, by inspection,

$$\frac{\partial}{\partial x} [\varphi(i, j, k)] = \left(\frac{N}{2L}\right) \{ \varphi(i+1, j, k) - \varphi(i-1, j, k) \} \quad (13-12)$$

The relative crudeness of this approximation becomes quite apparent when this expression is compared with the previous differencing formulas.

#### 14. CONTINUITY EQUATION

Let  $\hat{U}$  represent the mean-flow velocity vector, and  $\hat{u}$  the turbulent perturbation. We apply the law of conservation of mass to a small but finite control cell of volume  $\delta v$  and surface  $\delta S$ . Let  $\hat{n}$  be the outward normal unit vector at surface element  $dS$ . For the combined mean flow plus turbulence, this gives

$$\nabla \cdot (\hat{U} + \hat{u}) = \frac{1}{\delta v} \int_{\delta S} (\hat{U} + \hat{u}) \cdot \hat{n} dS = 0 \quad (14-1)$$

For reasons explained earlier, we have omitted the process of going to the limit of zero volume.

By averaging this equation over time (or over a statistical ensemble of macroscopically similar cases), we find that the mean flow itself must satisfy the following mass-conservation requirement, namely,

$$\nabla \cdot \hat{U} = \frac{1}{\delta v} \int_{\delta S} \hat{U} \cdot \hat{n} dS = 0 \quad (14-2)$$

Subtracting (14-2) from (14-1) gives the net mass-conservation relation for the turbulence itself, that is,

$$\nabla \cdot \hat{u} = D = \frac{1}{\delta v} \int_{\delta S} \hat{u} \cdot \hat{n} dS = 0 \quad (14-3)$$

The integral in (14-3) is evaluated over the surface of the element. But for the cubical control volumes here considered, the surface consists of six squares, each of area  $\delta S$ . Let the individual surfaces be represented by the index  $k=1,2,3,4,5,6$ . Note that area  $\delta S = (\frac{L}{N})^2$  and volume  $\delta v = (\frac{L}{N})^3$ . Therefore Eq. (14-3) may be reduced to the form

$$D = \left(\frac{N}{L}\right) \sum_{k=1}^6 \left\{ \frac{1}{\delta S} \int_{\delta S} \hat{u} \cdot \hat{n} dS \right\}_k = 0 \quad (14-4)$$

The quantity enclosed within braces represents the average mass flow per unit area through the kth bounding surface.

## 15. MOMENTUM EQUATION

We apply the momentum theorem of fluid flow to the same small but finite Eulerian control cell used in the previous section. The following nomenclature is used to denote the various forces per unit area (and per unit mass) acting on the differential surface element  $dS$ , namely,

$$\begin{aligned}\hat{F}_n &= \text{mean viscous force} \\ \hat{f}_n &= \text{turbulent viscous force} \\ \hat{\phi} &= \text{mean pressure} \\ \hat{\varphi} &= \text{turbulent pressure}\end{aligned}$$

For the combined mean flow plus turbulence, we obtain the equation

$$\begin{aligned}\frac{1}{\delta V} \int \frac{\partial}{\partial t} (\hat{U} + \hat{u}) dV &= - \frac{1}{\delta V} \int_{\delta S} (\hat{U} + \hat{u})(\hat{U} + \hat{u}) \cdot n dS \\ &+ \frac{1}{\delta V} \int_{\delta S} (\hat{F}_n + \hat{f}_n) dS - \frac{1}{\delta V} \int_{\delta S} (\hat{\phi} + \hat{\varphi}) n dS\end{aligned}\tag{15-1}$$

For the particular case of the simple uniform shear flow mainly considered in this report, the following simplifications apply to Eq. (15-1), namely,

$$\left( \frac{\partial \hat{U}}{\partial t} \right) = 0 \tag{15-2}$$

$$\int_{\delta S} \hat{\phi} n dS = 0 \tag{15-3}$$

$$\int_{\delta S} \hat{F}_n dS = 0 \tag{15-4}$$

$$U = \hat{i} \gamma \quad (15-5)$$

$$\int_{\delta S} \hat{U} \hat{U} \cdot \hat{n} dS = 0 \quad (15-6)$$

Furthermore, the turbulent viscous forces  $\hat{f}_n$  may be expressed specifically as  $\hat{f}_x$ ,  $\hat{f}_y$ ,  $\hat{f}_z$ , namely, the forces on faces normal to the x,y,z axes respectively. These, in turn may be written in the form

$$\hat{f}_x = \hat{i} \left( \frac{\tau_{xx}}{\rho} \right) + \hat{j} \left( \frac{\tau_{xy}}{\rho} \right) + \hat{k} \left( \frac{\tau_{xz}}{\rho} \right) \quad (15-7)$$

$$\hat{f}_y = \hat{i} \left( \frac{\tau_{yx}}{\rho} \right) + \hat{j} \left( \frac{\tau_{yy}}{\rho} \right) + \hat{k} \left( \frac{\tau_{yz}}{\rho} \right) \quad (15-8)$$

$$\hat{f}_z = \hat{i} \left( \frac{\tau_{zx}}{\rho} \right) + \hat{j} \left( \frac{\tau_{zy}}{\rho} \right) + \hat{k} \left( \frac{\tau_{zz}}{\rho} \right) \quad (15-9)$$

The viscous stresses themselves can be expressed in terms of velocity derivatives. For an incompressible fluid of constant viscosity

$$\left( \frac{\tau_{xx}}{\rho} \right) = \nu \nabla^2 \left( \frac{\partial u}{\partial x} \right) \quad (15-10) \quad \left( \frac{\tau_{yz}}{\rho} \right) = \left( \frac{\tau_{zy}}{\rho} \right) = \nu \left( \frac{\partial w}{\partial y} + \frac{\partial v}{\partial z} \right) \quad (15-13)$$

$$\left( \frac{\tau_{yy}}{\rho} \right) = \nu \nabla^2 \left( \frac{\partial v}{\partial y} \right) \quad (15-11) \quad \left( \frac{\tau_{zx}}{\rho} \right) = \left( \frac{\tau_{xz}}{\rho} \right) = \nu \left( \frac{\partial u}{\partial z} + \frac{\partial w}{\partial x} \right) \quad (15-14)$$

$$\left( \frac{\tau_{zz}}{\rho} \right) = \nu \nabla^2 \left( \frac{\partial w}{\partial z} \right) \quad (15-12) \quad \left( \frac{\tau_{xy}}{\rho} \right) = \left( \frac{\tau_{yx}}{\rho} \right) = \nu \left( \frac{\partial v}{\partial x} + \frac{\partial u}{\partial y} \right) \quad (15-15)$$

Of course, the various partial derivatives shown here must be expressed in terms of appropriate surface integrals, as explained earlier.

With the various conditions listed from (15-2) through (15-15) incorporated or implied, the basic momentum equation (15-1) is reducible to the form

$$\begin{aligned}
\frac{1}{\delta v} \int_{\delta v} \left( \frac{\partial \hat{u}}{\partial t} \right) dv = & - \Omega \frac{1}{\delta v} \int_{\delta S} y(\hat{i}\hat{u} + \hat{u}\hat{i}) \cdot \hat{n} dS - \frac{1}{\delta v} \int_{\delta S} \hat{u}\hat{u} \cdot \hat{n} dS \\
& + \frac{1}{\delta v} \int_{\delta S} \hat{f}_n dS - \frac{1}{\delta v} \int_{\delta S} \hat{c} n dS
\end{aligned} \tag{15-16}$$

This is the basic result required, although it is still in a somewhat unwieldy form. It is convenient to introduce some auxiliary notation as follows. Let

$$\frac{1}{\delta v} \int_{\delta v} \left( \frac{\partial \hat{u}}{\partial t} \right) dv = \left( \frac{\partial \hat{u}}{\partial t} \right) = \hat{u}_t \tag{15-17}$$

where  $\hat{u}_t$  is the mean time rate of change of  $\hat{u}$  over the volume  $\delta v$ , and is taken as the best available estimate of the local point value at the centroid of the element.

Let the remaining integrals be evaluated first over the six individual square bounding surfaces,  $k=1,2,3,4,5,6$ . Thus, let

$$\hat{S}_k = - \Omega \left\{ \frac{1}{\delta S} \int_{\delta S} y(\hat{i}\hat{u} + \hat{u}\hat{i}) \cdot \hat{n} dS \right\}_k \tag{15-18}$$

$$\hat{T}_k = - \left\{ \frac{1}{\delta S} \int_{\delta S} \hat{u}\hat{u} \cdot \hat{n} dS \right\}_k \tag{15-19}$$

$$\hat{H}_k = \left\{ \frac{1}{\delta S} \int_{\delta S} \hat{f}_n dS \right\}_k \tag{15-20}$$

$$\hat{P}_k = - \left\{ \frac{1}{\delta S} \int_{\delta S} \hat{c} n dS \right\}_k \tag{15-21}$$

Furthermore, let us introduce the abbreviation

$$\hat{R}_k = \hat{S}_k + \hat{T}_k + \hat{H}_k \quad (15-22)$$

With this notation, the basic momentum equation (15-16) reduces to the relatively simple statement

$$\hat{u}_t = \left(\frac{N}{L}\right) \sum_{k=1}^6 (\hat{R}_k + \hat{P}_k) \quad (15-23)$$

By way of interpretation, it might be remarked that all quantities (15-18) through (15-21) inclusive have the dimensions and character of mean stress over the  $k$ th face, that is, total force on the face divided by area. Furthermore,  $\hat{S}_k$  is the stress associated with the shear rate  $\Omega$  of the mean flow. The turbulent apparent stresses or momentum transport terms are represented by  $\hat{T}_k$ . These latter terms are quadratic in the velocities and are the only non-linear effects present. Purely viscous stresses are represented by  $\hat{H}_k$ . It has been shown that the  $\hat{H}_k$ , although linear, involve the partial derivatives of the turbulent velocity perturbations, rather than the velocities themselves.

It is convenient in the subsequent analysis to lump the terms  $(\hat{S}_k + \hat{T}_k + \hat{H}_k)$  together under the separate symbol  $\hat{R}_k$ . The reason is that these particular components can be calculated directly from the turbulent-velocity distribution, without any reference to pressure distribution. Determination of the pressure requires a separate and lengthy calculation, and the resulting average stress associated with the pressures is therefore represented by the separate symbol  $\hat{P}_k$ .

Turning to Eq. (15-23) it is seen that the terms have the character of net force per unit mass, that is to say, of acceleration. It turns out to be advantageous to employ the additional terminology below, namely,

$$\hat{F} = \left(\frac{N}{L}\right) \sum_{k=1}^6 \hat{R}_k \quad (15-24)$$

$$\nabla\phi = - \left(\frac{N}{L}\right) \sum_{k=1}^6 \hat{P}_k \quad (15-25)$$

Hence the basic momentum equation becomes finally

$$\hat{u}_t = \hat{F} - \nabla\phi \quad (15-26)$$

The term  $\hat{F}$  represents that part of the net accelerating force which can be calculated directly from the velocity distribution existing at a particular instant of time. The term  $(-\nabla\phi)$  is the net pressure force; it can be calculated only after the pressure distribution  $\phi$  has been found. The unknown pressure function  $\phi$  is itself fixed by the velocity distribution, but the relation is rather complex. However, it can be solved by the method outlined in the next section.

## 16. TURBULENT PRESSURE DISTRIBUTION

The momentum equation (15-26) has so far been used only to show how the local velocity-time derivative  $\hat{u}_t$  can be calculated when the direct velocity-induced forces  $\hat{F}$  and the pressure forces  $(-\nabla\phi)$  are known. It has been indicated that the forces  $\hat{F}$  can be calculated in a relatively straightforward manner when the instantaneous velocity distribution is known. The pressure forces, however, depend on the detailed distribution of the turbulent pressure  $\phi$ , and this quantity is so far still an unknown. The purpose of this section is to show how  $\phi$  itself is determined from the turbulent velocities.

To show this, we need only to apply the divergence operator term-by-term to the momentum equation (15-26). Thus

$$\nabla \cdot \hat{u}_t = \nabla \cdot \hat{F} - \nabla \cdot (\nabla\phi) \quad (16-1)$$

The three terms in this equation can be expressed in expanded form as follows:

$$\begin{aligned} \nabla \cdot (\nabla\phi) &= \nabla^2\phi = \frac{1}{\delta V} \int_{\delta S} (\nabla\phi) \cdot \hat{n} dS \\ &= \left(\frac{N}{L}\right) \sum_{k=1}^6 \left\{ \frac{1}{\delta S} \int_{\delta S} (\nabla\phi) \cdot \hat{n} dS \right\}_k \end{aligned} \quad (16-2)$$

$$\nabla \cdot \hat{F} = \frac{1}{\delta V} \int_{\delta S} \hat{F} \cdot \hat{n} dS = \left(\frac{N}{L}\right) \sum_{k=1}^6 \left\{ \frac{1}{\delta S} \int_{\delta S} \hat{F} \cdot \hat{n} dS \right\}_k \quad (16-3)$$

$$\begin{aligned} \nabla \cdot \hat{u}_t &= \frac{1}{\delta V} \int_{\delta S} \left( \frac{\partial \hat{u}}{\partial t} \right) \cdot \hat{n} dS = \frac{\partial}{\partial t} \left\{ \left(\frac{N}{L}\right) \sum_{k=1}^6 \left[ \frac{1}{\delta S} \int_{\delta S} \hat{u} \cdot \hat{n} dS \right]_k \right\} \\ &= \left( \frac{\partial D}{\partial t} \right) \end{aligned} \quad (16-4)$$

Consequently, with these definitions, the basic equation (16-1) may be rewritten in the concise form

$$\nabla^2 \phi = \nabla \cdot \hat{F} - \left( \frac{\partial D}{\partial t} \right) \quad (16-5)$$

This is the partial differential equation which fixes the pressure distribution  $\phi$ . The quantity  $\nabla \cdot \hat{F}$  on the right side is a known function of the turbulent velocity perturbations. The quantity  $\left( \frac{\partial D}{\partial t} \right)$  calls for some comment, however.

Strictly speaking, for an incompressible flow, the divergence  $D$  should vanish identically, in which case its time derivative will also vanish. In actual computations, however, because of round-off or other errors of approximation, the calculated divergence will usually differ from zero by some very small quantity  $\delta D$ . In order to prevent such small errors from accumulating and growing, it is desirable to assign the value of  $\left( \frac{\partial D}{\partial t} \right)$  in such a way as to tend to liquidate the error already present. Thus, we wish to eliminate the current divergence error  $\delta D$  within some small time interval  $\delta t'$ . But how shall this time interval be chosen? If the rate of error correction is too small, the divergence errors will tend to accumulate and grow, perhaps excessively. If the rate of error correction is too large, the associated pressure perturbations may become excessive; furthermore, the divergence error, instead of being eliminated, may be reversed in sign and possibly even increased in magnitude, thus leading to computational instability. Therefore, it is advisable to normalize  $\delta t'$  with respect to appropriate reference parameters of the turbulence. Cell size  $\frac{L}{N}$  and mean turbulent energy  $\bar{E}$  represent the natural reference parameters for this case. Hence we assign

$$\left( \frac{\partial D}{\partial t} \right) = - \left( \frac{\delta D}{\delta t} \right) = - C_D \frac{N}{L} \sqrt{2\bar{E}} \delta D \quad (16-6)$$

where  $C_D$  is a dimensionless coefficient whose optimum value can be established by numerical experimentation on the computer.

Consequently, the basic equation for the pressure distribution now becomes

$$\nabla^2 \phi = \nabla \cdot \hat{F} + C_D \frac{N}{L} \sqrt{2E} \delta D \quad (16-7)$$

where the right side is a known function of the space coordinates.

Therefore pressure  $\phi$  is the only unknown in Eq. (16-7). For accurate work, it is essential that the last term in this equation be of very small magnitude.

This relation lends itself to solution for the unknown pressure of  $\phi$  by a numerical relaxation technique. The essential principle of the method may be summarized as follows. The calculation starts with an arbitrary initial estimate or approximation for the unknown function  $\phi$ . The local values of  $\phi$  in the vicinity of the first grid point are then adjusted so that Eq. (16-7) becomes exactly satisfied for the first control cell. Then the values in the vicinity of the second cell are adjusted in a corresponding fashion. This process is continued systematically to cover the entire mesh. However, each time a local cell is adjusted, this process slightly upsets any previously made adjustments in adjacent cells. Nevertheless, each step of the computation produces a net reduction in the overall mean square error. Hence a complete sweep of the mesh in the above manner substantially improves the original approximation. Therefore the above procedure may be repeated as often as necessary, until the absolute residual error in Eq. (16-7) is everywhere less than some very small pre-assigned limit.

Calculation of the turbulent pressure distribution  $\phi$  by the above iteration method is quite straightforward in principle. The boundary conditions on the vertical faces of the block are simple because of the blockwise periodicity of the solution. The boundary conditions on the horizontal faces are somewhat tricky, however, owing to the relative sliding between successive rows of blocks, as explained in another section of this report. Owing to the number of iterations required to attain convergence, the pressure calculation is, of course,

quite lengthy. It consumes by far the greatest proportion of the total computing time.

17. BASIC SURFACE INTEGRALS FOR A FINITE ELEMENT:  
METHOD C

This discussion applies to any scalar function of position, say, for definiteness, the velocity component  $u$ . We choose differencing method C for this discussion because, as explained elsewhere, this was the method used in the program TURBOCODE, MARK V. We consider an arbitrary cubical element, of either family, and of length  $2a = L/N$ . The origin of coordinates is originally at the volume centroid, and the dimensionless coordinates  $\xi$ ,  $\eta$ ,  $\zeta$  take on values of  $\pm 1$  along the bounding surfaces.

The basic interpolation formula for this case is

$$u = A_0 + A_1\xi + A_2\eta + A_3\zeta + A_4\xi\eta + A_5\xi\zeta + A_6\eta\zeta + A_7\xi\eta\zeta + A_8(1-\xi^2)(1-\eta^2)(1-\zeta^2) \quad (17-1)$$

Consider the application of this equation to the bounding surfaces of the element. The surfaces in question may be those normal to either the  $x$ ,  $y$  or  $z$  axes, respectively; superscripts are used to distinguish these three orientations. Consequently, Eq. (17-1) may be reduced to one of the three forms below, namely,

$$u^x = A_0^x + A_1^x\eta + A_2^x\zeta + A_3^x\eta\zeta \quad (17-2)$$

$$u^y = A_0^y + A_1^y\zeta + A_2^y\xi + A_3^y\xi\zeta \quad (17-3)$$

$$u^z = A_0^z + A_1^z\xi + A_2^z\eta + A_3^z\xi\eta \quad (17-4)$$

The four constants in each equation depend only on the surface in question. They are uniquely determined by the values of the function at the four corners of the surface (this feature is one of the advantages of Method C.)

Consider the specific example indicated in Fig. 17.1. We drop the superscript notation for this portion of the discussion since there is no ambiguity in this case.

Upon substituting the coordinates of the points A, B, C, D into (17-4), and solving the resulting four equations for the four initially unknown constants, we obtain

$$A_0 = \frac{1}{4} [ + u_A + u_B + u_C + u_D ] \quad (17-5)$$

$$A_1 = \frac{1}{4} [ - u_A + u_B - u_C + u_D ] \quad (17-6)$$

$$A_2 = \frac{1}{4} [ - u_A - u_B + u_C + u_D ] \quad (17-7)$$

$$A_3 = \frac{1}{4} [ + u_A - u_B - u_C + u_D ] \quad (17-8)$$

An analogous treatment may be applied to the velocity components  $v$  and  $w$ . It is convenient to denote the corresponding constants by  $B$ 's and  $C$ 's, respectively.

Now a review of the basic continuity and momentum equations reveals that the surface integrals involved therein are of three main types. An example of each type is presented below for the case of a surface normal to the  $z$  axis. The extension of these results to other velocity components and other surfaces is easily made.

$$\frac{1}{(2a)^2} \int_{-1}^{+1} \int_{-1}^{+1} u(ad\xi)(ad\eta) = \frac{1}{4} \int_{-1}^{+1} \int_{-1}^{+1} [A_0 + A_1\xi + A_2\eta + A_3\xi\eta] d\xi d\eta = A_0 \quad (17-9)$$

$$-\frac{1}{(2a)^2} \int_{-1}^{+1} \int_{-1}^{+1} u(a\eta)(ad\xi)(ad\eta) = \frac{a}{4} \int_{-1}^{+1} \int_{-1}^{+1} [A_0 + A_1\xi + A_2\eta + A_3\xi\eta] \eta d\xi d\eta = \frac{1}{6} \left( \frac{L}{N} \right) A_2 \quad (17-10)$$

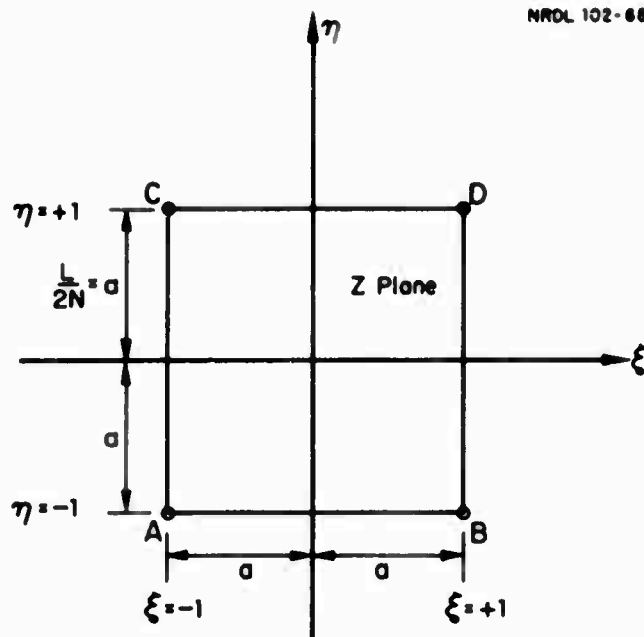


Fig. 17.1 Surface Element in  $Z$  Plane.

$$\begin{aligned}
\frac{1}{(2a)^2} \int_{-1}^{+1} \int_{-1}^{+1} uv(ad\xi)(ad\eta) &= \frac{1}{4} \int_{-1}^{+1} \int_{-1}^{+1} [A_0 + A_1\xi + A_2\eta + A_3\xi\eta] [B_0 + B_1\xi + B_2\eta + B_3\xi\eta] d\xi d\eta \\
&= A_0B_0 + \frac{1}{3}(A_1B_1 + A_2B_2) + \frac{1}{9} A_3B_3
\end{aligned} \tag{17-11}$$

Note that the form (17-9) represents a simple linear average value of the function  $u$  over the surface. All constants except  $A_0$  vanish from the result. In turn  $A_0$  is merely the arithmetic average of the four corner values. This result is consistent with elementary intuitive expectations.

In result (17-10) all terms vanish except the coefficient of  $\eta$ . The method of subscripting here used is such that for a  $z$  surface the non-vanishing component is  $A_2$ ; for an  $x$  surface, it would be constant  $A_1$ .

In this connection  $y$  surfaces are exceptional, for  $\eta$  is a constant in this case and may be moved outside the integral, thereby reducing the integral from the form (17-10) to the form (17-9). As a matter of fact, it is advantageous in dealing with surface integrals to shift the origin of coordinates from the centroid of the volume to the centroid of the surface directly involved. In this way we obtain for any  $y$  surface the result  $\eta = 0$ , whereupon the integral (17-10) simply vanishes.

Perhaps the most striking result is the integral (17-11). This goes well beyond what could be achieved by mere intuition, or by treatment of the surface as if it were an infinitesimal quantity. Note that all cross product terms drop out of the final result but that nevertheless, all eight original constants are significant and are retained. This undoubtedly represents a significant contribution to the accuracy of the method, especially for relatively coarse meshes. Recall that the integral (17-11) occurs in connection with the turbulent momentum stresses, and that the accurate evaluation of these stresses is one of the important goals of this study.

The results (17-9), (17-10) and (17-11) may be generalized by simple permutation of variables and subscripts so as to produce all the surface integrals required in this analysis, without further recourse to detailed integration. In this way the fundamental continuity, momentum and pressure relations may be reduced to algebraic difference equations which may then be directly programmed for the computer. The essential features of this algebraic development, and of the results, are summarized in Appendix A.

## 18. SCALE OF TURBULENCE

One of the fundamental aspects of turbulence is the linear scale which characterizes the phenomenon. It has already been pointed out that our method of analysis implies that, in some sense, cell size must be small, whereas block size must be large in relation to the scale of turbulence.

But how shall scale of turbulence be measured? Several approaches have already been indicated. One is based on the concept of correlation distance, another on the wavelength spectrum of the turbulence. A third method previously mentioned is associated with the idea of a critical cell size below which turbulence cannot be self-sustaining. All of these methods, however, involve lengthy and intricate calculations.

There is clearly a requirement for a much simpler measure of scale, which can be routinely calculated. To answer this need, a concept based on vorticity has been adopted.

From the point of view of the finite-element method, the vorticity vector at a grid point may be defined by the relation

$$\hat{\omega} = \frac{1}{\delta V} \int_{\delta S} \hat{n} \times \hat{u} dS \quad \text{sec}^{-1} \quad (18-1)$$

Considering the separate scalar components of vorticity, we have

$$\omega^2 = \omega_x^2 + \omega_y^2 + \omega_z^2 \quad \text{sec}^{-2} \quad (18-2)$$

Similarly, for the velocity components at any point

$$V^2 = u^2 + v^2 + w^2 = 2E \quad \text{ft}^2/\text{sec}^2 \quad (18-3)$$

where E represents kinetic energy per unit mass.

Both these quantities may be averaged by integration over the entire volume of the block, thus yielding root-mean-square values  $\sqrt{\overline{w^2}}$  and  $\sqrt{2\overline{E}}$  respectively.

Now a definition of scale  $\lambda$  may be written in the form

$$\lambda = C \sqrt{\frac{2\overline{E}}{\overline{w^2}}} \quad (18-4)$$

Note that the radical has the required physical dimension of length. A dimensionless normalizing constant  $C$  is introduced to permit adjustment of the units of scale. The value of  $C$  is assigned in such a way that the magnitude of  $\lambda$  acquires a clear physical significance for a certain simple limiting case.

The case in question may be represented by a hypothetical velocity distribution of the form illustrated (for  $v$ ) in Fig. 18.1. The equations are

$$u = P \sin \frac{2\pi z}{l} \sin \frac{2\pi y}{l} \quad (18-5)$$

$$v = Q \sin \frac{2\pi x}{l} \sin \frac{2\pi z}{l} \quad (18-6)$$

$$w = R \sin \frac{2\pi y}{l} \sin \frac{2\pi x}{l} \quad (18-7)$$

This is seen to represent a simple reference sine wave of wavelength  $l$ . The constant  $C$  is now chosen in such a way that the scale parameter  $\lambda$  for this simple case turns out to be exactly equal to the wavelength  $l$ . This same value of  $C$  is then retained as a fixed constant for all other cases as well. Consequently  $\lambda$  may be interpreted as a kind of generalized mean wavelength of the turbulence. (See Appendix C, Section 4.)

It is now proper to say concerning cell size  $\frac{L}{N}$ , normalized scale of turbulence  $\lambda$ , and block size  $L$  that we should ideally like to have

$$\frac{L}{N} \ll \lambda \ll L \quad (18-8)$$

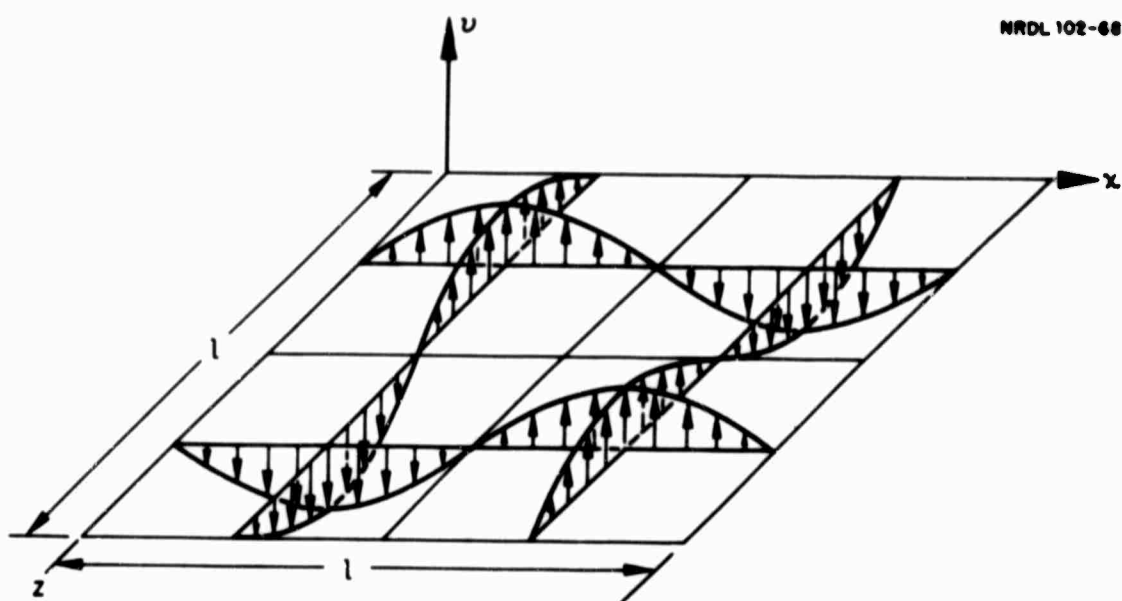


Fig. 18.1 Velocity Component  $v$  in Reference Wave.

However, if  $N$  be sharply limited by computer memory capacity, we are willing to accept the more modest statement

$$\frac{L}{N} < \lambda < L \quad (18-9)$$

## 19. MEAN EFFECTIVE TURBULENCE STRESSES

One of the important objectives of the present research is to improve our understanding of the so-called Reynolds stresses, that is, the mean effective values of apparent stress associated with the turbulent momentum transport. It is well known that turbulent fluctuations can be admitted into the Navier-Stokes equations of motion, and that the resulting expressions can then be averaged over time (or over an ensemble of macroscopically similar cases). When this process is carried out, the equations which are recovered are exactly similar to the ordinary Navier-Stokes equations for laminar flow, except for the presence of the additional Reynolds stresses. In effect, this result tells us how the mean motion is affected by the mean effective turbulence stresses. However, this is only part of the story. What is required to complete the solution is a knowledge of how the effective stresses, in turn, are affected by the mean motion.

Sometimes an attempt is made to express this latter relation by means of an analogy with the viscous stresses. The distortional components of the viscous stress tensor are known to be proportional to the corresponding components of the strain rate tensor based on the mean motion. The constant of proportionality is, of course, the ordinary molecular viscosity. It is sometimes assumed, therefore, that distortional components of the Reynolds stress may likewise be found by multiplication of corresponding components of the mean strain rate tensor by a suitable scalar factor of proportionality, the so-called eddy viscosity. If this analogy were strictly valid, it would represent a great simplification of the problem. Unfortunately, it is at best only a rough kind of approximation. The melancholy fact seems to be that there does not necessarily exist any single common scalar factor of proportionality between the various Reynolds stress components and the corresponding mean strain rate components. Consequently, a more fundamental approach to the problem is needed.

Since stress and strain rate are tensor concepts, it is advantageous for the present discussion to adopt Cartesian tensor notation and conventions. In particular, the coordinates  $x, y, z$  are replaced by  $x_1, x_2, x_3$  respectively. Hence the general component of the Reynolds stress may be written in the symbolic form.

$$\left( \frac{\tau_{1j}}{\rho} \right) = - \overline{u_1 u_j} \quad (19-1)$$

where  $\begin{matrix} 1 \\ j \end{matrix} = 1, 2, 3$

Contracting indices (and applying the usual summation convention), then dividing by 3 gives

$$\begin{aligned} \frac{1}{3} \left( \frac{\tau_{11}}{\rho} \right) &= - \frac{1}{3} (\overline{u_1 u_1}) = - \frac{1}{3} [\overline{u_1^2} + \overline{u_2^2} + \overline{u_3^2}] \\ &= - \frac{\bar{p}}{\rho} = - \frac{2}{3} \bar{E} \end{aligned} \quad (19-2)$$

where  $\bar{p}$  represents the equivalent "hydrostatic" pressure associated with the turbulence, while  $\bar{E}$  is the corresponding mean kinetic energy of turbulence.

The distortional Reynolds stresses are therefore expressible in the form

$$\left( \frac{\tau_{1j}}{\rho} \right) - \delta_{1j} \left( \frac{\bar{p}}{\rho} \right) = - \overline{u_1 u_j} + \delta_{1j} \frac{2}{3} \bar{E} \quad (19-3)$$

where  $\delta_{1j} = +1$  if  $1 = j$   
 $= 0$  if  $1 \neq j$  (19-4)

We now tackle the problem of identifying the specific parameters upon which the values of the stress tensor might depend. For this purpose it is useful to distinguish four types of turbulent flows as indicated in Table 19.1.

TABLE 19.1  
Types of Turbulent Flows

Type	I	II	III	IV
<u>Definition</u>				
Stationary?	No	Yes	Yes	No
Isotropic?	Yes	No	No	No
Homogeneous?	Yes	Yes	No	No
<u>Stress and Force Characteristics of Mean Flow</u>				
Distortional Stresses?	None	Present	Present	Present
Net Reynolds Forces?	None	None	Present	Present

Discussion elsewhere in this report shows that for Type-I flows, the distortional Reynolds stress tensor vanishes identically. Or to put the matter more simply, there can be no mean effective shear stresses in an isotropic flow field. Hence the Reynolds stress is of the purely "hydrostatic" type for this case. It follows that Type-I turbulence is too specialized in nature to provide information regarding a general state of stress.

Flows of Type II, on the other hand, are much more interesting in that non-vanishing shear stresses are now definitely involved. In fact this category represents the simplest possible case compatible with the existence of a general state of stress at a point. Therefore, it would seem to be the most profitable case to study initially for the purpose of establishing the parameters which determine the stresses at a point. The simple shear flow which is the subject of most of this report is a particular example of a Type-II flow.

Of some interest, besides the Reynolds stresses themselves, are the net resultant forces per unit volume exerted by the Reynolds stresses upon a small volume element enclosing an arbitrary point. These resultant forces are proportional to the gradients of the Reynolds stresses. However, in any homogeneous flow field, the stress gradients are everywhere zero, of course, and the net Reynolds forces vanish. (In fact the net viscous forces associated with the mean flow also vanish in this case.) Consequently, in any homogeneous flow, the Reynolds stresses are determined by the mean flow, but the mean flow is not influenced by the Reynolds stresses. This fact represents an important simplification of the overall problem.

Once the stress laws applicable to Type-II flows have been worked out, the study may be extended to the more complex flows of Type III and IV. There appear to be some grounds for the hope that the laws ultimately established for Type-II flows will need only minor elaboration to serve adequately for the more complex cases. In fact it might well be that under certain circumstances, the laws derived for Type-II flows may be applied unchanged to the other cases; however, much more work needs to be done before such a conclusion can be asserted with any degree of confidence.

Another important application of the foregoing stress laws arises in the following connection. In principle, the method of analyzing turbulence described in this report depends for its success on the creation of a mathematical model having a very large number of mesh points. Since not all possible difficulties can be faced and conquered simultaneously, it is tacitly assumed in much of the discussion in this report that the number of mesh points required for satisfactory results lies within the capabilities of the best modern computers, or at least within the capabilities of machines that will become available within a few years. In truth, however, this is probably an over-optimistic view. Hence there exists a need for simplifying the method to the extent that it does truly fall within the capabilities of now-

existing equipment. Naturally, any such simplification entails a certain loss of information. However, if the simplification is carried out judiciously, the loss of information need not be too serious.

The basis of simplification is obviously to use a coarser mesh than that demanded by the "exact" theory. This means that components of the turbulence of wavelength smaller than the minimum attainable cell size cannot be explicitly resolved in the analysis. However, if the mean effective Reynolds stresses associated with this range of wavelengths can be correctly simulated, the resulting error in the overall motion should be quite negligible.

As has been discussed earlier, it is believed that the above objective can be accomplished by means of an analysis in two stages. The first deals with the small-scale turbulence, the second with the large-scale turbulence. The cell size of the large-scale motion is taken as the block size of the small-scale motion. In the initial small-scale analyses, the full memory capacity of the computer is devoted entirely to resolving the small-wavelength turbulence. From these results, it should be possible to infer simplified rules for establishing the corresponding small-scale mean effective Reynolds stresses. Such stresses can subsequently be incorporated into the large-scale analysis to produce the required overall result.

For the remainder of this section, we revert now specifically to flows of Type II. Since the Reynolds stresses are uniquely determined whenever the mean motion is specified, we may hypothesize that these stresses are, in general, some unknown functions of the mean velocity components and of their various partial derivatives of all orders. Also, we observe that the Navier-Stokes equations of motion are valid with respect to any inertial frame. Furthermore, any coordinate frame moving at any constant velocity with respect to an initial frame is also an inertial frame. It follows, therefore, that the Reynolds stresses cannot depend on the velocity components themselves since these are different in different inertial frames, but must be functions

of the velocity derivatives alone. The velocity derivatives are invariant with respect to a shift of inertial frames. However, for any homogeneous flow field, all velocity derivatives vanish except those of first order. We conclude, therefore, that the six Reynolds stresses at any point are each functions of the nine quantities  $\left(\frac{\partial U_j}{\partial x_i}\right)$  where  $\begin{matrix} i) \\ j) \end{matrix} = 1, 2, 3$ .

The nine components of the unsymmetrical tensor  $\left(\frac{\partial U_j}{\partial x_i}\right)$  may be reorganized into six components of the symmetrical strain rate tensor  $\dot{\gamma}_{ij}$  and three components of the rotation vector  $\omega_k$ , as follows. Let

$$\dot{\gamma}_{ij} = \frac{1}{2} \left[ \frac{\partial U_j}{\partial x_i} + \frac{\partial U_i}{\partial x_j} \right] \quad (19-5)$$

$$\left. \begin{matrix} i) \\ j) \\ k) \end{matrix} \right\} = 1, 2, 3$$

$$\omega_k = \frac{1}{2} \left[ \frac{\partial U_j}{\partial x_i} - \frac{\partial U_i}{\partial x_j} \right] = \frac{1}{2} \epsilon_{ijk} \left( \frac{\partial U_j}{\partial x_i} \right) \quad (19-6)$$

where  $\epsilon_{ijk} = +1$  if  $i, j, k$  are in cyclic order  
 $= -1$  if  $i, j, k$  are in anti-cyclic order  
 $= 0$  if any two indices are equal

For any given state of the mean motion as defined by the mean velocity vectors

$$U_i = U_i(x_1, x_2, x_3) \quad (19-8)$$

the actual values of the six strain rate components  $\dot{\gamma}_{ij}$  and the three rotation components  $\omega_k$  will depend, of course, on the arbitrarily chosen orientation of the axes; consequently only three of the six components  $\dot{\gamma}_{ij}$  characterize the actual nature of the mean strain rate. This can be readily seen if the principal axes are chosen as coordinate axes, for in this case the strain rate tensor reduces merely to the three principal strain rates  $\dot{\gamma}_{11}, \dot{\gamma}_{22}, \dot{\gamma}_{33}$ , which now fully define the

character of the field. For the present discussion, however, it is more convenient to choose the axes in a somewhat different way; clearly, the choice of a particular axis orientation entails no loss of generality in the phenomenon itself - this still represents a general state of strain rate at a point.

We choose the axes  $x_1, x_2, x_3$  in such a way that  $x_1$  and  $x_2$  lie in that principal plane which contains both the algebraically largest and algebraically smallest principal strain rates. However, axes  $x_1$  and  $x_2$  are chosen to be at  $45^\circ$  with respect to the principal strain rate axes. Of course,  $x_3$  is the third principal axis, the one associated with an intermediate value of strain rate. The situation is shown in Fig. 19.1. Also shown are the familiar Mohr's circle representations for this strain rate condition, and for the associated Reynolds stresses.

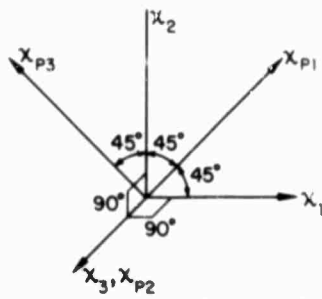
In this particular frame of reference, since  $x_3$  is a principal axis, we have  $\dot{\gamma}_{23} = \dot{\gamma}_{31} = 0$ . The non-vanishing components are  $\dot{\gamma}_{11}, \dot{\gamma}_{22}, \dot{\gamma}_{33}$  and  $\dot{\gamma}_{12}$ . However, in this case  $\dot{\gamma}_{11} = \dot{\gamma}_{22}$ , so that again there are just three independent degrees of freedom in the strain rates. Furthermore, we choose the axes such that  $\dot{\gamma}_{12}$  is positive. Since axes  $x_1$  and  $x_2$  are at  $45^\circ$  to the principal axes, it follows that the magnitude of  $\dot{\gamma}_{12}$  represents the maximum possible shearing rate. Reference to Fig. 19.1, the Mohr's circle diagram, should help make this clear.

In discussing either the stress or the strain rate tensors, it is frequently useful to distinguish between the isotropic and distortional components. The distortional components of strain rate are defined by

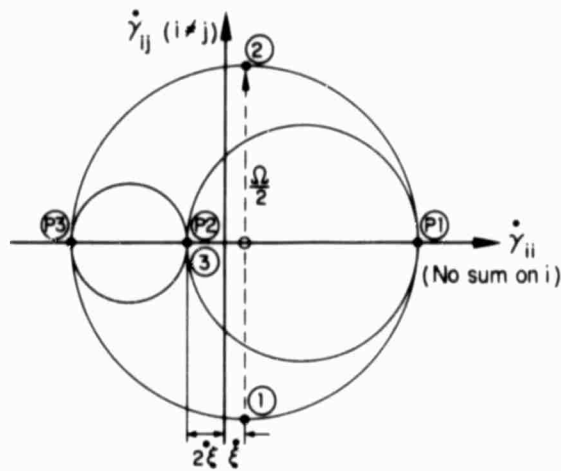
$$\dot{\gamma}'_{ij} = \dot{\gamma}_{ij} - \delta_{ij} \dot{\gamma} \quad (19-9)$$

$$\text{where } \dot{\gamma} = \frac{1}{3} \dot{\gamma}_{11} = \frac{1}{3} (\dot{\gamma}_{11} + \dot{\gamma}_{22} + \dot{\gamma}_{33}) \quad (19-10)$$

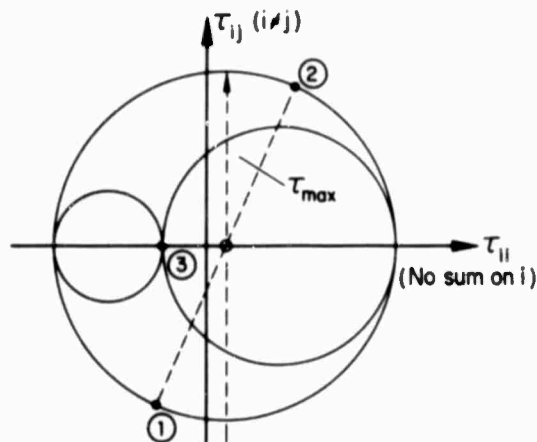
However, for the case of an incompressible fluid, which is the specific case to which this entire report is restricted, we have zero divergence, that is



(a) Reference Axes  $x_1, x_2, x_3$  and Principal Axes  $x_{p1}, x_{p2}, x_{p3}$  for Mean Strain Rate Tensor



(b) Mohr's Circles for Mean Flow Strain Rates



(c) Mohr's Circles for Reynolds Stresses

Fig. 19.1 Reference Axes and Mohr's Circles of Strain Rate and Stress.

- (a) Reference Axes  $x_1, x_2, x_3$  and Principal Axes  $x_{p1}, x_{p2}, x_{p3}$  for Mean Strain Rate Tensor.
- (b) Mohr's Circles for Mean Flow Strain Rates.
- (c) Mohr's Circles for Reynolds Stresses.

$$\dot{\gamma}_{11} = 3\dot{\gamma} = (\dot{\gamma}_{11} + \dot{\gamma}_{22} + \dot{\gamma}_{33}) = 0 \quad (19-11)$$

whereupon the distortional component becomes identical with the strain rate itself, that is,

$$\dot{\gamma}'_{1j} = \dot{\gamma}_{1j} \quad (19-12)$$

By reason of the zero divergence, which establishes another relation of constraint among the strain rate components, the number of independent degrees of freedom in the strain rate tensor is reduced from three to two. We may therefore at this point rewrite the strain rate components in the optional alternative form

$$\dot{\gamma}_{11} = \dot{\epsilon} \quad (19-13) \quad \dot{\gamma}_{23} = 0 \quad (19-16)$$

$$\dot{\gamma}_{22} = \dot{\epsilon} \quad (19-14) \quad \dot{\gamma}_{31} = 0 \quad (19-17)$$

$$\dot{\gamma}_{33} = 2\dot{\epsilon} \quad (19-15) \quad \dot{\gamma}_{12} = \frac{\Omega}{2} \quad (19-18)$$

where  $\dot{\epsilon}$  and  $\Omega$  now represent the two independent degrees of freedom in an explicit way. If we set  $\dot{\epsilon} = 0$  in this result, we obtain the strain rate tensor associated with simple two-dimensional shear flow, with shearing rate  $\Omega$ ; in fact the simple parallel shear flow which is the subject of most of this report is a particular flow of this type. The foregoing strain rate pattern with  $\dot{\epsilon} \neq 0$  is therefore a generalization to three dimensions of the simple two-dimensional shear flow; the meaning of  $\Omega$  has been appropriately generalized in a corresponding manner.

We may summarize the argument to this point by stating that for homogeneous flows, the Reynolds stress components must be functions of the form

$$\left( \frac{\overline{\tau_{1j}}}{\rho} \right) = -\overline{u_1 u_j} = f_{1j}(\dot{\epsilon}, \Omega, w_1, w_2, w_3) \quad (19-19)$$

This relation may be simplified even further by dimensional analysis. Using reference parameters  $\rho$ ,  $v$  and  $\Omega$ , we set up the dimensionless forms of the various variables as follows:

$$\tau_{ij}^* = \frac{\tau_{ij}}{\rho v \Omega} \quad (19-20) \quad \dot{e}^* = \frac{\dot{e}}{\Omega} \quad (19-23)$$

$$\rho^* = \frac{\rho}{\rho} = 1 \quad (19-21) \quad \Omega^* = \frac{\Omega}{\Omega} = 1 \quad (19-24)$$

$$u_1^* = \frac{u_1}{\sqrt{\lambda}} \quad (19-22) \quad w_1^* = \frac{w_1}{\Omega} \quad (19-25)$$

Consequently we obtain at last

$$\overline{\tau_{ij}^*} = - \overline{u_i^* u_j^*} = f_{ij}^*(\dot{e}^*, w_1^*, w_2^*, w_3^*) \quad (19-26)$$

Each of the six dimensionless stresses is therefore a function of just four variables, as shown. This is the general form of the relation which we initially desired to ascertain.

In the case of a mean flow which is purely two-dimensional, this relation simplifies drastically, for in this case

$$\dot{e}^* = 0, \text{ and } w_1^* = w_2^* = 0 \quad (19-27)$$

Consequently

$$\overline{\tau_{ij}^*} = - \overline{u_i^* u_j^*} = f_{ij}^*(w_3^*) \quad (19-28)$$

where, from considerations of symmetry, two of the six stresses vanish, namely,

$$\overline{\tau_{23}^*} = \overline{\tau_{31}^*} = 0 \quad (19-29)$$

Hence for turbulence in a two-dimensional homogeneous mean flow, the four dimensionless non-vanishing Reynolds stresses are functions of only

a single parameter,  $w_3^*$ , the dimensionless rotation vector. This analysis makes evident the desirability of an early investigation of the two-dimensional homogeneous flow in which  $w_3^*$  varies over a range of values.

Furthermore, for the special case of the simple parallel shear flow considered in this report

$$w_3^* = -\frac{1}{2} \quad (19-30)$$

Consequently for this particular case, the dimensionless Reynolds stresses reduce to four specific constants.

Note that the foregoing method is free of any arbitrary or speculative assumptions regarding eddy viscosity, mixing lengths or the like, although it is, of course, restricted to flows of Type II.

An interesting question arises in connection with the principal axes of stress and strain rate. The principal axes of the strain rate tensor are, by definition, axes of zero strain rate. Similarly, the principal axes of the Reynolds stress tensor are axes of zero shear stress. According to our usual rheological notions of stress and strain, we would expect that along axes of zero shear strain rate the shear stress would also be zero. In other words, the principal axes of mean flow strain rate and Reynolds stress would be expected to coincide. But do these particular rheological relations necessarily apply to the case of fluid turbulence? There appears to be no definite proof that they do apply in general. This is an item on which it should be possible to obtain useful information by the methods of numerical simulation considered in this report.

Elementary theory can also shed some light on this question. For this purpose, let indices i, j, k now refer specifically to the principal axes of strain rate. Now if any principal plane  $x_1x_j$  is also a plane of symmetry of the mean flow, then it follows from this symmetry that  $\overline{\tau_{k1}^*} = 0$  and  $\overline{\tau_{jk}^*} = 0$ . However, in any such plane of symmetry, it again follows

that  $w_1^* = 0$  and  $w_j^* = 0$ . It would appear that the converse must also be true. That is, if  $w_1^* = 0$  and  $w_j^* = 0$ , then also  $\overline{\tau_{k1}^*} = 0$  and  $\overline{\tau_{jk}^*} = 0$ , where the three indices  $i, j, k$  are all distinct. Thus,

$$\text{If } w_1^* = 0 \text{ and } w_2^* = 0, \text{ then } \overline{\tau_{31}^*} = 0 \text{ and } \overline{\tau_{23}^*} = 0 \quad (19-31)$$

$$\text{if } w_2^* = 0 \text{ and } w_3^* = 0, \text{ then } \overline{\tau_{12}^*} = 0 \text{ and } \overline{\tau_{31}^*} = 0 \quad (19-32)$$

$$\text{if } w_3^* = 0 \text{ and } w_1^* = 0, \text{ then } \overline{\tau_{23}^*} = 0 \text{ and } \overline{\tau_{12}^*} = 0 \quad (19-33)$$

It follows also that if the mean flow be irrotational, the principal axes of stress and strain rate are then coincident. The implication is that for highly rotational mean flows, the principal axes of stress and strain may cease to coincide.

## 20. COMPUTATIONAL VERSUS HYDRODYNAMIC INSTABILITY

The discussion in earlier sections should make it abundantly clear that considerable ingenuity and care are required to devise grid patterns and calculation procedures which will yield maximum accuracy and resolution for a given computational effort and cost. A special difficulty that presents itself in various guises concerns the stability and convergence of the calculation procedure. This is one of the fundamental problems generally associated with numerical methods. The particular difficulty in the present application is that turbulence itself is an instability phenomenon. There is always the lurking danger of introducing inadvertently some subtle cause of instability in the calculation procedure, and confounding the results with the true physical instability which is turbulence.

One common if indirect method of coping with questions of computational accuracy and stability is to compare results obtained by numerical methods with some known exact theoretical results. Unfortunately, in the turbulence problem, there are no known theoretical results to serve as standards of comparison.

An alternative is to compare with experimental data. There is an enormous amount of experimental data available on various aspects of turbulence. Nevertheless adequate experimental data specifically applicable to the present boundary conditions might not be available or readily found. It may eventually prove necessary to undertake an independent experimental program for this express purpose.

A more direct approach is to attempt to analyze theoretically the stability characteristics of the numerical method being used. Some tentative guide lines are available in this connection, although there does not seem to be available any standard and definitive technique. The present problem is especially difficult owing to the great length and complexity of the basic difference equations involved, and owing to

their non-linearity. Hence the theoretical approach to stability is a full-fledged research problem in its own right.

It is, however, a very important problem, and efforts will be made to pursue it as circumstances may permit. A successful theoretical analysis would provide definite and rational criteria of stability and should thereby improve the efficiency of the calculation procedure and the reliability of the results obtained.

Meanwhile, the difficulty is being faced in a pragmatic way. Various common sense safeguards and criteria of a heuristic kind have already been provided in the program TURBOCODE, MARK V. Thus, for example, the degree of convergence demanded in the iteration procedure which fixes the pressure distribution is readily adjustable. A parameter is also provided to limit the maximum displacement of any fluid particle in any time step to any desired small fraction of a single cell length. Preliminary numerical experiments are producing useful guide lines concerning the optimum settings for these parameters, and concerning the corresponding level of residual error or noise produced in the calculation sequence. Furthermore, it is well known that the sovereign remedy for most instability problems is a reduction in the size of space and time increments. Hence it is believed that stability problems are not likely to defeat the goals of the investigation, although they might very well increase the effort and cost required to attain these goals.

Incidentally, it is believed that the comparatively sophisticated finite-element techniques being used in this problem are far less susceptible to instability problems than the looser methods based merely on replacing differentials by finite differences. It must be conceded, however, that no method of differencing, however refined, is altogether exempt from the hazard of possible computational instability.

## 21. GENERATION VERSUS ANALYSIS OF TURBULENCE DATA

The numerical description of a flow field involves the use of a suitable grid of coordinate points in that field. For the ordinary case of a cubical region of length  $L$  on a side, subdivided into cubical cells of length  $L/N$  on a side according to Method A, there are  $N^3$  cells. Since a grid point is placed at the centroid of each cell, there are  $N^3$  grid points. In the program TURBOCODE, MARK V, a staggered scheme of cells is employed, Method C, which involves  $2N^3$  independent grid points. Since MARK V may use values up to  $N = 8$ , the number of grid points may reach 1024 in all.

The state of the turbulent flow at any instant of time may be adequately described by specification of the values of the three velocity components and of the pressure perturbation at each point. Hence we have, in MARK V, at least  $8N^3$  items of data involved for each time step, that is, up to 4096 items per step. (Actually, certain additional items of information are also needed near the top and bottom surfaces, but this is immaterial for the present discussion.)

Now the basic purpose of TURBOCODE, MARK V is to follow the evolution of the turbulence resulting from an arbitrary initial perturbation. Since the number of time steps involved in any adequate overall time period is large, it is clear that we are confronted with an enormous volume of data - a veritable torrent. It becomes a major problem as to what to do with this data, how to store it, how to process it, and so on.

The basic tenet has been adopted that the generation of the basic data and its subsequent processing for various analytical purposes should not be confounded within the same program. Accordingly, TURBOCODE, MARK V is intended solely to generate the data. The processing involved therein is minimal and is confined to those few statistical features which are clearly indispensable for providing a general indication of

the state of turbulence. These include (for each time step) space mean values of kinetic energy, turbulent shear stress and scale of turbulence. Consequently the generation of the data is accomplished with maximum efficiency and in minimum time.

The results thereby generated are recorded and stored on magnetic tape for subsequent analysis and processing by a separate program or series of programs, according to the type of information desired. However, for conservation of tape and recording time, provision is made to sample the generated data and to retain only such selected portions as are required for the subsequent analysis. This avoids the indiscriminate taping of huge amounts of data far in excess of any realistic need.

In a sense, the generation and sampling of data in the present study plays a role comparable to that of physical experimentation in conventional research. The subsequent analysis and manipulation of the data so obtained is a more or less distinct and separate step.

## 22. PARTIAL SUMMARY OF PRINCIPAL CONCEPTS

The mean flow field is a steady, incompressible, parallel and uniform shear flow in which the mean velocity  $U$  is of the form

$$U = \hat{i} \hat{\Omega} y \quad (22-1)$$

where  $\hat{\Omega}$  represents the constant shear rate, and  $\hat{i}$  is a unit vector in the  $x$  direction. Physical boundaries of the flow are at  $y = \pm \infty$ .

The turbulence is homogeneous, that is, all statistical properties of the turbulence are uniform over the flow field. However, the field is anisotropic, that is, properties in one direction are in general different from those in another direction.

All physical quantities are non-dimensionalized in terms of the reference parameters: density  $\rho$ , kinematic viscosity  $\nu$ , and shear rate  $\hat{\Omega}$ . All possible uniform shear flows of the above type, when non-dimensionalized in this way, reduce to a single definite and unique case.

The energy spectrum of the turbulence is largely confined within a limited range of wavelengths. If we neglect some arbitrary but very small fraction of the total turbulent energy at each end of the spectrum, two corresponding limits of wavelength are thereby defined, say  $L_{\min}$  and  $L_{\max}$ , between which nearly all of the turbulent energy lies.

The flow field is subdivided into large cubical blocks of length  $L$  on a side. Each block is in turn subdivided into many small cubical control volumes or cells of length  $(L/N)$  on a side. The integer  $N$  fixes the fineness of the cubical mesh. In the ideal case, it is desirable that  $L \geq L_{\max}$  and  $(L/N) \leq L_{\min}$ . This implies that  $N \geq L_{\max}/L_{\min}$ .

Since the computer memory requirements are roughly proportional to  $N^3$ , it will probably be impossible to meet the above criterion. In that case, the turbulence must be subdivided into small-scale and large-scale components, and analyzed in two successive stages. The method lies beyond the scope of this summary, but is detailed in the main text of the report.

The large cubical blocks into which the flow field is subdivided are arranged in horizontal rows. The horizontal mid-plane of each row has zero velocity with respect to the mean flow. Because of the shear rate  $\Omega$  of the mean flow, there is a relative velocity of magnitude  $\Omega L$  between any two successive rows. At times  $t = 0, 1/\Omega, 2/\Omega, 3/\Omega, \dots$  all rows are aligned in an unstaggered cubical array, such that all vertical faces of all blocks coincide and form continuous vertical planes. At all other times the blocks in successive rows are staggered with respect to one another. See Fig. 5.1.

At time  $t = 0$ , a set of non-divergent velocity perturbations is assigned at the centroids of all the control cells. The perturbation is arbitrary except that all possible wavelengths in the range of interest are present. The initial distribution of the perturbation velocities is taken as identical for all blocks, that is all cells in corresponding positions in all blocks are assigned identical perturbations. Consequently, the subsequent motion throughout all blocks remains identical thereafter. This spatial periodicity of the solution makes the subsequent boundary conditions along the block surfaces perfectly definite and unique.

The flow field passes through an initial transient in which the spectral distribution gradually changes from its arbitrary initial form. Ultimately, some definite equilibrium form and amplitude are attained, and thereafter, the turbulence remains in an essentially stationary state. The resulting velocity components and pressures over the entire block may be sampled for any desired number of successive time steps. With methods suggested in the main body of this report, this data may be analyzed to establish any desired statistical properties of the turbulence, such as the mean kinetic energy, Reynolds stresses, scale of turbulence, energy spectrum, various correlation coefficients, etc.

The initial state of the system is defined by the distributions of the three velocity components and the pressure. However, it may be shown that the equations of motion and continuity, along with the

boundary conditions, suffice to determine the pressure distribution uniquely whenever the velocities are fully specified. Hence the pressure distribution is a derived function which cannot be specified independently. Furthermore, not all of the velocity components are independent, for it may be shown from the condition of continuity and from the specified spacewise periodicity of the turbulence that if any two of the velocity components are specified throughout the grid, the third component is thereby uniquely determined. Hence there are just two arbitrary initial degrees of freedom for each distinct grid point of the block. Strictly speaking, these arbitrary degrees of freedom exist only at the initial time  $t = 0$ , for the entire subsequent motion is wholly determined thereafter.

Determination of the pressure distribution which must co-exist with any specified distribution of the velocity components involves a lengthy process of computation by successive approximations until the results converge to within the required degree of accuracy. This entire iteration process must be repeated every time the velocities change, which is to say, for every time step. Hence the pressure computation takes by far the biggest part of the total computation time.

The small but finite cells are used as fixed control volumes in an Eulerian sense. The continuity and momentum equations are applied to these control volumes. This involves evaluation of the forces and of the mass and momentum fluxes pertaining to the six square bounding surfaces which enclose each cell. The evaluation is accomplished by means of complete and detailed surface integrals. Similarly, average values of momentum and energy enclosed within the cell are evaluated by means of detailed volume integrals. This painstaking integration technique constitutes the heart of the so-called finite-element method. It contrasts strongly with most ordinary differencing methods which use much cruder estimates of the required forces and fluxes. The difference in accuracy is particularly important for relatively coarse meshes, such as those which are necessarily involved in the present study.

For evaluation of the above surface and volume integrals with good accuracy, it is essential to have a suitable interpolation rule which specifies how the various quantities vary in the space between the principal grid points. For this purpose a linear interpolation rule is employed. It is postulated that values vary linearly along any straight line parallel to any one of the three coordinate axes. It turns out that this rule determines the distribution uniquely throughout the entire space when values are specified at the principal grid points.

In connection with the evaluation of various volume integrals, it is further postulated that the volume average of any quantity within any cell also constitutes the best available estimate of the local value of that quantity at the centroid of that cell.

The finite-element technique is a method of approximation which employs a minimum number of definite basic postulates, and proceeds thereafter in a completely determinate and unambiguous manner consistent with these postulates. The necessity for any subsequent ad hoc assumptions is eliminated. The numerical accuracy and stability thereby attained is probably the maximum attainable in relation to the coarseness of the grid employed.

The basic idea of the present calculation method is that if the velocity distribution is completely known at some instant of time, the new velocity distribution a short time later can consequently be found. First of all, the pressure distribution corresponding to the initial velocity must be calculated by the iteration method mentioned earlier. Next, the equations of motion are applied to the control cells to establish the time rates of change of the velocity components at the centroids of the cells. Finally, the new velocities are computed.

The above cycle of calculations is repeated for every time step. Hence the motion of the system may be followed indefinitely, or as long as necessary to obtain the desired information.

A particular feature of the above calculation procedure relates to the maintenance of a continuously non-divergent velocity distribution.

Because of round-off and other errors, the velocity distribution at the beginning of any time step may deviate very slightly from the required condition of non-divergence. This is corrected in the following way. A very small correction term is included in the pressure distribution. This term influences the motion during the subsequent time step very slightly and in such a way as to tend to restore zero divergence. Hence there is built into the calculation sequence a divergence correction which continuously compensates for accumulating round-off and other errors.

An important question in connection with any numerical method, including this one, pertains to the stability of the calculation procedure. Owing to the great complexity of the final difference equations in the present problem, this aspect has not yet received adequate study. However, a number of common-sense precautions have been taken to minimize the danger of computational instability. The main precaution involves limiting the time intervals to very small values such that the maximum displacement of any fluid particle is restricted to some small fraction of the cell size. It is known that reducing the time increment cures most problems of computational instability. Furthermore, the improved accuracy associated with the finite-element method itself provides an enhanced resistance to instability difficulties.

The basic assumptions and concepts here summarized suffice to establish a method for the computer simulation of the detailed stationary turbulence in a uniform shear flow. The data generated in this way is in some respects comparable to that which might in principle be obtained by direct experimental measurement. The computed data, however, pertains to a very fundamental case but one which would be rather difficult to set up experimentally. Furthermore, the computed results are incomparably more comprehensive than any that could reasonably be obtained by experiment. The detailed data so generated represents fundamental information which may subsequently be analyzed from various points of view to establish corresponding overall statistical and phenomenological characteristics of the turbulence.

### 23. TYPICAL COMPUTER RESULT

Table 23.1 and Fig. 23.1 show some results of a typical computer run. For internal consistency this data is included merely as an example; no detailed conclusions are offered at this time. More comprehensive data and analysis are planned for the near future. Nevertheless, the particular result shown supports the idea, advanced on theoretical grounds in an earlier section of this report, that for block size  $L$  below some critical value,  $L_{cr}$ , the initial turbulence dies away and laminar flow is restored. The data also shows that the normalized divergence errors (column DBIG) and the inherent noise level in the computer solution are extremely small.

The data listed in Table 23.1 represents only the gross overall features of the turbulence. (Most of the columns are self-explanatory: ENERGY = energy of turbulence per unit mass; UVBAR = Reynolds shear stress; SCALE = scale of turbulence as discussed elsewhere in this report; NITER = number of pressure iterations for convergence.) Not shown, but available from this same computer run, is an enormous mass of detail showing the individual velocity components and pressures at every point in the grid for every time step.

Table 23.1 Typical Computer Output

```
TURBOCODE MARK V
PROBLEM NUMBER 32
MESH SIZE 5 BY 5 BY 5 BY 2

INITIAL STATE
KINETIC ENERGY .100-01
SPECTRAL PARAMETER 1.000
SIZE OF BLOCK .500+01

INTERNAL CONTROL
MAX. ITERATIONS 999
CONVERGENCE PARAMETER .100-02
MAX. TIME INCREMENT .100+00
DIVERGENCE COEFF .100+07
TIME STABILITY PARAMETER .0250

OUTPUT CONTROL
OUTPUT TAPE UNIT NUMBER 28
LENGTH OF OUTPUT BURSTS (CYCLES) 1
SPACE BETWEEN BURSTS (CYCLES) 70
```

1CYCLE	TIME	ENERGY	UVRAR	SCALE	NITER	DB16	OUT
0	.00000	.100-01	-.116-11	.486+01 *	0	.000 *	0
1	.26419-02	.990-02	.248-07	.486+01 *	24	.000 *	0
2	.76419-02	.972-02	.314-06	.486+01 *	12	-.188-07 *	0
3	.12642-01	.954-02	.965-06	.486+01 *	12	.205-07 *	0
4	.17642-01	.936-02	.195-05	.486+01 *	12	.245-07 *	0
5	.22642-01	.919-02	.325-05	.486+01 *	12	.249-07 *	0
6	.27642-01	.902-02	.483-05	.486+01 *	17	.218-07 *	0
7	.32642-01	.885-02	.666-05	.486+01 *	12	.187-07 *	0
8	.37642-01	.869-02	.873-05	.486+01 *	12	.200-07 *	0
9	.42642-01	.853-02	.110-04	.486+01 *	12	-.181-07 *	0
10	.47642-01	.837-02	.134-04	.486+01 *	12	-.210-07 *	0
11	.52642-01	.822-02	.160-04	.486+01 *	12	-.218-07 *	0
12	.57642-01	.807-02	.187-04	.486+01 *	12	-.238-07 *	0
13	.62642-01	.792-02	.216-04	.486+01 *	12	-.290-07 *	0
14	.67642-01	.778-02	.244-04	.486+01 *	12	-.324-07 *	0
15	.72642-01	.763-02	.274-04	.486+01 *	12	-.377-07 *	0
16	.77642-01	.750-02	.303-04	.486+01 *	12	-.406-07 *	0
17	.82642-01	.736-02	.333-04	.486+01 *	16	.461-07 *	0
18	.87642-01	.723-02	.362-04	.486+01 *	12	.310-07 *	0
19	.92642-01	.710-02	.391-04	.486+01 *	12	.436-07 *	0
20	.97642-01	.697-02	.419-04	.486+01 *	16	.486-07 *	0
21	.10264+00	.685-02	.446-04	.486+01 *	12	.371-07 *	0
22	.10764+00	.672-02	.473-04	.486+01 *	12	.402-07 *	0
23	.11264+00	.660-02	.498-04	.486+01 *	12	.449-07 *	0
24	.11764+00	.649-02	.521-04	.486+01 *	12	.474-07 *	0
25	.12264+00	.637-02	.544-04	.486+01 *	16	.502-07 *	0
26	.12764+00	.626-02	.564-04	.486+01 *	16	.312-07 *	0
27	.13264+00	.615-02	.583-04	.486+01 *	16	.251-07 *	0

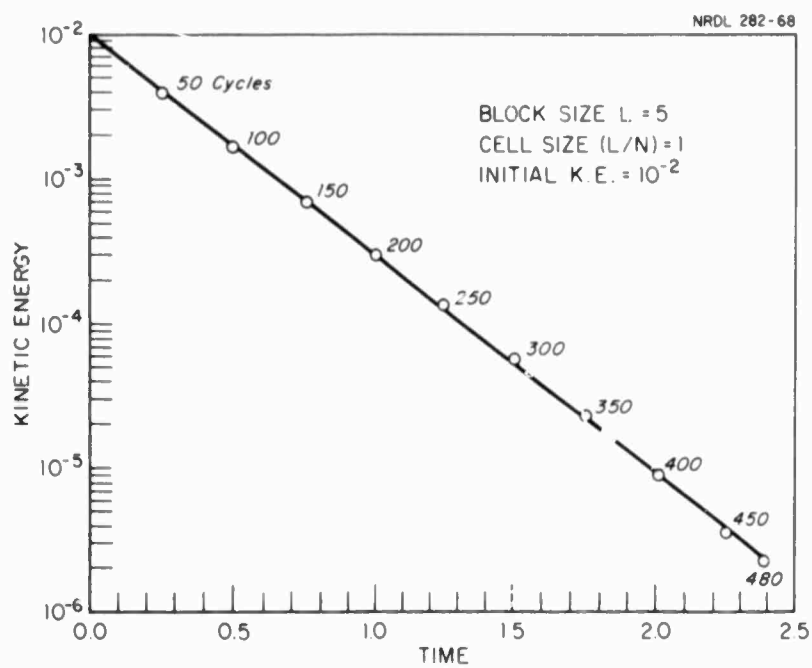


Fig. 23.1 Dissipation of Turbulent Energy for Sub-Critical Block Size.

## 24. POSTSCRIPT

The purpose of this postscript is to record two important concepts whose value and significance were not fully appreciated at the time the main body of this report was written.

The first idea pertains to a simplified analysis of turbulence by treatment on a purely two-dimensional basis. One could set  $w = 0$ ,  $\frac{\partial}{\partial z}$  (any function)  $= 0$ , and treat  $u$ ,  $v$  and  $\phi$  as functions of  $x$ ,  $y$  and  $t$  only. Actually this approach was considered earlier, but was initially rejected on the ground that true turbulence is inherently three dimensional and should be treated as such. Nevertheless, it appears that an analysis of two-dimensional "pseudo turbulence" would be of considerable value and interest as an interim step toward the final goal. It would undoubtedly resemble true three-dimensional turbulence in many significant respects. As a two-dimensional problem in the space coordinates, it falls well within the range of existing computer capabilities. It would enable us to increase the important mesh resolution parameter  $N$  without involving prohibitively large computer storage requirements. It would also facilitate all subsequent steps such as spectral analysis and the like. While obviously not a complete substitute for the full three-dimensional treatment, it would certainly be a valuable complement to the latter. It would be particularly useful and most relevant in the earlier stages of investigation as a tool for establishing basic concepts and methods. The idea of using simplifications of this type is nothing new; somewhat similar simplifications have been made by Emmons (Ref. 2), Kraichman (Ref. 3) and others.

The second concept is a further generalization of the idea of equivalent reference frames, as outlined in Section 5 of the report. In Section 5 the basic unit of fluid to which the concept of equivalence has been applied has been the cubical block of length  $L$  on a side. But it is both possible and advantageous to go further. We can apply the

concept of equivalence to the individual cubical cell, of length  $\frac{L}{N}$  on a side. In this case, the condition of equivalence can be reduced to the statement that the centroid of each cell shall have zero velocity with respect to the mean flow. This amounts to adoption of a kind of Lagrangian System, in the sense explained in Appendix D. The scheme has obvious merit in that all control volumes are truly equivalent. The equations of motion are identical in form for all control cells; there are no terms needed to reflect differences in mean flow velocity at the centroids. Consequently, the complexities and peculiarities of the sliding boundary condition, which is associated with the Eulerian system of rigid reference blocks, simply vanish from the analysis.

If the control cells are rigid cubes of length  $(\frac{L}{N})$  on a side, and if the centroids of these cells move with the main flow, the effect is as shown in Fig. 26.1. At the initial (dimensionless) time  $t^* = 0$ , and at subsequent integral values of  $t^* = 1, 2, 3, \dots$ , the cells form a simple cubical array as shown. At other times the individual layers become staggered as shown. The basic unit of analysis is now not a rigid block, but a stack of slabs measuring  $L$  by  $L$  horizontally, by  $(\frac{L}{N})$  vertically.

The differencing formulas to be used in this case will contain the time variable  $t$ , since they must account for the continuously changing geometry of the system. However, the basic method of deriving these formulas in terms of surface integrals still applies in the usual way. There seem to be no basic difficulties involved. Nevertheless, some care is needed in defining the interpolation spaces which now also vary with time.

Consider the set of parallelopipeds formed by connecting principal grid points by straight lines. In horizontal planes these grid lines form squares of size  $\frac{L}{N}$ , in the usual way. In vertical planes  $z = \text{constant}$ ; however, owing to the continuous shearing motion, the "vertical" lines of the grid lie at an angle  $\alpha$  with respect to the  $y$  direction, as shown. This angle changes continuously with time. We impose the restriction,

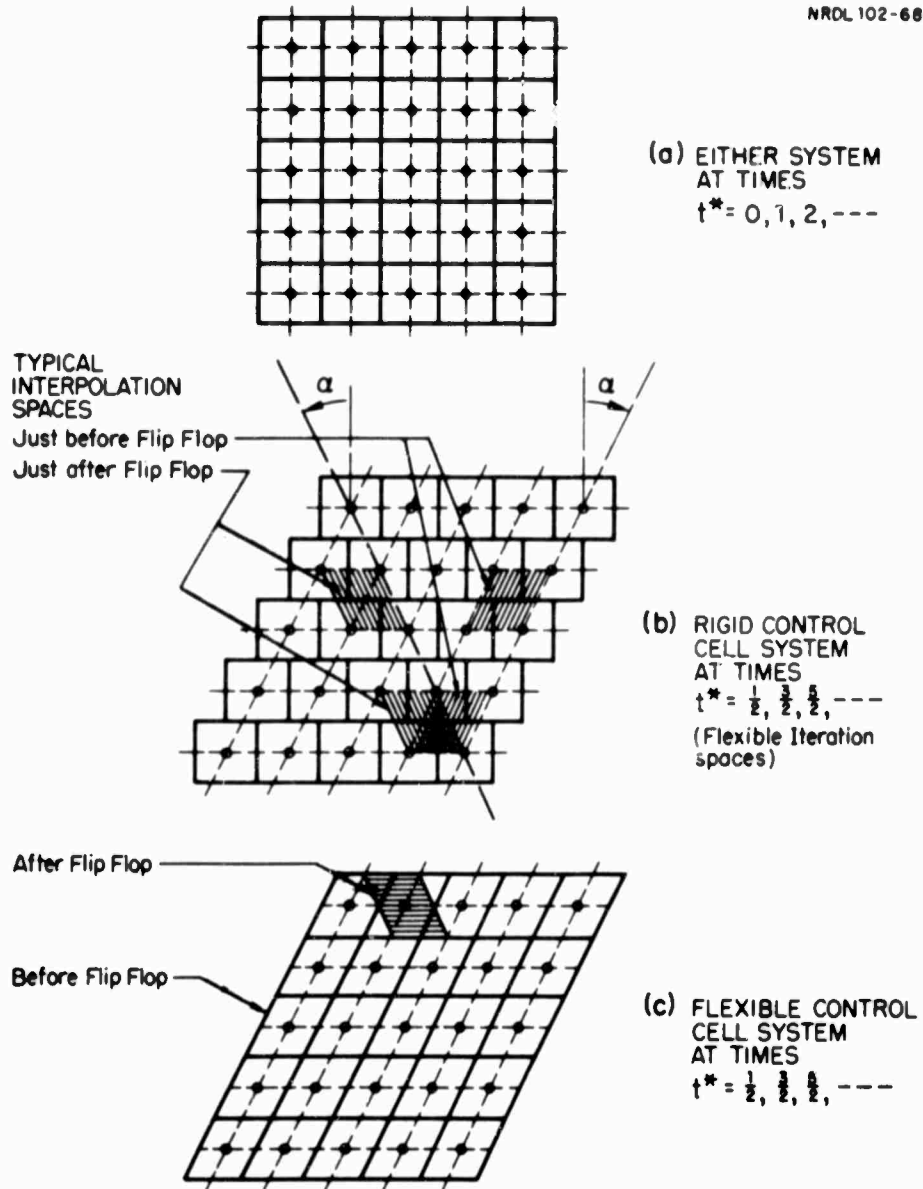


Fig. 26.1 Differencing Method for Grid Points Which Move with Mean Flow.

however, that at all times the angle  $\alpha$  must lie between the limits

$$- 1/2 \leq \tan \alpha \leq + 1/2 \quad (26-1)$$

These limits are reached at dimensionless times  $t^* = 1/2, 3/2, 5/2, \dots$ . Each time the upper limit  $\tan \alpha = + 1/2$  is reached, the lines are all instantaneously flipped back to  $\tan \alpha = - 1/2$  in order to satisfy (26-1). The angle then smoothly increases again to the upper limit, whereupon the above instantaneous flip-flop action is repeated. The corresponding grid lines define a system of time-varying interpolation spaces. The moving lines form the edges of these spaces. It is quite natural to adopt the rule that within each interpolation space, the variation of all quantities shall be linear along any line parallel to any grid line.

The use of interpolation spaces whose shape varies with time in a linear/cyclic pattern suggests that the control volumes might be allowed to change in shape in an exactly analogous manner. This is indeed entirely feasible, and probably advantageous from a computational standpoint. At any rate, the choice between rigid or time-dependent control cell shapes can be made on the basis of convenience, since either choice is correct. However, time-dependent shape of control cells seems slightly more consistent with the time-dependent shape of the interpolation spaces. If this idea is adopted consistently, we will have at times  $t^* = 0, 1, 2, \dots$  all control cells and interpolation spaces instantaneously cubical. Similarly, at times  $t^* = 1/2, 3/2, 5/2, \dots$ , all control cells and interpolation spaces flip-flop instantaneously from  $\tan \alpha = + 1/2$  to  $\tan \alpha = - 1/2$ . However, the principal grid points themselves continue to move on with a majestic Lagrangian dignity, utterly unperturbed by the periodic flip-flop of the reference grid lines.

The gist of this postscript is that there is an early requirement for a simplified two-dimensional treatment of turbulence, and that future work should employ coordinates which move with the mean flow.

#### REFERENCES

1. Schlichting, H., Boundary Layer Theory, 4th Ed., McGraw-Hill, 1960, p. 492.
2. Emmons, H. W., "The Numerical Solution of the Turbulence Problem," Proceedings of the First Symposium in Applied Mathematics, Brown University, 1949, pp. 67-71.
3. Kraichnan, R. H., "Inertial Ranges in Two Dimensional Turbulence," Office of Naval Research, Research Report No. 11, Task NR 062-309, Contract Nonr 4307(00).

## APPENDIX A

### DEVELOPMENT OF BASIC DIFFERENCE EQUATIONS (METHOD C)

#### A.1 LOCATION OF GRID POINTS

In each of the horizontal directions  $x$  and  $z$ , and for both families of points, the number of grid rows needed is  $N$ . In the vertical or  $y$  direction, however, two extra rows are needed at the bottom and two at the top, to meet the special boundary conditions at these locations. Hence the number of stations needed in the vertical direction is  $(N+4)$ . Consequently the indices  $i, j, k$  in the two families vary over the following ranges

$$\begin{aligned} i^I &= i^{II} = 1, 2, 3, \dots, N \\ j^I &= j^{II} = 1, 2, 3, \dots, (N+4) \\ k^I &= k^{II} = 1, 2, 3, \dots, N \end{aligned} \quad (A1-1)$$

Spacing between any two successive rows in the same family is  $(L/N)$ . Any point  $(i, j, k)^{II}$  of family II is staggered by the amount  $(L/2N)$  in each of the positive  $x, y, z$  directions with respect to the corresponding point  $(i, j, k)^I$  of family I. In the vertical direction, the lowest row is at  $j^I = 1$ , the highest at  $j^{II} = (N+4)$ ; the reference plane  $y = 0$  is chosen to lie exactly midway between the lowest and highest grid rows, for the sake of symmetry in the  $S$  forces. In the  $x$  and  $z$  directions, the origin of coordinates is immaterial, and is arbitrarily placed at  $i^{II} = k^{II} = 0$ .

The following grid point locations satisfy the above requirements:

$$x_1^I = \frac{L}{N} (1 - \frac{1}{2})$$

$$x_1^{II} = \frac{L}{N} 1$$

$$y_j^I = \frac{L}{N} (j - \frac{11}{4} - \frac{N}{2})$$

$$y_j^{II} = \frac{L}{N} (j - \frac{9}{4} - \frac{N}{2}) \quad (A1-2)$$

$$z_k^I = \frac{L}{N} (k - \frac{1}{2})$$

$$z_k^{II} = \frac{L}{N} k$$

The constants  $C^I = \frac{11}{4}$  and  $C^{II} = \frac{9}{4}$  in the above results are found from the conditions

$$y_j^{II} - y_j^I = -\frac{L}{N} (C^{II} - C^I) = +\frac{L}{2N} \quad (A1-3)$$

$$y_1^I + y_{N+4}^{II} = +\frac{L}{N} (5 - C^I - C^{II}) = 0$$

Locations, other than those at the principal grid points themselves, are denoted by dimensionless coordinates  $\xi, \eta, \zeta$ . Thus within a volume cell of family I, with centroid at  $(i, j, k)^I$ , or anywhere along the bounding surfaces of this cell, which are surfaces passing through points of family II, we have

$$-1 \leq \xi = \frac{N}{2L} (x - x_1^I) \leq +1$$

$$-1 \leq \eta = \frac{N}{2L} (y - y_j^I) \leq +1 \quad (A1-4)$$

$$-1 \leq \zeta = \frac{N}{2L} (z - z_k^I) \leq +1$$

Similarly, within a volume cell of family II, with centroid at  $(i, j, k)^{II}$ , or anywhere along the bounding surfaces of this cell, which are surfaces passing through points of family I, we have

$$-1 \leq \xi = \frac{N}{2L} (x_1^{II} - x) \leq +1 \quad (A1-5)$$

$$-1 \leq \eta = \frac{N}{2L} (y_j^{II} - y) \leq +1$$

$$-1 \leq \zeta = \frac{N}{2L} (z_k^{II} - z) \leq +1$$

## A.2 SURFACE CONSTANTS

Surfaces passing through points of family I, and perpendicular to the x, y or z axes, are denoted by superscripts Ix, Iy or Iz, respectively. For surfaces passing through points of family II, we use superscripts IIX, IIy or IIz in like manner.

The three velocity components u, v, w are assumed to vary linearly along any line parallel to the x, y or z axes. Hence along a typical surface - let us say a surface Ix - we have

$$\begin{aligned} u &= A_0^{Ix} + A_1^{Ix} \eta + A_2^{Ix} \zeta + A_3^{Ix} \eta\zeta \\ v &= B_0^{Ix} + B_1^{Ix} \eta + B_2^{Ix} \zeta + B_3^{Ix} \eta\zeta \\ w &= C_0^{Ix} + C_1^{Ix} \eta + C_2^{Ix} \zeta + C_3^{Ix} \eta\zeta \end{aligned} \quad (A2-1)$$

where the A's, B's and C's are constants whose values are to be determined from the known values of the u's, v's and w's at the four grid points which constitute the corners of the surface. (This approach, Method C, ignores the additional data available from the two other nearby grid points, lying off the surface on either side of its centroid.)

Equations similar to (A2-1) may also be written for the other five surfaces denoted by superscripts Iy, Iz, IIX, IIy, IIz.

Taking for illustration only the expression for u in (A2-1), we have at the four corners

$$\begin{aligned} u &= u^I(i, j, k) & \eta &= 0 & \zeta &= 0 \\ u &= u^I(i, j+1, k) & \eta &= +1 & \zeta &= 0 \\ u &= u^I(i, j, k+1) & \eta &= 0 & \zeta &= +1 \\ u &= u^I(i, j+1, k+1) & \eta &= +1 & \zeta &= +1 \end{aligned} \quad (A2-2)$$

On the other hand, for the corresponding surface of family II, we have at the corners

$$\begin{aligned}
 u &= u^{II}(1, j, k) & \eta &= +1 & \zeta &= +1 \\
 u &= u^{II}(1, j-1, k) & \eta &= 0 & \zeta &= +1 \\
 u &= u^{II}(1, j, k-1) & \eta &= +1 & \zeta &= 0 \\
 u &= u^{II}(1, j-1, k-1) & \eta &= 0 & \zeta &= 0
 \end{aligned} \tag{A2-3}$$

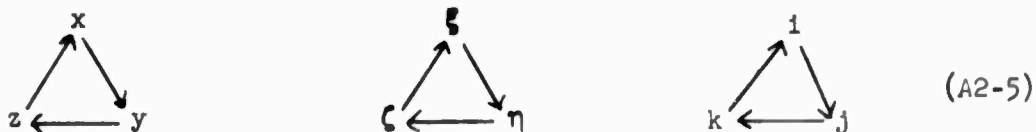
Now from (A2-1) and (A2-2) the solution for the A's becomes

$$\begin{aligned}
 A_0^{Ix}(1, j, k) &= \frac{1}{4} \left[ u^I(1, j, k) + u^I(1, j+1, k) + u^I(1, j, k+1) + u^I(1, j+1, k+1) \right] \\
 A_1^{Ix}(1, j, k) &= \frac{1}{4} \left[ -u^I(1, j, k) + u^I(1, j+1, k) - u^I(1, j, k+1) + u^I(1, j+1, k+1) \right] \\
 A_2^{Ix}(1, j, k) &= \frac{1}{4} \left[ -u^I(1, j, k) - u^I(1, j+1, k) + u^I(1, j, k+1) + u^I(1, j+1, k+1) \right] \\
 A_3^{Ix}(1, j, k) &= \frac{1}{4} \left[ +u^I(1, j, k) - u^I(1, j+1, k) - u^I(1, j, k+1) + u^I(1, j+1, k+1) \right]
 \end{aligned} \tag{A2-4A}$$

Similarly for the other family

$$\begin{aligned}
 A_0^{IIx}(1, j, k) &= \frac{1}{4} \left[ +u^I(1, j-1, k-1) + u^I(1, j, k-1) + u^I(1, j-1, k) + u^{II}(1, j, k) \right] \\
 A_1^{IIx}(1, j, k) &= \frac{1}{4} \left[ -u^I(1, j-1, k-1) + u^I(1, j, k-1) - u^I(1, j-1, k) + u^I(1, j, k) \right] \\
 A_2^{IIx}(1, j, k) &= \frac{1}{4} \left[ -u^I(1, j-1, k-1) - u^I(1, j, k-1) + u^I(1, j-1, k) + u^I(1, j, k) \right] \\
 A_3^{IIx}(1, j, k) &= \frac{1}{4} \left[ +u^I(1, j-1, k-1) - u^I(1, j, k-1) - u^I(1, j-1, k) + u^I(1, j, k) \right]
 \end{aligned} \tag{A2-4B}$$

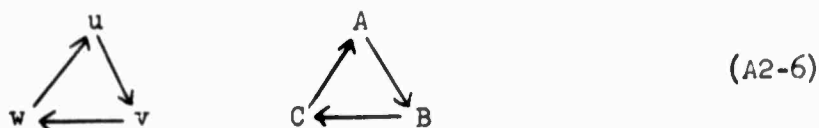
The above results may be extended to the other surfaces by cyclic permutations as symbolized by the diagrams



In other words, starting with any valid equation, and changing each variable or index thereof by a single step forward in the above diagrams, produces another valid equation.

On the other hand, the subscripts as in  $A_0, A_1, A_2, A_3$  do not change during the above permutations.

Furthermore, the results can also be extended to the other velocity components by the permutations symbolized below, namely



In sum we can say that Eqs. (A2-4A) and A2-4B), along with the permutation rules (A2-5) and (A2-6), fix all the A's, B's, and C's on the x, y and z surfaces of both families. The final expressions obtained are in terms of the u's, v's, or w's; that is, in terms of the velocities at the corner grid points.

In the sections which follow, various quantities needed for the continuity and momentum equations are derived and expressed in terms of the above surface constants - the A's, B's and C's. If desired, these constants can then be eliminated from the resulting expressions by substitution of the equations of this section. Hence the results required can be expressed directly in terms of the velocity components themselves. Such expanded formulas were actually used in TURBOCODE, MARK V in order to avoid the large computer storage which would be required for storing the many surface constants. (It can be shown that the number of storage places required for this purpose is approximately  $72N^2(N+4)$ .) The expanded formulas are very long, however, and it is considered impractical to give them in this appendix.

### A.3 DIVERGENCE

In terms of the surface constants, the expressions for divergence in the two families become

$$\begin{aligned}
 D^I(i, j, k) = \frac{N}{L} \{ & [A_0^{IIx}(i, j, k) - A_0^{IIx}(i-1, j, k)] \\
 & + [B_0^{IIy}(i, j, k) - B_0^{IIy}(i, j-1, k)] \\
 & + [C_0^{IIz}(i, j, k) - C_0^{IIz}(i, j, k-1)] \}
 \end{aligned} \tag{A3-1}$$

$$\begin{aligned}
 D^{II}(i, j, k) = \frac{N}{L} \{ & [A_0^{Ix}(i+1, j, k) - A_0^{Ix}(i, j, k)] \\
 & + [B_0^{Iy}(i, j+1, k) - B_0^{Iy}(i, j, k)] \\
 & + [C_0^{Iz}(i, j, k+1) - C_0^{Iz}(i, j, k)] \}
 \end{aligned} \tag{A3-2}$$

#### A.4 MEAN STRESSES FROM IMPOSED SHEAR RATE

The shear stress components associated with the interaction of the turbulent eddies with the mean shear rate  $\Omega^* = 1$ , and defined by Eq. (15-18), are as follows. For family -

$$\begin{aligned} S_x^{Ix}(1, j, k) &= - \left(\frac{L}{N}\right) \left\{ \left(j - \frac{9}{4} - \frac{N}{2}\right) 2A_0^{Ix}(1, j, k) + \frac{1}{3} A_1^{Ix}(1, j, k) \right\} \\ S_y^{Ix}(1, j, k) &= - \left(\frac{L}{N}\right) \left\{ \left(j - \frac{9}{4} - \frac{N}{2}\right) B_0^{Ix}(1, j, k) + \frac{1}{6} B_1^{Ix}(1, j, k) \right\} \\ S_z^{Ix}(1, j, k) &= - \left(\frac{L}{N}\right) \left\{ \left(j - \frac{9}{4} - \frac{N}{2}\right) C_0^{Ix}(1, j, k) + \frac{1}{6} C_1^{Ix}(1, j, k) \right\} \end{aligned} \quad (A4-1)$$

$$\begin{aligned} S_x^{Iy}(1, j, k) &= - \left(\frac{L}{N}\right) \left( j - \frac{11}{4} - \frac{N}{2} \right) B_0^{Iy}(1, j, k) \\ S_y^{Iy}(1, j, k) &= 0 \\ S_z^{Iy}(1, j, k) &= 0 \end{aligned} \quad (A4-2)$$

$$\begin{aligned} S_x^{Iz}(1, j, k) &= - \left(\frac{L}{N}\right) \left\{ \left(j - \frac{9}{4} - \frac{N}{2}\right) C_0^{Iz}(1, j, k) + \frac{1}{6} C_2^{Iz}(1, j, k) \right\} \\ S_y^{Iz}(1, j, k) &= 0 \\ S_z^{Iz}(1, j, k) &= 0 \end{aligned} \quad (A4-3)$$

Similarly, for family II

$$\begin{aligned}
 s_x^{IIx}(1,j,k) &= - \left(\frac{L}{N}\right) \left\{ \left(j - \frac{11}{4} - \frac{N}{2}\right) 2A_0^{IIx}(1,j,k) + \frac{1}{3} A_1^{IIx}(1,j,k) \right\} \\
 s_y^{IIx}(1,j,k) &= - \left(\frac{L}{N}\right) \left\{ \left(j - \frac{11}{4} - \frac{N}{2}\right) B_0^{IIx}(1,j,k) + \frac{1}{6} B_1^{IIx}(1,j,k) \right\} \\
 s_z^{IIx}(1,j,k) &= - \left(\frac{L}{N}\right) \left\{ \left(j - \frac{11}{4} - \frac{N}{2}\right) C_0^{IIx}(1,j,k) + \frac{1}{6} C_1^{IIx}(1,j,k) \right\} \quad (A4-4) \\
 s_x^{IIy}(1,j,k) &= - \left(\frac{L}{N}\right) \left(j - \frac{9}{4} - \frac{N}{2}\right) B_0^{IIy}(1,j,k) \\
 s_y^{IIy}(1,j,k) &= 0 \\
 s_z^{IIy}(1,j,k) &= 0 \\
 s_x^{IIz}(1,j,k) &= - \left(\frac{L}{N}\right) \left\{ \left(j - \frac{11}{4} - \frac{N}{2}\right) C_0^{IIz}(1,j,k) + \frac{1}{6} C_2^{IIz}(1,j,k) \right\} \\
 s_y^{IIz}(1,j,k) &= 0 \\
 s_z^{IIz}(1,j,k) &= 0
 \end{aligned}$$

## A.5 MOMENTUM FLUX

The components of the quadratic momentum flux stresses defined by Eq. (15-19) are given below

$$\begin{aligned}
 T_x^{Ix}(1,j,k) &= - \left[ A_0^{Ix}(1,j,k) \right]^2 + \frac{1}{3} \left[ A_1^{Ix}(1,j,k) \right]^2 \\
 &\quad + \frac{1}{3} \left[ A_2^{Ix}(1,j,k) \right]^2 + \frac{1}{9} \left[ A_3^{Ix}(1,j,k) \right]^2 \} \\
 T_y^{Ix}(1,j,k) &= - \left\{ B_0^{Ix}(1,j,k) A_0^{Ix}(1,j,k) + \frac{1}{3} B_1^{Ix}(1,j,k) A_1^{Ix}(1,j,k) \right. \\
 &\quad \left. + \frac{1}{3} B_2^{Ix}(1,j,k) A_2^{Ix}(1,j,k) + \frac{1}{9} B_3^{Ix}(1,j,k) A_3^{Ix}(1,j,k) \right\} \\
 T_z^{Ix}(1,j,k) &= - \left\{ C_0^{Ix}(1,j,k) A_0^{Ix}(1,j,k) + \frac{1}{3} C_1^{Ix}(1,j,k) A_1^{Ix}(1,j,k) \right. \\
 &\quad \left. + \frac{1}{3} C_2^{Ix}(1,j,k) A_2^{Ix}(1,j,k) + \frac{1}{9} C_3^{Ix}(1,j,k) A_3^{Ix}(1,j,k) \right\} \quad (A5-1)
 \end{aligned}$$

These results suffice to fix the pattern. The remaining equations may be found by application of the permutation rules (A2-5) and (A2-6). Exactly similar expressions apply to the surfaces of family II; it is necessary only to change superscript I to II. There are nine separate equations in each family, or eighteen equations in all for the T components.

## A.6 LOCAL VISCOUS STRESSES

The local viscous stresses at a point follow the pattern below.

For family I, the local normal and shear stresses are, respectively, of the form

$$\begin{aligned}\tau_{xx}^I(1,j,k) &= \frac{2N}{L} \left[ A_0^{IIx}(1,j,k) - A_0^{IIx}(1-1,j,k) \right] - \frac{2}{3} D^I(1,j,k) \\ \tau_{yz}^I(1,j,k) &= \frac{N}{L} \left\{ \left[ C_0^{IIy}(1,j,k) - C_0^{IIy}(1,j-1,k) \right] \right. \\ &\quad \left. + \left[ B_0^{IIz}(1,j,k) - B_0^{IIz}(1,j,k-1) \right] \right\}\end{aligned}\tag{A6-1}$$

For family II, the corresponding forms are

$$\begin{aligned}\tau_{xx}^{II}(1,j,k) &= \frac{2N}{L} \left[ A_0^{Ix}(1+1,j,k) - A_0^{Ix}(1,j,k) \right] - \frac{2}{3} D^{II}(1,j,k) \\ \tau_{yz}^{II}(1,j,k) &= \left(\frac{N}{L}\right) \left\{ \left[ C_0^{Iy}(1,j+1,k) - C_0^{Iy}(1,j,k) \right] \right. \\ &\quad \left. + \left[ B_0^{Iz}(1,j,k+1) - B_0^{Iz}(1,j,k) \right] \right\}\end{aligned}\tag{A6-2}$$

The other four stresses of each family are found by the usual permutations of (A6-1) and (A6-2).

The divergences  $D^I$  and  $D^{II}$  which occur in these equations are of the order of the round-off error only and may be neglected if desired.

## A.7 MEAN VISCOUS STRESSES

The mean effective viscous stresses over the surface as defined by Eq. (15-20) are computed from the local viscous stresses according to the following format

For family I

$$\begin{aligned}
 H_X^{Ix}(1,j,k) &= \frac{1}{4} \left[ \tau_{xx}^I(1,j,k) + \tau_{xx}^I(1,j+1,k) \right. \\
 &\quad \left. + \tau_{xx}^I(1,j,k+1) + \tau_{xx}^I(1,j+1,k+1) \right] \\
 H_Y^{Ix}(1,j,k) &= \frac{1}{4} \left[ \tau_{xy}^I(1,j,k) + \tau_{xy}^I(1,j+1,k) \right. \\
 &\quad \left. + \tau_{xy}^I(1,j,k+1) + \tau_{xy}^I(1,j+1,k+1) \right] \\
 H_Z^{Ix}(1,j,k) &= \frac{1}{4} \left[ \tau_{zx}^I(1,j,k) + \tau_{zx}^I(1,j+1,k) \right. \\
 &\quad \left. + \tau_{zx}^I(1,j,k+1) + \tau_{zx}^I(1,j+1,k+1) \right] \quad (A7-1)
 \end{aligned}$$

The components on the other two surfaces are now found by the usual permutation.

For family II only the indices differ. The first equation suffices to establish the sequence

$$\begin{aligned}
 H_X^{IIx}(1,j,k) &= \frac{1}{4} \left[ \tau_{xx}^{II}(1,j-1,k-1) + \tau_{xx}^{II}(1,j,k-1) \right. \\
 &\quad \left. + \tau_{xx}^{II}(1,j-1,k) + \tau_{xx}^{II}(1,j,k) \right] \quad (A7-2)
 \end{aligned}$$

etc.

The local stresses may be eliminated from (A7-1) and (A7-2) by use of (A6-1) and (A6-2). The process is lengthy but not difficult. A single typical result is the equation

$$\begin{aligned}
 H_x^{IIx}(1,j,k) = \frac{N}{2L} \{ & A_0^{IIx}(1,j,k) + A_0^{IIx}(1,j+1,k) + A_0^{IIx}(1,j,k+1) \\
 & + A_0^{IIx}(1,j+1,k+1) - A_0^{IIx}(1-1,j,k) - A_0^{IIx}(1-1,j+1,k) \\
 & - A_0^{IIx}(1-1,j,k+1) - A_0^{IIx}(1-1,j+1,k+1) \} \\
 & - \frac{1}{6} \{ D^I(1,j,k) + D^I(1,j+1,k) + D^I(1,j,k+1) \\
 & + D^I(1,j+1,k+1) \}
 \end{aligned} \tag{A7-3}$$

The extension of these results to all eighteen components follows in the usual way.

#### A.8 RESULTANT PRIMARY STRESSES

The sum of the S, T and H stresses as given by Eq. (15-22) is termed the resultant primary stress R. These R stresses are of the form

$$R_X^{Ix}(i,j,k) = S_X^{Ix}(i,j,k) + T_X^{Ix}(i,j,k) + H_X^{Ix}(i,j,k) \quad (A8-1)$$

Eq. (A8-1) represents the x component on the Ix face. Components in the y and z directions are indicated by corresponding subscripts, and the other surfaces are indicated by corresponding superscripts. There are eighteen R stresses in all. Note, however, that eight of the eighteen S components in Eq. (A8-1) are zeros.

## A.9 NET PRIMARY FORCES

According to Eq. (15-24) the net primary forces are found by summation of the primary stresses over the six bounding surfaces of the volume element. The results are of the following form.

For volume elements with centroids of family I, bounded by surfaces of family II -

$$\begin{aligned} F_x^I(1,j,k) = \left(\frac{N}{L}\right) \{ & [R_x^{IIx}(1,j,k) - R_x^{IIx}(1-1,j,k)] \\ & + [R_x^{IIy}(1,j,k) - R_x^{IIy}(1,j-1,k)] \\ & + [R_x^{IIz}(1,j,k) - R_x^{IIz}(1,j,k-1)] \} \end{aligned} \quad (A9-1)$$

Similarly, for volume elements with centroids of family II, bounded by surfaces of family I

$$\begin{aligned} F_x^{II}(1,j,k) = \left(\frac{N}{L}\right) \{ & [R_x^{Ix}(1+1,j,k) - R_x^{Ix}(1,j,k)] \\ & + [R_x^{Iy}(1,j+1,k) - R_x^{Iy}(1,j,k)] \\ & + [R_x^{Iz}(1,j,k+1) - R_x^{Iz}(1,j,k)] \} \end{aligned} \quad (A9-2)$$

Of course the corresponding y and z components are found by changing all subscripts accordingly in Eqs. (A9-1) and (A9-2). There are three force components in each family, or six in all.

## A.10 MEAN PRIMARY FORCES

Note from Eq. (16-3) that in order to determine the divergence of the net primary forces, it is necessary to evaluate quantities of the form

$$G = \frac{1}{\delta S} \int_{\delta S} \hat{F} \cdot \hat{n} \, dS \quad (A10-1)$$

We call these quantities the mean primary forces. By the usual interpolation rules of Method C, the mean value over the surface  $\delta S$  is simply taken as the mean of the four corner values.

Thus for surfaces of family I, we obtain the form

$$G_x^{Ix} = \frac{1}{4} \left[ F_x^I(i, j, k) + F_x^I(i, j+1, k) + F_x^I(i, j, k+1) + F_x^I(i, j+1, k+1) \right] \quad (A10-2)$$

and similarly for the y and z components.

Thus for surfaces of family II

$$G_x^{IIx} = \frac{1}{4} \left[ F_x^{II}(i, j, k) + F_x^{II}(i, j-1, k) + F_x^{II}(i, j, k-1) + F_x^{II}(i, j-1, k-1) \right] \quad (A10-3)$$

and similarly for the y and z components.

The total number of components is six, namely,  $G_x^{Ix}$ ,  $G_y^{Iy}$ ,  $G_z^{Iz}$ ,  $G_x^{IIx}$ ,  $G_y^{IIy}$ ,  $G_z^{IIz}$ . Note that the subscript and superscript letters are always in agreement.

## A.11 PRESSURE COMPATIBILITY EQUATION

It is convenient for this section to adopt a simple letter symbol for the divergence quantity  $\nabla \cdot \hat{\mathbf{F}}$ . We arbitrarily choose the letter Q for this purpose.

From Eq. (16-3) we obtain

$$\begin{aligned} Q^I(1,j,k) = & \left(\frac{N}{L}\right) \left\{ \left[ G_x^{IIx}(1,j,k) - G_x^{IIx}(1-1,j,k) \right] \right. \\ & + \left[ G_y^{IIy}(1,j,k) - G_y^{IIy}(1,j-1,k) \right] \\ & \left. + \left[ G_z^{IIz}(1,j,k) - G_z^{IIz}(1,j,k-1) \right] \right\} \end{aligned} \quad (A11-1)$$

$$\begin{aligned} Q^{II}(1,j,k) = & \left(\frac{N}{L}\right) \left\{ \left[ G_x^{Ix}(1+1,j,k) - G_x^{Ix}(1,j,k) \right] \right. \\ & + \left[ G_y^{Iy}(1,j+1,k) - G_y^{Iy}(1,j,k) \right] \\ & \left. + \left[ G_z^{Iz}(1,j,k+1) - G_z^{Iz}(1,j,k) \right] \right\} \end{aligned} \quad (A11-2)$$

Substituting these results into Eq. (16-7) then fixes the pressure-compatibility equation, namely

$$\nabla^2 \varphi^I(1,j,k) = Q^I(1,j,k) + C_D \frac{N}{L} \sqrt{2\bar{E}} D^I(1,j,k) \quad (A11-3)$$

$$\nabla^2 \varphi^{II}(1,j,k) = Q^{II}(1,j,k) + C_D \frac{N}{L} \sqrt{2\bar{E}} D^{II}(1,j,k) \quad (A11-4)$$

These results fix the required values of  $\nabla^2 \phi$  throughout most of the grid. Near the top and bottom of the block, however, special considerations apply because of the sliding boundary conditions. In the first place the pressure-compatibility equations (All-3) and (All-4) are not even needed for the four rows  $j = 1$ ,  $j = 2$ ,  $j = N+3$ ,  $j = N+4$ . The reason is that these are extra rows outside the block. The velocities in these rows are not computed by the usual method, but are found indirectly by taking advantage of the sliding blockwise periodicity of the phenomena. Hence values of  $\nabla^2 \phi$  are needed only over the range  $3 \leq j \leq (N+2)$ . It turns out that Eq. (All-3) is valid over this range except for the single value  $j^I = 3$ . Similarly, Eq. (All-4) is valid over the required range, except for the single value  $j^{II} = N+2$ . Modified equations are required for these two particular rows. The necessary special equations are derived in Appendix B.

Tracing back the Q terms in Eqs. (All-3) and (All-4) shows that they are definite and known functions of the turbulent-velocity distributions. Hence they represent a constraint on  $\nabla^2 \phi$  such as to make the resulting distribution of the pressure function  $\phi$  compatible with the already existing velocity perturbations. The last term on the right of (All-3) and (All-4) represents a correction for error divergence. The positive dimensionless constant  $C_D$  should be large enough to provide good divergence correction, but not so high as to cause computational instability; its optimum value is best found by numerical experimentation on the computer itself.

## A.12 SOLUTION FOR PRESSURE BY ITERATION

By application of the differencing formula (13-10) we can express  $\partial\varphi/\partial x = \varphi_x$  at any grid point in terms of the values of  $\varphi$  at adjacent grid points.

A repetition of this procedure gives  $\partial^2\varphi/\partial x^2 = \partial\varphi_x/\partial x = \varphi_{xx}$  at any point in terms of adjacent grid point values of  $\varphi$ . By cyclic permutation of subscripts, corresponding results can be found for  $\partial^2\varphi/\partial y^2 = \partial\varphi_y/\partial y = \varphi_{yy}$  and for  $\partial^2\varphi/\partial z^2 = \partial\varphi_z/\partial z = \varphi_{zz}$ . Adding these three results finally gives an expression for  $\nabla^2\varphi = (\varphi_{xx} + \varphi_{yy} + \varphi_{zz})$  at any grid point in terms of the values of  $\varphi$  at nearby grid points. The procedure, while lengthy, is not difficult.

It is convenient to multiply through by the factor  $\frac{3}{2} (L/N)^2$  in order to simplify the expression. In this way we obtain the result

$$\begin{aligned} \frac{3}{2} \left(\frac{L}{N}\right)^2 \nabla^2 \varphi^I(i, j, k) = & \varphi^I(i, j, k) + \frac{1}{6} \left[ \varphi^I(i-1, j, k) + \varphi^I(i, j-1, k) \right. \\ & + \varphi^I(i, j, k-1) + \varphi^I(i+1, j, k) + \varphi^I(i, j+1, k) \\ & \left. + \varphi^I(i, j, k+1) \right] - \frac{1}{8} \left[ \varphi^I(i-1, j-1, k-1) + \varphi^I(i-1, j-1, k+1) \right. \\ & + \varphi^I(i-1, j+1, k-1) + \varphi^I(i-1, j+1, k+1) + \varphi^I(i+1, j-1, k-1) \\ & \left. + \varphi^I(i+1, j-1, k+1) + \varphi^I(i+1, j+1, k-1) + \varphi^I(i+1, j+1, k+1) \right] \\ & - \frac{1}{12} \left[ \varphi^I(i-1, j-1, k) + \varphi^I(i-1, j, k-1) + \varphi^I(i-1, j, k+1) \right. \\ & + \varphi^I(i-1, j+1, k) + \varphi^I(i, j-1, k-1) + \varphi^I(i, j-1, k+1) \\ & + \varphi^I(i, j+1, k-1) + \varphi^I(i, j+1, k+1) + \varphi^I(i+1, j-1, k) \\ & \left. + \varphi^I(i+1, j, k-1) + \varphi^I(i+1, j, k+1) + \varphi^I(i+1, j+1, k) \right] \quad (A12-1) \end{aligned}$$

Exactly analogous results apply to the other family; it is necessary only to change all superscripts from I to II. Hence a single explanation will serve to cover both cases.

Suppose we have available a set of trial values of the function  $\phi$  at all grid points. If this is in fact the correct function, then it will satisfy Eq. (A12-1) at all grid points; the left side of this equation is known, of course, from the calculations of the previous section. However, if the trial solution is not correct, the terms on the right side of (A12-1) will not in general equal the known values required on the left.

We must therefore devise a method for adjusting the  $\phi$ 's on the right so that the required value on the left can always be obtained at any specified point  $(i,j,k)$ . This procedure is then applied in succession to each point in the field, for both families of points. The entire field is swept in this way again and again until, at length, the values of the required corrections become everywhere less than some very small pre-assigned error. This then fixes the required pressure distribution.

An essential constraint upon the solution is that the average pressure for each family of points is zero. This follows from the very definition of the turbulent pressure perturbation as the net deviation from the prevailing mean pressure. Consequently either the procedure for adjusting the  $\phi$ 's should leave the mean value unchanged, or it must be followed eventually by another correction which restores the zero mean. This restoration is easily accomplished by addition of the appropriate constant to the values of  $\phi$  at all points in the field. An additive constant leaves all differences unaffected.

The simplest method of adjustment is to correct the value of  $\phi^I(i,j,k)$ , which is the first term on the right side of Eq. (A12-1), so as to bring this equation into balance. This is the method that has been adopted in TURBOCODE, MARK V. This procedure pulls the solution away from zero mean, but this is easily corrected later in the manner indicated above.

It is not difficult to modify the adjustment procedure so that it does not disturb the mean value in the first place. For this purpose it is necessary only to adjust not only  $\phi^I(i,j,k)$ , but also the next group of six points as well. These six points are all adjusted by equal amounts. This additional degree of freedom may be used to keep the mean value unchanged while Eq. (A12-1) is brought into balance.

More elaborate relaxation procedures are also possible. Note that the 27 terms on the right side consist of the term  $\phi^I(i,j,k)$  itself, plus three other groups of six, eight and twelve members, respectively. If a separate correction quantity is assigned to each of these four categories, this provides four degrees of freedom. One of these is used to satisfy Eq. (A12-1), another to maintain zero mean. The remaining two may be utilized to minimize the square of the error. This leads to perfectly definite relaxation formulas. It is somewhat dubious, however, whether these more elaborate procedures have any real computational advantages. Hence they have not been utilized up to now. However, the matter may be worthy of further study.

Each time the solution is advanced by one time increment, the above relaxation procedure must be repeated. The previously existing pressure distribution is taken as the first approximation for the new pressure. If time increments are small, the pressure distribution does not change much during any one time step, and the pressure solution converges in comparatively few iterations.

Attention is invited to the fact that the pressures  $\phi^I$  and  $\phi^{II}$  appear to be virtually independent of each other. This arises from the manner of differencing in method C. Such apparent separation cannot occur in differencing methods B or A. This circumstance might also make the pressure iteration procedure in method C somewhat more susceptible to instability difficulties than would be the case with either of the other methods.

### A.13 NET PRESSURE FORCES

Once the pressure distribution  $\varphi$  has been found, the net pressure forces are easily determined. The relevant difference equations for the two families follow the patterns below, namely

$$\begin{aligned} \varphi_x^I(i, j, k) = & + \frac{N}{4L} \left\{ \varphi^{II}(i, j, k) + \varphi^{II}(i, j-1, k) + \varphi^{II}(i, j, k-1) \right. \\ & + \varphi^{II}(i, j-1, k-1) - \varphi^{II}(i-1, j, k) - \varphi^{II}(i-1, j-1, k) \\ & \left. - \varphi^{II}(i-1, j, k-1) - \varphi^{II}(i-1, j-1, k-1) \right\} \end{aligned} \quad (A13-1)$$

$$\begin{aligned} \varphi_x^{II}(i, j, k) = & \frac{N}{4L} \left\{ \varphi^I(i+1, j+1, k+1) + \varphi^I(i+1, j, k+1) + \varphi^I(i+1, j+1, k) \right. \\ & + \varphi^I(i+1, j, k) - \varphi^I(i, j+1, k+1) - \varphi^I(i, j, k+1) - \varphi^I(i, j+1, k) \\ & \left. - \varphi^I(i, j, k) \right\} \end{aligned} \quad (A13-2)$$

The other two components in each family are found by the usual cyclic permutations of these equations.

#### A.14 VELOCITY TIME DERIVATIVES

The local velocity time derivatives are now of the form

$$u_t^I(i,j,k) = v_x^I(i,j,k) - \varphi_x^I(i,j,k) \quad (A14-1)$$

Cyclic permutation gives the corresponding results for  $v_t^I$  and  $w_t^I$ .  
The expressions for family II are exactly similar.

#### A.15 NEW VELOCITIES

The new velocities at the end of a time increment  $\tau$  are of the form

$$u_N^I(i,j,k) = u^I(i,j,k) + \tau u_t^I(i,j,k) \quad (A15-1)$$

The extension to the other components and to the other family is the same as in the previous section.

This step completes the calculation of the new velocity distributions at the end of the time interval. The whole process is then repeated for the next time interval.

## APPENDIX B

### DIVERGENCE CORRECTION AT SLIDING BOUNDARIES

#### B.1 SLIDING INTERPOLATION

It has already been pointed out in Appendix A that in the y direction calculation of velocities, forces, pressures, and so on proceeds in the normal manner only over the range  $j = 3, 4, 5, \dots, N+2$ . Values outside this range are obtained by an interpolation process which takes into account the sliding boundary conditions. Thus values at  $j = 1$  and  $j = 2$  are obtained by this sliding interpolation method from the known values at  $j = N+1$  and  $j = N+2$ , respectively. Similarly, the values at  $j = N+3$  and  $j = N+4$  are obtained by sliding interpolation from the known values at  $j = 3$  and  $j = 4$ , respectively. It will be shown that this circumstance affects the divergences and the required divergence corrections in rows  $j^I = 3$  and  $j^{II} = N+2$ .

The interpolation procedure is based on the fact that the entire solution is blockwise periodic. This means, for example, that at any time  $t$

$$u^I(1,2,k) = u^I(1+Nt,N+2,k) \quad (B1-1)$$

$$u^{II}(1,N+3,k) = u^{II}(1-Nt,3,k)$$

The complication arises, however, that the quantities  $(1+Nt)$  and  $(1-Nt)$  are usually not integers, and therefore usually represent positions which lie somewhere between grid points. Nevertheless, values at such intermediate locations can be estimated by linear interpolation

between the known values at the two adjacent grid points on either side of the desired location.

Any real numbers can always be divided into two parts, one of which is an integer, the other a fraction of magnitude smaller than unity. It is convenient to introduce the notation

$$\begin{aligned} I(s) &= \text{integral part of } s \\ F(s) &= \text{fractional part of } s \end{aligned} \quad (\text{B1-2})$$

from which it is obvious that for any  $s$

$$s = I(s) + F(s) \quad (\text{B1-3})$$

It follows from this that the required intermediate point falls between two adjacent grid points according to the relations

$$I(1 + Nt) \leq (1 + Nt) < I(1 + Nt) + 1 \quad (\text{B1-4})$$

$$\text{or} \quad I(1 - Nt) \leq (1 - Nt) < I(1 - Nt) + 1$$

The various integers in (B1-4) may or may not fall within the range from 1 thru  $N$ , inclusive. However, because of the periodicity of the solution we may shift each integer by any exact integral multiple of  $N$  such that the shifted value does lie within the above range. To express this idea we introduce a shift operator  $S( )$  such that

$$1 \leq S(s) = s + KN < N \quad (\text{B1-5})$$

where  $K$  is an integer whose value is uniquely fixed by the above inequalities.

With this notation we may now define the following quantities:

$$\begin{array}{lcl}
 t' = F(t) & & \\
 i_L = S [I(1+Nt')] & \left. \begin{array}{l} \\ \\ \\ \\ \end{array} \right\} & t' = \text{truncated time} \\
 i_{LP} = S [I(1+Nt') + 1] & & \text{Shifted indices (integers)} \\
 i_U = S [I(1-Nt')] & & \text{for interpolation at} \\
 i_{UP} = S [I(1-Nt') + 1] & & \text{upper and lower} \quad (B1-6) \\
 & & \text{boundaries}
 \end{array}$$

$$\begin{array}{lcl}
 w_U = w_{LP} = F(Nt') & \left. \begin{array}{l} \\ \\ \end{array} \right\} & \text{Weighting factors} \\
 w_L = w_{UP} = 1 - F(Nt') & &
 \end{array}$$

Consequently, the relations implied by (B1-1) can now be written explicitly in the form

$$\begin{array}{l}
 u^I(1,2,k) = w_L u^I(i_L, N+2, k) + w_{LP} u^I(i_{LP}, N+2, k) \\
 u^{II}(1, N+3, k) = w_U u^{II}(i_U, 3, k) + w_{UP} u^{II}(i_{UP}, 3, k) \quad (B1-7)
 \end{array}$$

Note that these interpolation formulas are based on the values of the  $i$ 's and  $w$ 's as evaluated at the beginning of the time interval. The subsequent discussion will show the usefulness also of interpolation formulas based on  $i$ 's and  $w$ 's evaluated at the end of the time step.

Using subscript  $N$  to denote new values at the end of the time step  $\tau$ , we write

$$\begin{array}{lcl}
 t_N = t + \tau & \text{New time} & \\
 t'_N = F(t_N) & \text{Truncated new time} & \\
 i_{LN} = S [I(1+Nt'_N)] & \left. \begin{array}{l} \\ \\ \\ \\ \end{array} \right\} & \text{New shifted indices} \quad (B1-8) \\
 i_{LPN} = S [I(1+Nt'_N) + 1] & & \\
 i_{UN} = S [I(1-Nt'_N)] & & \\
 i_{UPN} = S [I(1-Nt'_N) + 1] & &
 \end{array}$$

$$\left. \begin{aligned} w_{UN} &= w_{LPN} = F(Nt'_N) \\ w_{LN} &= w_{UPN} = 1 - F(Nt'_N) \end{aligned} \right\} \begin{array}{l} \text{New weighting} \\ \text{factors} \end{array}$$

Of course, for the functions being interpolated, like velocities, pressures, forces, and so on, only the initial values are known at the particular stage of calculation here involved. Hence, for these quantities, only the initial values are involved, in any case. To distinguish the following interpolated values from those of (B1-7) we add the subscript s. Then

$$\begin{aligned} u_S^I(1,2,k) &= w_{LN} u^I(i_{LN}, N+2, k) + w_{LPN} u^I(i_{LPN}, N+2, k) \\ u_S^{II}(1, N+3, k) &= w_{UN} u^{II}(i_{UN}, 3, k) + w_{UPN} u^{II}(i_{UPN}, 3, k) \end{aligned} \quad (B1-9)$$

In certain calculations it will be useful to evaluate the small differences between the values given by the two different interpolation formulas (B1-7 and B1-9). Hence we introduce the further definitions..

$$\begin{aligned} \Delta u_S^I(1,2,k) &= u_S^I(1,2,k) - u^I(1,2,k) \\ \Delta u_S^{II}(1, N+3, k) &= u_S^{II}(1, N+3, k) - u^{II}(1, N+3, k) \end{aligned} \quad (B1-10)$$

A similar notation is applied to interpolated forces and pressure gradients.

## B.2 DIVERGENCE CORRECTIONS

The divergence at the lower boundary  $j^I = 3$  may be written out in full as follows:

$$D^I(1,3,k) =$$

$$\begin{aligned} & \left(\frac{N}{4L}\right) \left\{ u^{II}(1,3,k) + u^{II}(1,3,k-1) - u^{II}(1-1,3,k) - u^{II}(1-1,3,k-1) \right. \\ & + v^{II}(\text{"}) + v^{II}(\text{"}) + v^{II}(\text{"}) + v^{II}(\text{"}) \\ & + w^{II}(\text{"}) - w^{II}(\text{"}) + w^{II}(\text{"}) - w^{II}(\text{"}) \left. \right\} \\ & + \left(\frac{N}{4L}\right) \left\{ u^{II}(1,2,k) + u^{II}(1,2,k-1) - u^{II}(1-1,2,k) - u^{II}(1-1,2,k-1) \right. \\ & - v^{II}(\text{"}) - v^{II}(\text{"}) - v^{II}(\text{"}) - v^{II}(\text{"}) \\ & + w^{II}(\text{"}) - w^{II}(\text{"}) + w^{II}(\text{"}) - w^{II}(\text{"}) \left. \right\} \quad (B2-1) \end{aligned}$$

To facilitate subsequent operations, we adopt the following abbreviated notation to represent the above result, namely,

$$D^I(1,3,k) = \left(\frac{N}{4L}\right) \left\{ u^{II}(1,3,k) + \dots \right\} + \left(\frac{N}{4L}\right) u^{II} \left\{ (1,2,k) + \dots \right\} \quad (B2-2)$$

This equation represents the situation at some arbitrary time  $t$ , regarded as the initial time of the current time step. Using subscript  $N$  to denote new values at the end of the time step, we may write

$$D_N^I(1,3,k) = \left(\frac{N}{4L}\right) \left\{ u_N^{II}(1,3,k) + \dots \right\} + \left(\frac{N}{4L}\right) \left\{ u_N^{II}(1,2,k) + \dots \right\} \quad (B2-3)$$

We subtract these two equations and impose the condition that the new divergence shall be zero. Then upon rearrangement -

$$\begin{aligned}
 D_N^I(1,3,k) = 0 = D^I(1,3,k) \\
 + \left(\frac{N}{4L}\right) \left\{ \left[ u_N^{II}(1,3,k) - u^{II}(1,3,k) \right] + \text{-----} \right\} \\
 + \left(\frac{N}{4L}\right) \left\{ \left[ u_N^{II}(1,2,k) - u^{II}(1,2,k) \right] + \text{-----} \right\}
 \end{aligned} \tag{B2-4}$$

The velocity changes on the right side of (B2-4) are computed from the equation of motion. The situation is regular at  $j = 3$ , therefore

$$\left[ u_N^{II}(1,3,k) - u^{II}(1,3,k) \right] = \tau \left[ F_x^{II}(1,3,k) - \phi_x^{II}(1,3,k) \right] \tag{B2-5}$$

However, at  $j = 2$ , the interpolation rule applies. In particular, the new velocities here are of the form

$$\begin{aligned}
 u_N^{II}(1,2,k) = \\
 -w_{LN} \left\{ u^{II}(1_{LN}, N+2, k) + \tau \left[ F_x^{II}(1_{LN}, N+2, k) - \phi_x^{II}(1_{LN}, N+2, k) \right] \right\} \\
 +w_{LPN} \left\{ u^{II}(1_{LPN}, N+2, k) + \tau \left[ F_x^{II}(1_{LPN}, N+2, k) \right. \right. \\
 \left. \left. - \phi_x^{II}(1_{LPN}, N+2, k) \right] \right\}
 \end{aligned} \tag{B2-6}$$

Upon regrouping of the terms on the right side of this equation, and employment of the definitions of (B1-9), this result may be re-written in the concise form

$$u_N^{II}(1,2,k) = u_S^{II}(1,2,k) + \tau \left[ F_{XS}^{II}(1,2,k) - \phi_{XS}^{II}(1,2,k) \right] \tag{B2-7}$$

Next we subtract the original velocity to find the net velocity change. Using the notation of (B1-10), we obtain

$$\begin{aligned} & [u_N^{II}(1,2,k) - u^{II}(1,2,k)] \\ & = \Delta u_S^{II}(1,2,k) + \tau \left[ F_{xS}^{II}(1,2,k) - \phi_x^{II}(1,2,k) - \Delta \phi_{xS}^{II}(1,2,k) \right] \quad (B2-8) \end{aligned}$$

It is instructive to compare this result with (B2-5). This shows the difference in the velocity change between a regular interior point  $j=3$ , and a point  $j=2$  exterior to the block.

Upon substitution of the expressions of type (B2-5) and (B2-9) into (B2-4) and rearrangement, the basic divergence equation may be reduced to the following form. The various groups of terms are identified by number, to facilitate the subsequent discussion.

$$\begin{aligned} & \left(\frac{N}{4L}\right) \left\{ \left[ \phi_x^{II}(1,3,k) + \dots \right]^{(1)} + \left[ \phi_x^{II}(1,2,k) + \dots \right] \right\} \\ & + \left(\frac{N}{4L}\right) \left\{ \Delta \phi_x^{II}(1,2,k) + \dots \right\}^{(2)} \\ & = \nabla^2 \phi^{(3)}(1,3,k) = \left(\frac{N}{4L}\right) \left\{ \left[ F_x^{II}(1,3,k) + \dots \right]^{(4)} \right. \\ & + \left. \left[ F_{xS}^{II}(1,2,k) + \dots \right]^{(5)} \right\} + \frac{1}{\tau} D^I(1,3,k)^{(6)} \\ & + \frac{1}{\tau} \left(\frac{N}{4L}\right) \left\{ \Delta u^{II}(1,2,k) + \dots \right\}^{(7)} \quad (B2-9) \end{aligned}$$

This result establishes both the required value of  $\nabla^2 \phi$ , term (3), and the corresponding pressure solution. The required value of  $\nabla^2 \phi$  is fixed by the terms on the right, which depend only on the existing velocity distribution. Terms (4) and (5) together represent the main effect. This is exactly of the same form as found in the interior regions of the block, except that the term (5) involves the modified

interpolation formulas as signified by the s subscript. Term (6) is the usual divergence-correction term. The new term is (7) which represents an additional correction associated purely with the sliding-boundary condition.

On the left side, the term (1) is found to represent the usual solution for  $\nabla^2 \phi$  which may be expressed directly in terms of the pressures themselves. Term (2) is a small correction associated with the sliding boundary condition. This correction must be included in the iteration solution for the pressures, in order to obtain a divergence free result.

In expanded form, the two corrections associated with the sliding boundary condition are found to be as follows:

$$\begin{aligned} & \frac{1}{\tau} \left( \frac{N}{4L} \right) \left\{ \Delta u^{II(7)}_{(1,2,k)} + \dots \right\} \\ & = \frac{1}{\tau} \left( \frac{N}{4L} \right) \left\{ \Delta u^{II}_{(1,2,k)} + \Delta u^{II}_{(1,2,k-1)} - \Delta u^{II}_{(1-1,2,k)} - \Delta u^{II}_{(1-1,2,k-1)} \right. \\ & \quad - \Delta v^{II} \left( \begin{array}{c} " \\ " \end{array} \right) - \Delta v^{II} \left( \begin{array}{c} " \\ " \end{array} \right) - \Delta v^{II} \left( \begin{array}{c} " \\ " \end{array} \right) - \Delta v^{II} \left( \begin{array}{c} " \\ " \end{array} \right) \\ & \quad \left. + \Delta w^{II} \left( \begin{array}{c} " \\ " \end{array} \right) - \Delta w^{II} \left( \begin{array}{c} " \\ " \end{array} \right) - \Delta w^{II} \left( \begin{array}{c} " \\ " \end{array} \right) + \Delta w^{II} \left( \begin{array}{c} " \\ " \end{array} \right) \right\} \quad (B2-10) \end{aligned}$$

$$\begin{aligned} & \left( \frac{N}{4L} \right) \left\{ \Delta \phi^{II(2)}_{(1,2,k)} + \dots \right\} = \frac{3}{2} \left( \frac{N}{L} \right)^2 \left\{ \frac{1}{2} \Delta \phi^I_{(1,3,k)} + \dots \right. \\ & - \frac{1}{12} \left[ \Delta \phi^I_{(1-1,3,k)} + \Delta \phi^I_{(1,3,k-1)} + \Delta \phi^I_{(1+1,3,k)} + \Delta \phi^I_{(1,3,k+1)} \right] \\ & - \frac{1}{24} \left[ \Delta \phi^I_{(1-1,3,k-1)} + \Delta \phi^I_{(1-1,3,k+1)} + \Delta \phi^I_{(1+1,3,k-1)} \right. \\ & \left. \left. + \Delta \phi^I_{(1+1,3,k+1)} \right] \right\} \quad (B2-11) \end{aligned}$$

The corresponding results for the upper boundary may now be found by a systematic permutation of superscripts and indices. Hence we obtain

$$\begin{aligned}
& - \frac{N}{4L} \left\{ \left[ \overset{(1)}{\varphi_x^I(1, N+2, k) + \dots} \right] + \left[ \varphi_x^I(1, N+3, k) + \dots \right] \right\} \\
& - \left( \frac{N}{4L} \right) \left\{ \overset{(2)}{\Delta \varphi_x^I(1, N+3, k) + \dots} \right\} = \overset{(3)}{\nabla^2 \varphi^{II}(1, N+2, k)} \\
& = - \left( \frac{N}{4L} \right) \left\{ \left[ \overset{(4)}{F_x^I(1, N+2, k) + \dots} \right] + \left[ \overset{(5)}{F_{xs}^I(1, N+3, k) + \dots} \right] \right\} \\
& + \frac{1}{\tau} D^{II}(1, N+2, k) - \frac{1}{\tau} \left( \frac{N}{4L} \right) \left\{ \overset{(6)}{\Delta u^I(1, N+3, k) + \dots} \right\} \quad (B2-12)
\end{aligned}$$

where the required correction terms are

$$\begin{aligned}
& - \frac{1}{\tau} \left( \frac{N}{4L} \right) \left\{ \overset{(7)}{\Delta u^I(1, N+3, k) + \dots} \right\} \\
& = - \frac{1}{\tau} \left( \frac{N}{4L} \right) \left\{ \Delta u^I(1, N+3, k) + \Delta u^I(1, N+3, k+1) - \Delta u^I(1+1, N+3, k) - \Delta u^I(1+1, N+3, k+1) \right. \\
& \quad - \Delta v^I( \quad ) - \Delta v^I( \quad ) - \Delta v^I( \quad ) - \Delta v^I( \quad ) \\
& \quad \left. + \Delta w^I( \quad ) - \Delta w^I( \quad ) - \Delta w^I( \quad ) + \Delta w^I( \quad ) \right\} \quad (B2-13)
\end{aligned}$$

$$\begin{aligned}
& \text{and} \quad (2) \\
& - \left( \frac{N}{4L} \right) \left\{ \Delta \varphi_x^I(1, N+3, k) + \dots \right\} = + \frac{3}{2} \left( \frac{N}{L} \right)^2 \left\{ + \frac{1}{2} \Delta \varphi^{II}(1, N+2, k) + \dots \right. \\
& + \frac{1}{12} \left[ \Delta \varphi^{II}(1+1, N+2, k) + \Delta \varphi^{II}(1, N+2, k+1) + \Delta \varphi^{II}(1-1, N+2, k) \right. \\
& + \Delta \varphi^{II}(1-1, N+2, k-1) \left. \right] - \frac{1}{24} \left[ \Delta \varphi^{II}(1+1, N+2, k+1) + \Delta \varphi^{II}(1+1, N+2, k-1) \right. \\
& \left. + \Delta \varphi^{II}(1-1, N+2, k+1) + \Delta \varphi^{II}(1-1, N+2, k-1) \right] \left. \right\} \quad (B2-14)
\end{aligned}$$

This completes the required divergence corrections at the sliding boundaries.

## APPENDIX C

### EVALUATION OF KINETIC ENERGY, REYNOLDS STRESSES, VORTICITY AND SCALE OF TURBULENCE

#### C.1 REYNOLDS STRESSES AND ENERGY

In differencing method C, the distributions over the volume element of typical velocity components, say  $u$  and  $v$ , are assumed to be of the form below, for control volumes of either family.

$$u = A_0 + A_1\xi + A_2\eta + A_3\zeta + A_4\eta\zeta + A_5\xi\zeta + A_6\xi\eta + A_7\xi\eta\zeta + A_8(1-\xi^2)(1-\eta^2)(1-\zeta^2) \quad (C1-1)$$

$$v = B_0 + B_1\xi + B_2\eta + B_3\zeta + B_4\eta\zeta + B_5\xi\zeta + B_6\xi\eta + B_7\xi\eta\zeta + B_8(1-\xi^2)(1-\eta^2)(1-\zeta^2)$$

The typical mean quadratic product  $\overline{uv}$  over the volume element is then found by evaluation of the integral

$$\overline{uv} = \frac{1}{8} \int_{-1}^{+1} \int_{-1}^{+1} \int_{-1}^{+1} uv \, d\xi d\eta d\zeta \quad (C1-2)$$

Since components  $u$  and  $v$  each have nine terms per Eq. (C1-1), the integral in (C1-2) has 81 terms in all. Fortunately, most of these vanish in the integration. The following basic types of integrals are encountered in the above calculation, namely

$$\int_{-1}^{+1} \xi^n d\xi = 0 \quad \text{for } n \text{ odd}$$

$$= \frac{2}{n+1} \quad \text{for } n \text{ even}$$

$$\int_{-1}^{+1} (1-\xi^2) d\xi = \frac{4}{3}$$

$$\int_{-1}^{+1} (1-\xi^2) \xi d\xi = 0$$

$$\int_{-1}^{+1} (1-\xi^2)^2 d\xi = \frac{16}{15} \quad (C1-3)$$

and similarly for the variables  $\eta$  and  $\zeta$ .

Consequently, the required mean product reduces finally to the form

$$\overline{uv} = \left\{ A_0 B_0 + \frac{1}{3} (A_1 B_1 + A_2 B_2 + A_3 B_3) + \frac{1}{9} (A_4 B_4 + A_5 B_5 + A_6 B_6) \right.$$

$$\left. + \frac{1}{27} (A_7 B_7) + \frac{8}{27} (A_0 B_8 + A_8 B_0) + \frac{512}{3375} A_8 B_8 \right\} \quad (C1-4)$$

The first term on the right represents the product of the mean centroidal values. The remaining terms reflect the fact that the mean product over the volume differs appreciably from the simple product of the two centroidal mean values.

The overall mean product is then found by averaging of the above quantity over all the volume elements that constitute the block. Moreover, the averaging must be carried out over the volume elements of both families. Hence the total volume is covered twice. This is a peculiarity of differencing method C.

By means of the usual method of permutation, the foregoing result may be extended to include all six of the possible quadratic mean products, namely,  $\overline{uu}$ ,  $\overline{vv}$ ,  $\overline{ww}$ ,  $\overline{vw}$ ,  $\overline{wu}$  and  $\overline{uv}$ . These represent the six Reynolds stresses. Furthermore, the sum of the first three of the above quantities represents twice the mean kinetic energy  $2\bar{E}$ . In fact this summation yields the result

$$\begin{aligned}
 2\bar{E} = & \left[ A_0^2 + B_0^2 + C_0^2 \right] + \frac{1}{3} \left[ (A_1^2 + A_2^2 + A_3^2) + (B_1^2 + B_2^2 + B_3^2) \right. \\
 & \left. + (C_1^2 + C_2^2 + C_3^2) \right] \\
 & + \frac{1}{9} \left[ (A_4^2 + A_5^2 + A_6^2) + (B_4^2 + B_5^2 + B_6^2) + (C_4^2 + C_5^2 + C_6^2) \right] \\
 & + \frac{1}{27} \left[ A_7^2 + B_7^2 + C_7^2 \right] + \frac{16}{27} \left[ A_0 A_8 + B_0 B_8 + C_0 C_8 \right] \\
 & + \frac{512}{3375} \left[ A_8^2 + B_8^2 + C_8^2 \right]
 \end{aligned}$$

(C1-5)

## C.2 VORTICITY

The three vorticity components at an arbitrary point within a given control volume are expressed by the relations

$$\begin{aligned} \omega_x &= \left( \frac{2N}{L} \right) \left( \frac{\partial w}{\partial \eta} - \frac{\partial v}{\partial \zeta} \right) \\ \omega_y &= \left( \frac{2N}{L} \right) \left( \frac{\partial u}{\partial \zeta} - \frac{\partial w}{\partial \xi} \right) \\ \omega_z &= \left( \frac{2N}{L} \right) \left( \frac{\partial v}{\partial \xi} - \frac{\partial u}{\partial \eta} \right) \end{aligned} \quad (C2-1)$$

These expressions would be exact if the derivatives appearing in them were known exactly. Unfortunately, only the approximate information represented by equations of the form (C1-1) is available. Direct analytical differentiation of (C1-1) degrades the accuracy somewhat, although the subsequent volume integration explained below tends to offset this error. The results obtained are of the form

$$\begin{aligned} \left( \frac{L}{2N} \right) \omega_x &= (C_2 - B_3) + (C_6 - B_5)\xi - B_4\eta - C_4\zeta \\ &\quad - B_7\xi\eta + C_7\xi\zeta - 2C_8(1-\xi^2)\eta(1-\zeta^2) \\ &\quad + 2B_8(1-\xi^2)(1-\eta^2)\zeta \end{aligned} \quad (C2-2)$$

The components  $\omega_y$  and  $\omega_z$  follow from this by cyclic permutation. The mean square vorticity finally required is defined by the integral

$$\overline{\omega^2} = \frac{1}{8} \int_{-1}^{+1} \int_{-1}^{+1} \int_{-1}^{+1} [\omega_x^2 + \omega_y^2 + \omega_z^2] d\eta d\zeta d\xi \quad (C2-3)$$

Fortunately most of the integrals involved in the evaluation of (C2-3) vanish identically. The integration, although quite lengthy, is not difficult. The result finally obtained is

$$\begin{aligned}
 \left(\frac{L}{2N}\right)^2 \overline{w^2} = & \left[ (A_3 - C_1)^2 + (B_1 - A_2)^2 + (C_2 - B_3)^2 \right] + \frac{1}{3} \left[ (A_4 - C_6)^2 \right. \\
 & + (B_5 - A_4)^2 + (C_6 - B_5)^2 + A_5^2 + A_6^2 + B_6^2 + B_4^2 + C_4^2 + C_5^2 \left. \right] \\
 & + \frac{2}{9} \left[ A_7^2 + B_7^2 + C_7^2 \right] + \frac{512}{675} \left[ A_8^2 + B_8^2 + C_8^2 \right] \\
 & + \frac{16}{27} \left[ (A_6 B_8 + B_6 A_8) + (B_4 C_8 + C_4 B_8) + (C_5 A_8 + A_5 C_8) \right] \quad (C2-4)
 \end{aligned}$$

This result must, of course, be averaged over all the volume elements of both families, in the same manner as for the kinetic energy.

### C.3 SURFACE CONSTANTS

Consider a typical control volume with a centroidal point of family I. The eight corners and the centroid may be designated as follows:

$$\begin{aligned}
 u_P &= u^{II}(1, j, k) & u_{P'} &= u^{II}(1-1, j-1, k-1) \\
 u_A &= u^{II}(1-1, j, k) & u_{A'} &= u^{II}(1, j-1, k-1) \\
 u_B &= u^{II}(1, j-1, k) & u_{B'} &= u^{II}(1-1, j, k-1) \\
 u_C &= u^{II}(1, j, k-1) & u_{C'} &= u^{II}(1-1, j-1, k)
 \end{aligned} \tag{C3-1}$$

$$u_O = u^I(1, j, k)$$

Similarly, consider a typical control volume with a centroidal point of family II. The nine corresponding points may be designated as follows

$$\begin{aligned}
 u_P &= u^I(1+1, j+1, k+1) & u_{P'} &= u^I(1, j, k) \\
 u_A &= u^I(1, j+1, k+1) & u_{A'} &= u^I(1+1, j, k) \\
 u_B &= u^I(1+1, j, k+1) & u_{B'} &= u^I(1, j+1, k) \\
 u_C &= u^I(1+1, j+1, k) & u_{C'} &= u^I(1, j, k+1)
 \end{aligned} \tag{C3-2}$$

$$u_O = u^{II}(1, j, k)$$

Now in either of the above cases we may apply Eq. (C1-1) to all nine characteristic points of the control volume, thus obtaining nine simultaneous equations. These are easily solved for the nine surface constants  $A_0$  through  $A_8$ , with the following results.

$$A_0 = \frac{1}{8} \{ + u_P + u_A + u_B + u_C + u_C' + u_B' + u_A' + u_P' \}$$

$$A_1 = \frac{1}{8} \{ + u_P - u_A + u_B + u_C - u_C' - u_B' + u_A' - u_P' \}$$

$$A_2 = \frac{1}{8} \{ + u_P + u_A - u_B + u_C - u_C' + u_B' - u_A' - u_P' \}$$

$$A_3 = \frac{1}{8} \{ + u_P + u_A + u_B - u_C + u_C' - u_B' - u_A' - u_P' \}$$

$$A_4 = \frac{1}{8} \{ + u_P + u_A - u_B - u_C - u_C' - u_B' + u_A' + u_P' \}$$

$$A_5 = \frac{1}{8} \{ + u_P - u_A + u_B - u_C - u_C' + u_B' - u_A' + u_P' \}$$

$$A_6 = \frac{1}{8} \{ + u_P - u_A - u_B + u_C + u_C' - u_B' - u_A' + u_P' \}$$

$$A_7 = \frac{1}{8} \{ + u_P - u_A - u_B - u_C + u_C' + u_B' + u_A' - u_P' \}$$

$$A_8 = u_0 - A_0$$

Similarly, the B's are computed from the v's and the C's from the w's. Thereupon the mean energy is calculated from (C1-5) and the mean square vorticity from (C2-4).

#### C.4 SCALE OF TURBULENCE

Consider a hypothetical velocity perturbation of the form

$$\begin{aligned} u &= P \sin \frac{2\pi y}{l} \sin \frac{2\pi z}{l} \\ v &= Q \sin \frac{2\pi x}{l} \sin \frac{2\pi z}{l} \\ w &= R \sin \frac{2\pi x}{l} \sin \frac{2\pi y}{l} \end{aligned} \quad (C4-1)$$

where P, Q, R and l are arbitrary constants.

The mean kinetic energy  $\bar{E}$  is then given by

$$2\bar{E} = \frac{1}{l^3} \int_0^l \int_0^l \int_0^l [u^2 + v^2 + w^2] dx dy dz = \frac{1}{l} (P^2 + Q^2 + R^2) \quad (C4-2)$$

The vorticity is defined by

$$\omega_x = \left( \frac{\partial w}{\partial y} - \frac{\partial v}{\partial z} \right) \quad (C4-3)$$

and similarly for  $\omega_y$  and  $\omega_z$  by cyclic permutation.

Upon differentiating, squaring and integrating, we obtain for the mean square vorticity

$$\overline{\omega^2} = \frac{1}{l^3} \int_0^l \int_0^l \int_0^l [\omega_x^2 + \omega_y^2 + \omega_z^2] dx dy dz = \left( \frac{2\pi}{l} \right)^2 \frac{1}{2} (P^2 + Q^2 + R^2) \quad (C4-4)$$

The scale of turbulence  $\lambda$  is defined by the equation

$$\lambda = C \sqrt{\frac{2\bar{E}}{\overline{\omega^2}}} \quad (C4-5)$$

where C is a constant whose value we wish to establish. We choose this constant in such a way that the hypothetical perturbation of (C4-1) shall be deemed to have a scale of turbulence  $\lambda$  which is equal to its wavelength  $\ell$ . The logic of this choice is evident from inspection of (C4-1). Hence we substitute from (C4-2) and (C4-4) into (C4-5) and set  $\lambda = \ell$ .

The result obtained thereby is

$$\lambda = 2 \sqrt{2} \pi \sqrt{\frac{2E}{\omega^2}} \quad (C4-6)$$

Note that the arbitrary amplitude parameters P, Q, R cancel from this result, so that the constant of proportionality given above is independent of these quantities.

Equation (C4-6) is now taken as the definition of the scale of turbulence  $\lambda$ , and is regarded as applicable to all types of perturbations. It may be interpreted as a kind of root mean square wavelength.

## APPENDIX D

### FOURIER ANALYSIS OF TURBULENCE IN A UNIFORM SHEAR FLOW

#### D.1 COORDINATE SYSTEMS

In this appendix, all quantities are non-dimensional in the sense explained elsewhere in this report.

Consider an arbitrary point which moves along with the mean flow. Let  $x, y, z, t$  represent the ordinary time-coordinates of the point in a rigid Cartesian axis system; we term these the Eulerian coordinates. Let  $\xi, \eta, \zeta, \tau$  represent the corresponding Lagrangian coordinates of the point. The Lagrangian coordinates are defined in terms of the Eulerian coordinates as follows:

$$\begin{aligned}\xi &= x_t = 0 \\ \eta &= y_t = 0 \\ \zeta &= z_t = 0 \\ \tau &= t\end{aligned}\tag{D1-1}$$

Thus at time  $t = 0$ , both sets of coordinates coincide.

Note that for a point moving with the mean flow, the Lagrangian space coordinates  $\xi, \eta, \zeta$  are constants, whereas the Eulerian space coordinates  $x, y, z$  are, in general, functions of time. Conversely, for a point fixed in space and not moving with the mean flow, coordinates  $x, y, z$  are constants, whereas  $\xi, \eta, \zeta$  are functions of time.

In the present case of a uniform parallel shear flow whose (dimensionless) shear rate  $\Omega$  equals unity, we see that for a point moving with the mean flow, the relations simplify to

$$\begin{aligned} x &= \xi + \eta t = \xi + y t \quad (\xi = \text{constant}) \\ y &= \eta = \text{constant} \\ z &= \zeta = \text{constant} \\ t &= \tau \end{aligned} \quad (D1-2)$$

Therefore it suffices for this case to take  $x, y, z, t$ , as the Eulerian coordinates, and  $\xi, \eta, \zeta, \tau$  as the Lagrangian coordinates.

Consider a set of simple cubic grid points in the fixed or Eulerian system of reference. Let space and time points be defined as follows:

$$\begin{aligned} x_i &= \frac{L}{N} \left( i - \frac{1}{2} \right) & i &= 1, 2, 3, \dots, N \\ y_j &= \frac{L}{N} \left( j - \frac{1}{2} \right) - \frac{L}{2} & j &= 1, 2, 3, \dots, N \\ z_k &= \frac{L}{N} \left( k - \frac{1}{2} \right) & k &= 1, 2, 3, \dots, N \\ t_m &= \frac{T}{M} \left( m - \frac{1}{2} \right) & m &= 1, 2, 3, \dots, M \end{aligned} \quad (D1-3)$$

Let us establish a corresponding set of Lagrangian grid points, which move with the mean flow. At time  $t = 0$ , however, let the moving Lagrangian grid coincide with the fixed Eulerian grid. Let indices  $\alpha, j, k, m$  represent space time points in the moving system. In particular, for such a moving grid point, we have

$$x(\alpha, j, k, m) = \frac{L}{N} \left( \alpha - \frac{1}{2} \right) + \frac{L}{N} \left( j - \frac{1}{2} - \frac{N}{2} \right) \frac{T}{M} \left( m - \frac{1}{2} \right) \quad (D1-4)$$

where the indices  $\alpha, j, k, m$  vary over the ranges previously indicated. The  $y, z$  and  $t$  coordinates remain as given in (D1-3).

## D.2 FOURIER SERIES APPROXIMATION FOR VELOCITY PERTURBATIONS

It has been shown elsewhere in this report that it is permissible for purposes of approximation to treat turbulence as if it were periodic in space, provided that the wavelength is made sufficiently large and the cell size sufficiently small. Corresponding considerations apply also to the time dimension. In principle, therefore, the space time structure of turbulence is representable by a four-dimensional Fourier series with a very large number of terms. The adequacy of such a representation in practice depends on the number of terms which it is feasible to retain, and also on the accuracy and precision with which the Fourier coefficients can be computed and expressed.

We introduce the auxiliary variable

$$\theta = \frac{2\pi}{L} (px + qy + rz) + \frac{2\pi}{T} (st) \quad (D2-1)$$

where  $\begin{matrix} p \\ q \\ r \end{matrix} = 1, 2, 3, \dots, N$

$s = 1, 2, 3, \dots, M$

Now the  $u$  velocity component is expressible in the form of the Fourier series

$$\frac{u(x, y, z, t)}{\sqrt{2E}} = \sum_{p=1}^N \sum_{q=1}^N \sum_{r=1}^N \sum_{s=1}^M \left\{ A(p, q, r, s) \frac{\sin \theta}{(1/\sqrt{2})} + D(p, q, r, s) \frac{\cos \theta}{(1/\sqrt{2})} \right\} \quad (D2-2)$$

In this equation the velocity component  $u$  is normalized with respect to the root mean square turbulent velocity as represented by  $\sqrt{2\bar{E}}$ , where  $\bar{E}$  is the mean turbulent kinetic energy. The variables  $\sin \theta$  and  $\cos \theta$  are also normalized by their respective root mean square values, both of which equal  $1/\sqrt{2}$ . Such normalizing is optional, but does confer upon the Fourier coefficients, the A's and D's, certain advantageous properties, as will be seen. The matrices  $A(p,q,r,s)$  and  $D(p,q,r,s)$  are four-dimensional arrays, each array consisting of  $N^3M$  constants.

Specifically at the moving Lagrangian grid points themselves, Eqs. (D2-1) and (D2-2) reduce to the forms

$$\theta = \frac{2\pi}{N} \left[ p\left(\alpha - \frac{1}{2}\right) + q\left(j - \frac{N+1}{2}\right) + r\left(k - \frac{1}{2}\right) \right] + \frac{2\pi}{M} \left[ s\left(m - \frac{1}{2}\right) \right]$$

$$\frac{u(\alpha, j, k, m)}{\sqrt{2\bar{E}}} = \sum_{p=1}^N \sum_{q=1}^N \sum_{r=1}^N \sum_{s=1}^M \left\{ A(p,q,r,s) \frac{\sin \theta}{(1/\sqrt{2})} + D(p,q,r,s) \frac{\cos \theta}{(1/\sqrt{2})} \right\} \quad (D2-3)$$

Corresponding expressions for the other two velocity components can be written by permuting the foregoing equations according to the pattern



Certain features of the above results are noteworthy. First of all, it may be seen that once the Fourier coefficients (as well as the normalizing mean energy  $\bar{E}$ ) are known, the turbulent velocities are fully defined. The Fourier coefficients are the six arrays of constants namely, the A's, B's, C's, D's, E's and F's. The total number of Fourier coefficients is therefore  $6N^3M$ , or just twice the total number of

velocity components in the complete space time grid block. Theoretically, these coefficients define the turbulent motion to just that degree of resolution permitted by the constants  $N$  and  $M$  which fix the fineness of the coordinate mesh. The adequacy and resolution of this mathematical model theoretically improve as the constants  $N$  and  $M$  are increased. However, as the number of Fourier coefficients increases, the number of significant figures required for each constant also increases, in order to prevent difficulties arising from round-off errors.

Of course, the velocity components defined by Eqs. (D2-2) or (D2-3) are referred to the moving Lagrangian coordinate system. However, if a transformation to fixed Eulerian coordinates is required, this is easily found by use of Eqs. (D1-2). The reason for introducing Lagrangian coordinates in the first place is that the sliding boundary conditions along the top and bottom of the rigid Eulerian block are thereby satisfied.

It should be stressed that the above Fourier representation is complete in the sense that it duplicates the actual turbulence to within the allotted degree of resolution. Hence any or all statistical or phenomenological quantities that can be calculated from a finite-difference approximation of the velocity history, can also be calculated directly from the Fourier coefficients themselves.

Inasmuch as the Fourier coefficients depend only on the wave numbers  $\frac{p}{L}$ ,  $\frac{q}{L}$ ,  $\frac{r}{L}$  and  $\frac{s}{T}$  but not on the space variables,  $\xi$ ,  $y$ ,  $z$ , the turbulence is homogeneous. Also, since the Fourier coefficients are independent of the time variable  $t$ , the turbulence is stationary.

An important advantage of the Fourier representation, as compared with the direct velocity components themselves, is that it more clearly reveals the structure of the turbulence. The direct velocity components in physical space seem so chaotic as almost to defy any efforts to analyze or order them. On the other hand, the Fourier spectral coefficients can be expected to vary in some smooth and orderly fashion within the wave number domain. Hence there can be some hope of charting

this spectral variation, and perhaps of expressing it graphically or analytically in some greatly condensed and simplified form. If this can be accomplished it will mean that the problem of turbulence in a uniform shear flow is then essentially solved. However, since the wave number domain is four-dimensional, to summarize conditions in this realm in a way which is both simple and adequate may or may not be possible. Detailed numerical data is required before this question can be settled.

Attention is invited to the fact that the Fourier solution contains equal numbers of sine and cosine terms. From this fact, it follows that the overall turbulence is resolvable into components at each point of wave number space which are in certain sense out of phase or orthogonal to each other. This is important for the adequate description of turbulence. Conventional experimental methods of obtaining spectral information about turbulence usually fail to disclose these phase relationships, and are therefore incomplete in a very significant respect. (In fact for a complete description, information on phase relationships is just as essential as information about amplitudes; in quantitative terms we may assert that exactly half the needed information concerns amplitude, the other half concerns phase.)

In principle, the equation of continuity and the three equations of motion could be written directly in terms of the Fourier coefficients themselves rather than in the more usual way, in terms of velocity components. These equations could then be solved for the unknown Fourier coefficients. This method, however, seems to involve extreme analytical complexities and numerical difficulties, and has been discarded as being too unpromising. On the other hand, a feasible method of solution has been developed which establishes the velocities directly, without any reference to Fourier coefficients. Thus far in this discussion we have considered how unknown velocities may be expressed in terms of known Fourier coefficients. In the present circumstances, however, the velocities are the knowns and the Fourier coefficients the unknowns. Hence we face the problem of inverting the previous solution. Fortunately, it is characteristic of Fourier methods that the fundamental equations can be readily inverted.

### D.3 SOLUTION FOR THE FOURIER COEFFICIENTS

For the purpose of inverting the basic equation (D2-2), we introduce the following notation

$$\theta = \frac{2\pi}{L} (p\xi + qy + rz) + \frac{2\pi}{T} (st)$$

$$\theta' = \frac{2\pi}{L} (p'\xi + q'y + r'z) + \frac{2\pi}{T} (s't)$$

$$I_{ss} = \int_{t=0}^T \int_{z=0}^L \int_{y=0}^L \int_{\xi=0}^L \frac{\sin \theta}{(1/\sqrt{2})} \frac{\sin \theta'}{(1/\sqrt{2})} \frac{d\xi dy dz dt}{L^3 T} \quad (D3-1)$$

$$I_{cc} = \int_{t=0}^T \int_{z=0}^L \int_{y=0}^L \int_{\xi=0}^L \frac{\cos \theta}{(1/\sqrt{2})} \frac{\cos \theta'}{(1/\sqrt{2})} \frac{d\xi dy dz dt}{L^3 T}$$

$$I_{sc} = \int_{t=0}^T \int_{z=0}^L \int_{y=0}^L \int_{\xi=0}^L \frac{\sin \theta}{(1/\sqrt{2})} \frac{\cos \theta'}{(1/\sqrt{2})} \frac{d\xi dy dz dt}{L^3 T}$$

It can be verified by direct integration that the following orthogonality relations are valid, namely,

$$(a) \quad I_{ss} = +1 \text{ provided } \begin{cases} p' = p \\ q' = q \\ r' = r \\ s' = s \end{cases} \\ = 0 \text{ otherwise}$$

$$(b) \quad I_{cc} = +1 \quad \text{provided} \quad \begin{cases} \rho' = p \\ q' = q \\ r' = r \\ s' = s \end{cases} \quad (D3-2)$$

$= 0 \text{ otherwise}$

(c)  $I_{sc} = 0$  for all values of the indices.

We now multiply Eq. (D2-2) through by  $\frac{\sin \theta}{(1/\sqrt{2})} \frac{d\xi \, dy \, dz \, dt}{L^3 T}$

and integrate over the limits indicated in (D3-1). Upon invoking the orthogonality relations (D3-2), we obtain

$$\int_{t=0}^T \int_{z=0}^L \int_{y=0}^L \int_{\xi=0}^L \frac{u(\xi, y, z, t)}{\sqrt{2E}} \frac{\sin \theta}{(1/\sqrt{2})} \frac{d\xi \, dy \, dz \, dt}{L^3 T} = A(p, q, r, s) \quad (D3-3)$$

For purposes of approximate numerical evaluation, the integrals on the left may be replaced by corresponding finite summations. These are formed by multiplication of each principal grid value of  $u$  by the cell volume  $(\frac{L}{N})^3$  and time interval  $(\frac{T}{M})$ , and then summation over the full extent of the space time block. Upon rearranging, we obtain the result

$$A(p, q, r, s) = \frac{1}{N^3 M} \sum_{\alpha=1}^N \sum_{j=1}^N \sum_{k=1}^N \sum_{m=1}^M \frac{u(\alpha, j, k, m)}{\sqrt{2E}} \frac{\sin \theta}{(1/\sqrt{2})} \quad (D3-4)$$

Proceeding in like fashion with the cosine term we obtain the corresponding result

$$D(p, q, r, s) = \frac{1}{N^3 M} \sum_{\alpha=1}^N \sum_{j=1}^N \sum_{k=1}^N \sum_{m=1}^M \frac{u(\alpha, j, k, m)}{\sqrt{2E}} \frac{\cos \theta}{(1/\sqrt{2})} \quad (D3-5)$$

The remaining Fourier coefficients may be found in like manner by permutation in accordance with (D2-4).

The velocity components on the right side of Eqs. (D3-4) and (D3-5) are evaluated at the Lagrangian grid points. These may be obtained by interpolation from the previously computed and known values at the Eulerian grid points.

A further important result is obtained from energy considerations. First, both sides of Eq. (D2-2) are squared and integrated over the space time block. In this process, the right side is greatly simplified through the application of the orthogonality relations. The same procedure is also applied to the other two components, and the three equations are then added together. The following result is thereby obtained, namely,

$$\sum_{p=1}^N \sum_{q=1}^N \sum_{r=1}^N \sum_{s=1}^M \left\{ \left[ A^2(p,q,r,s) + D^2(p,q,r,s) \right] + \left[ B^2(p,q,r,s) + E^2(p,q,r,s) \right] + \left[ C^2(p,q,r,s) + F^2(p,q,r,s) \right] \right\} = 1 \quad (D3-6)$$

The physical interpretation is simple. Each quadratic term represents the fraction of the total kinetic energy of turbulence stored at the corresponding location in wave number space. The sum of all such energy fractions must equal unity. This simple form of result is the consequence of the normalizing procedures employed in the analysis.

It is perhaps worth mentioning that a shift in the origin of the Lagrangian space time coordinates will affect all of the Fourier coefficients, but in a simple way. The total energy stored at each point in wave number space remains unchanged, but the separate sine and cosine components each undergo a simple phase shift.

It might also be mentioned that all results obtained in this appendix by use of Fourier series have an equivalent representation in terms of truncated Fourier integrals. The difference is mainly one of

form, the series form being somewhat more convenient for numerical methods. In the integral method, the Fourier coefficients are treated not as discrete constants but as continuous density functions in wave number space. Conversely, the discrete Fourier constants may be interpreted as pointwise approximations to functions which are, in fact, distributed continuously in wave number space. The distinction is largely academic. There is no difference in the final computational formulas which are obtained!

This completes the essential features of the Fourier analysis. It is now possible to derive further interesting and useful results concerning quantities such as the Reynolds stresses, various correlation coefficients, and so on, but such additional topics lie beyond the scope of the present discussion.

As a final cautionary note, we again observe that calculation of the Fourier coefficients from Eqs. (D3-4) and D3-5) is subject to inaccuracy from round-off errors, especially for high values of  $N^3M$ . It will be necessary to retain a sufficiently large number of significant figures in the calculations. It is a curious fact that if  $N^3M$  is small, round-off error in the individual coefficients is small, but detailed resolution of the turbulence is poor. On the other hand if  $N^3M$  is high, resolution is good, but round-off error is high. This circumstance somewhat resembles the well known indeterminacy principle of Heisenberg!

## DOCUMENT CONTROL DATA - R &amp; D

(Security classification of title, body of abstract and indexing annotation must be entered when the overall report is classified)

1. ORIGINATING ACTIVITY (Corporate author) Naval Radiological Defense Laboratory San Francisco, California 94135		2a. REPORT SECURITY CLASSIFICATION UNCLASSIFIED	
		2b. GROUP	
3. REPORT TITLE TURBULENCE IN AN UNBOUNDED, UNIFORM SHEAR FLOW: A COMPUTER ANALYSIS			
4. DESCRIPTIVE NOTES (Type of report and inclusive dates)			
5. AUTHOR(S) (First name, middle initial, last name) T. H. Gawain John W. Pritchett			
6. REPORT DATE (Distribution) 6 November 1968		7a. TOTAL NO. OF PAGES 175	7b. NO. OF REFS 3
8a. CONTRACT OR GRANT NO.		8a. ORIGINATOR'S REPORT NUMBER(S) NRDL-TR-68-86	
b. PROJECT NO. ARPA, Order No. 961, Program Code 7F40, Task 5.		8b. OTHER REPORT NO(S) (Any other numbers that may be assigned this report)	
10. DISTRIBUTION STATEMENT This document has been approved for public release and sale; its distribution is unlimited.			
11. SUPPLEMENTARY NOTES		12. SPONSORING MILITARY ACTIVITY Advanced Research Projects Agency Washington, D. C. 20301	
13. ABSTRACT <p>→ Fluid turbulence is of crucial significance in many problems of scientific and technical importance. Current developments in computer technology offer the possibilities of solving the fundamental equations of turbulent flow in a way never before possible. In order to accomplish this aim, however, it is first necessary to formulate the essential theoretical concepts in a suitable manner. This report summarizes the progress achieved to date in this connection. Various essential basic equations are derived, but the emphasis is as much on fundamental concepts as on mathematical details. More specifically, a method is established for the computer simulation of the detailed stationary turbulence in a uniform shear flow. The results obtainable in this way are far more comprehensive than any which could reasonably be obtained by physical experiment. The data generated represents fundamental information which may be subsequently analyzed to establish overall phenomenological characteristics of the turbulence. The concepts in this report should provide a sound basis for a systematic, sustained and productive research plan. They have already been successfully applied to a computer program which is now going into operation. Results of a typical computer run are included and illustrate qualitative agreement with theoretical predictions; it is hoped to present far more comprehensive and definitive numerical results in future reports.</p>			